

Wireless ATM Network Access and Control

by

Tung Chong Wong

A thesis
presented to the University of Waterloo
in fulfilment of the
thesis requirement for the degree of
Doctor of Philosophy
in
Electrical Engineering

Waterloo, Ontario, Canada, 1999

©Tung Chong Wong 1999



**National Library
of Canada**

**Acquisitions and
Bibliographic Services**

**395 Wellington Street
Ottawa ON K1A 0N4
Canada**

**Bibliothèque nationale
du Canada**

**Acquisitions et
services bibliographiques**

**395, rue Wellington
Ottawa ON K1A 0N4
Canada**

Your file Votre référence

Our file Notre référence

The author has granted a non-exclusive licence allowing the National Library of Canada to reproduce, loan, distribute or sell copies of this thesis in microform, paper or electronic formats.

The author retains ownership of the copyright in this thesis. Neither the thesis nor substantial extracts from it may be printed or otherwise reproduced without the author's permission.

L'auteur a accordé une licence non exclusive permettant à la Bibliothèque nationale du Canada de reproduire, prêter, distribuer ou vendre des copies de cette thèse sous la forme de microfiche/film, de reproduction sur papier ou sur format électronique.

L'auteur conserve la propriété du droit d'auteur qui protège cette thèse. Ni la thèse ni des extraits substantiels de celle-ci ne doivent être imprimés ou autrement reproduits sans son autorisation.

0-612-44781-2

The University of Waterloo requires the signatures of all persons using or photocopying this thesis. Please sign below, and give address and date.

Abstract

Wireless Asynchronous Transfer Mode (ATM) networks are attractive because they can provide a wide variety of new wireless broadband services providing true portability and support for personal, integrated broadband services currently envisioned for wired ATM systems only. A wireless ATM access network has to provide a reasonable user-transparent Quality of Service (QoS) for different service classes as well as seamless integration across an interconnection of wireless and wired ATM networks. A Medium Access Control (MAC) protocol has been designed, which allows seamless integration of the wireless access segments to the wired ATM network and takes into consideration the characteristics of the various classes of services to provide good QoS. This protocol is based on the Time Division Multiple Access with Dynamic Reservation (TDMA/DR) protocol. The performance of the MAC protocol is studied: a) by computer simulation for voice, Markov Modulated Poisson Process (MMPP) or Motion Picture Experts Group (MPEG) video and data traffic; b) by mathematical analysis for delay-sensitive voice and MMPP video traffic.

This research work is also concerned with the Connection Admission Control (CAC) and the Usage Parameter Control (UPC) issues in a cellular wireless ATM access network. The proposed two CAC approaches are based on equivalent capacity for heterogeneous traffic. The performance of one of these approaches is studied by mathematical analysis and the other approach by computer simulation. The UPCs used to police the heterogeneous traffic are leaky buckets with the token generation rates set at the equivalent capacities of the heterogeneous traffic. The performance of the UPC is studied by computer simulation for heterogeneous traffic and mathematical analysis for voice and MMPP video traffic.

Acknowledgements

I would like to thank my supervisor, Professor Jon W. Mark for invaluable guidance, support, patient and understanding, throughout these years.

I would like to thank Professor Stefan Leue, Professor Sherman Shen and Professor Johnny W. Wong for their constructive comments and guidance.

I would like to thank Professor Victor Leung for coming to University of Waterloo as my external examiner for my Ph.D. oral defense.

I would like to thank Professor Amir K. Khandani for his understanding and support.

I would like to thank my director, Professor Lye Kin Mun and deputy director, Professor Chua Kee Chaing of Centre for Wireless Communications, National University of Singapore, for their support, understanding and encouragement.

I would like to thank my colleagues at University of Waterloo for their friendship and valuable help: Michael Cheung, Dr. Nasir Ghani, Vincent Wong, Fred Ma, Edwin Iun, Salim Manji, Dr. Majid Barazande-Pour, Dr. Meenan Vishnu, Dr. Byoung Joon Lee, Dr. Robert Lehr, Dr. Atsushi Yamada, Shamir Mukhi, James Qiu, Joseph Zhang, Jian Zhu Zhang, Nainesh Agarwal, Wei Cui, Xiao Ning Yang, Janaki Bandara, Salman Akbar, Yu Zeng and Jun Ye.

I would like to thank Wendy Boles and Jenniffer Werth for their administration support.

I would like to thank my former colleague and friend, Wee Teck Ng, at University of Michigan for his encouragement, support and valuable help.

I would like to thank my colleagues at Centre for Wireless Communications, National University of Singapore, for their encouragement and support: Kuck Jong Yong, Guang

Yi Wang, Chin Ming Pang, Dr. Winston Seah, Dr. Anthony Lo, Dr. Chew Yong Huat, Dr. Brahim Bensaou.

I would also like to thank my parents, Sun Foon Wong and Ah Noy Heng, for their patient understanding, support and encouragement.

This research has been supported by the Natural Sciences and Engineering Research Council of Canada under grant no. A7779 and the Singapore National Science and Technology Board Scholarship.

Contents

Chapter 1 Introduction	1
1.1 Introduction	1
1.2 Literature Review	3
1.3 Motivation	8
1.4 Overview of Thesis	9
Chapter 2 Wireless ATM Network Design	11
2.1 Introduction	11
2.2 Integration of Wireless ATM Access Network to Wireline ATM Network	13
2.3 Transmission Frames	14
2.3.1 Uplink Slots	16
2.3.1.1 Guard Time	16
2.3.1.2 Service Type Field	17
2.3.1.3 QoS Parameter Field	18
2.3.1.4 Cyclic Redundant Check Field	18
2.3.1.5 Packet Sequence Number Field	19
2.3.1.6 Handoff Indicator Field	19
2.3.1.7 ATM Fields	19
2.3.1.8 Uplink TDMA Frame Size	20
2.3.2 Downlink Slots	21
2.3.2.1 Destination Address	22

2.3.2.2 Service Type Field	22
2.3.2.3 Start of Information Slot Position in the Uplink	22
2.3.2.4 End of Information Slot Position in the Uplink	22
2.3.3 Slot Timing for Uplink and Downlink	23
2.4 Medium Access Control Protocol	23
2.4.1 Bandwidth Allocation	27
2.5 Usage Parameter Control	27
2.6 Connection Admission Control	29
Chapter 3 Medium Access Control	33
3.1 Introduction	33
3.2 Simulation Model	34
3.2.1 Simulation Model Processes	34
3.2.2 Arrival Processes	35
3.2.2.1 Voice Arrival Process	36
3.2.2.2 Video Arrival Process	38
3.2.2.3 Data Arrival Process	39
3.2.3 Request Slot Contention Processes	40
3.2.4 Information Slot Allocation Process	41
3.3 Simulation Results	42
3.3.1 Voice Performance	44
3.3.2 MMPP Video Performance	46
3.3.3 Data Performance and Overall Channel Utilization	47
3.4 Performance Analyses	48

3.4.1 Voice Traffic	48
3.4.2 MMPP Video Traffic	56
3.5 Numerical Results	61
3.5.1 Voice Performance	61
3.5.2 MMPP Video Performance	62
3.6 Summary	64
Chapter 4 Usage Parameter Control	66
4.1 Introduction	66
4.2 Simulation Models	67
4.2.1 Voice Traffic	67
4.2.2 MMPP Video Traffic	67
4.2.3 Data Traffic	68
4.3 Simulation Results	69
4.3.1 Voice Performance	69
4.3.2 MMPP Video Performance	72
4.3.3 Data Performance	75
4.4 Performance Analyses	76
4.4.1 Voice Traffic	78
4.4.2 MMPP Video Traffic	79
4.5 Numerical Results	82
4.5.1 Voice Performance	82
4.5.2 MMPP Video Performance	83
4.6 Summary	84

Chapter 5 MPEG Video Traffic	87
5.1 Introduction	87
5.2 Simulation Model	87
5.2.1 MPEG Arrival Process	88
5.2.2 MAC Protocols	88
5.2.2.1 Protocol 1	88
5.2.2.2 Protocol 2	88
5.2.3 “Equivalent” number of MPEG video sources	88
5.3 MAC Performance	89
5.3.1 Simulation Results	89
5.3.1.1 Protocol 1	90
5.3.1.2 Protocol 2	93
5.4 UPC Performance	96
5.4.1 Simulation Results	96
5.4.1.1 Protocol 1	96
5.4.1.1 Protocol 2	97
5.5 Summary	98
Chapter 6 Connection Admission Control	100
6.1 Introduction	100
6.2 Performance Analysis	101
6.3 Numerical and Simulation Results	106
6.4 Summary	114
Chapter 7 Conclusions	116

7.1 Overview	116
7.2 Contributions	117
Appendices	120
Appendix A. Flow diagrams for uplink MAC protocol	120
Appendix B. Derivation of the probability of the number of frame delay, F , for voice packets	127
Bibliography	129

List of Tables

2.1	Mean delay spread for various type of environment	17
2.2	TDMA frame size for various voice bit rate	20
2.3	Overhead ratio due to the number of request slots in a TDMA frame of size 11.75 ms with request slot size of (a) 4.8 μ s and (b) 5.6 μ s	21
3.1	Traffic types and their QoS requirements	36
4.1	MMPP video loss	84
6.1	Number of base stations in a VCT that can be supported by a root ATM switch for an overload probability of 1 %	109
6.2	Number of base stations in a VCT that can be supported by a root ATM switch for 1 % of overload period	110
6.3	Minimum and maximum mean frequency of handoffs to surrounding VCTs based on the overload probability	113
6.4	Minimum and maximum mean frequency of handoffs to surrounding VCTs based on the % overload period	113

List of Figures

1.1	Network Configuration of cellular wireless ATM access segments connected to a ATM switch through a propriety ATM multiplexer/demultiplexer	2
2.1	General concept of integrating the cellular wireless ATM network to the wired ATM network	14
2.2	Uplink TDMA/DR frame format	15
2.3	Uplink request slot format	16
2.4	Uplink information slot format	16
2.5	Downlink control slot format	21
2.6	Downlink information slot format	21
2.7	Slot timing for the uplink and the downlink	23
2.8	Model of an arrival process to a portable terminal passing through the base station scheduler and a leaky bucket at the base station	28
2.9	A virtual connection tree	30
2.10	CAC model for a virtual connection tree	32
3.1	Simulation model for the cellular wireless ATM uplink MAC protocol	35
3.2	On-Off source model for voice arrival process	37
3.3	Packetized voice process for the case where the start of the next talkspurt period falls within the last packetization period for the last voice packet in the previous talkspurt	37
3.4	8-state MMPP for video arrival process	38
3.5	Poisson process for data message arrival with a geometric number of	

packets for data arrival process	40
3.10 Probability of more than zero outstanding voice request collisions	44
3.11 Percentage voice clippings	45
3.12 Distribution of voice packet access delay with 60 request slots	45
3.13 Distribution of voice packet access delay variation with 60 request slots	46
3.14 Mean MMPP video packet delay	47
3.15 Distribution of MMPP video packet access delay with 60 request slots	47
3.16 Distribution of MMPP video packet access delay variation with 60 request slots	47
3.17 Mean data packet access delay	48
3.18 Total information slot utilization	48
3.19 Mean voice packet queueing delay	62
3.20 Distribution of voice packet queueing delay	62
3.21 Mean MMPP video packet queueing delay	63
3.22 Distribution of MMPP video packet queueing delay	63
4.1 Simulation model of a voice traffic arriving to a portable terminal passing through the base station scheduler and a leaky bucket at the base station	67
4.2 Simulation model of a MMPP video traffic arriving to a portable terminal passing through the base station scheduler and a leaky bucket at the base station	68
4.3 Simulation model of a data traffic arriving to a portable terminal passing through the base station scheduler and a leaky bucket at the base station	68
4.4 Voice losses with respect to input voice buffer	70

4.5	Mean voice delays with respect to input voice buffer	71
4.6	Voice losses with respect to total buffer size	71
4.7	Mean voice delays with respect to total buffer size	72
4.8	MMPP video loss with respect to the input video buffer	73
4.9	Mean MMPP video delays with respect to the input video buffer	74
4.10	MMPP video loss with respect to total buffer size	74
4.11	Mean MMPP video delays with respect to total buffer size	75
4.12	Data loss with respect to the input data buffer	76
4.13	Mean data delays with respect to the input data buffer	76
4.14	Data loss with respect to the total buffer size	77
4.15	Mean data delays with respect to total buffer size	78
4.16	Voice losses with respect to the total buffer size	83
4.17	“On” period distribution to the leaky bucket	83
4.18	“Off” period distribution to the leaky bucket	84
5.1	Mean video packet queueing delay with Protocol 1	90
5.2	Distribution of video packet queueing delay with 60 request slots with Protocol 1	91
5.3	Percentage voice clippings for 100 voice users, 19 MPEG video and 10 data users with Protocol 1	92
5.4	Percentage voice clipping for 100 voice users, 2 MMPP video users and 100 data users with Protocol 1	92
5.5	Voice clippings with respect to the number of MPEG video users (with 100 voice users and 100 data users) for Protocol 1	93

5.6	Mean video packet queueing delay with Protocol 2	94
5.7	Distribution of video packet queueing delay with 60 request slots for Protocol 2	94
5.8	Percentage voice clipping with 100 voice users, 19 MPEG video users and 100 data users for Protocol 2	96
5.9	MPEG video loss with respect to total buffer size (with 100 voice users, 5 MPEG video users and 100 data users) for Protocol 1	97
5.10	MPEG video loss with respect to total buffer size (with 100 voice users, 19 MPEG video users and 100 data users) for Protocol 2	98
6.1	Maximum equivalent capacity connection admissibility based upon guaranteed overload probability	108
6.2	Maximum equivalent capacity connection admissibility based upon % overload period	110
6.3	Configurations for hexagon cell(s) in a VCT with the minimum values of p : (a) $B=1$, (b) $B=2$, (c) $B=3$, (d) $B=4$, (e) $B=5$, (f) $B=6$, (g) $B=7$, (h) $B=8$, (i) $B=9$ and (j) $B=10$	112
6.4	Configuration for hexagon cells in a VCT with the maximum value of p	113
6.5	Configuration for hexagon cells in a VCT which does not allow the same VCT configurations to be connected together efficiently for $B=8$ but gives the minimum value of p	113
A.1	Flow diagram for the algorithm followed by each portable terminal for data traffic	121
A.2	Flow diagram for the algorithm followed by each portable terminal for	

voice traffic	122
A.3 Flow diagram for the algorithm followed by each portable terminal for video traffic	123
A.4a Flow diagram for the algorithm followed by the base station for information slot allocation (part 1)	124
A.4b Flow diagram for the algorithm followed by the base station for information slot allocation (part 2)	125
A.4c Flow diagram for the algorithm followed by the base station for information slot allocation (part 3)	126

Glossary of Symbols

α	mean “on” period of the output video process from the uplink MAC protocol
a	token generation rate of a leaky bucket
A_i	number of voice requests that arrive to the available request slots in the i th TDMA frame
A_{i1}	number of voice requests that arrive to the available request slots in the i th TDMA frame and the voice users are in the silent states at the beginning of the frame
A_{i2}	number of voice requests that arrive to the available request slots in the i th TDMA frame and the voice users become silent during the frame
β	mean “off” period of the output video process from the uplink MAC protocol
b	peak burst rate of a input source to a leaky bucket
\bar{B}	number of MMPP video packets arriving during a TDMA frame
$B(u, v; N_A)$	probability that there are u successful requests given that there are v requests were transmitted in N_A slots
B	number of base stations supported by a given VCT
B_{data}	input data buffer to a leaky bucket
$B_{data,token}$	data token buffer in a leaky bucket
B_d	sum of input data buffer and data token buffer in a leaky bucket
B_{video}	input video buffer to a leaky bucket
$B_{video,token}$	video token buffer in a leaky bucket
B_{vi}	sum of input video buffer and video token buffer in a leaky bucket

B_{voice}	input voice buffer to a leaky bucket
$B_{voice,token}$	voice token buffer in a leaky bucket
B_v	sum of input voice buffer and voice token buffer in a leaky bucket
C	speed of propagation in radio domain or number of voice request collisions
C_0	allocated capacity of the test base station
C_i	number of outstanding collisions in the i th TDMA frame
C_{ik}	equivalent capacity of the i th connection belonging to the k th class
C_N	equivalent capacity of the entire VCT
C_R	equivalent capacity that must be reserved at the root of the VCT
C_S	standby capacity
C_t	equivalent capacity used in the test base station
d_{video}	MMPP video generation slot time
\tilde{D}	number of MMPP video packets arriving during an interval of length t
\tilde{D}_1	time interval from the time the tagged voice packet arrives in a TDMA frame to the “beginning” of the next TDMA frame
\tilde{D}_2	a single TDMA frame that the voice packet has to wait if $F=0$ as it can only be transmitted in the next TDMA frame, or two TDMA frame time if $F=1$
\tilde{D}_3	a request slot subframe that the tagged voice packet has to wait
\tilde{D}_4	time interval that the tagged voice packet has to wait before it can be transmitted in the information slot assigned to it by the base station in the previous frame
\tilde{D}_j	time interval from the time that a tagged video packet arrives (j th arrival) in a

	TDMA frame to the beginning of the next TDMA frame in the i th frame
\tilde{D}_6	one TDMA frame that the tagged video packet has to wait in the $(i+1)$ th frame
	frame
\tilde{D}_7	a request slot subframe that the tagged video packet has to wait in the $(i+2)$ th frame
	frame
\tilde{D}_8	delay due to voice packet being transmitted before the video packets and the time interval the tagged video packet has to wait for other video packets to be transmitted first in the $(i+2)$ th frame
	frame
\tilde{D}_9	delay due to voice packets being transmitted before the video packets in the $(i+2)$ th frame
	frame
\tilde{D}_{10}	time interval that the tagged video packet has to wait for other video packets to be transmitted first in the $(i+2)$ th frame
	frame
D	maximum propagation distance in the cell
h	mean “on” period of an input source to a leaky bucket
h_i	probability of being in phase i in steady state for a MMPP video source
\tilde{G}	number of Poisson arrivals in any interval of length t
H	phase transition probability matrix in a MMPP video slot time
\bar{F}	mean frequency of handoffs to adjacent/surrounding VCTs
F	number of TDMA frame(s) incurred by the voice requests due to contention for the request slot subframe
i	number of ways that a mobile user can move out of a VCT
k	mean “off” period of an input source to a leaky bucket

K	total number of traffic classes supported
$K_{D,i}$	number of voice requests transmitting in slots that are different from that of the tagged voice request in the i th TDMA frame
$K_{S,i}$	number of voice requests transmitting in the same slot as the tagged voice request in the i th TDMA frame
$\bar{\lambda}$	mean number of MMPP cells generated per second
λ	MMPP video arrival rate matrix
$\lambda_{data,i}$	mean message arrival rate for data user i
λ_i	MMPP video cell generation rate while in phase i
$\lambda_{i,sec}$	MMPP video cell generation rate per second while in phase i
$\lambda_{i,slot}$	MMPP video cell generation rate per video slot while in phase i
$\eta(u,v)$	number of combinations that u requests are successful given that v requests have been transmitted randomly in N_i slots
n_{jk}	number of class k connections in the j th base station
\tilde{N}	number of voice users in the active (on) state or the number of voice packets for transmission in a TDMA frame
\tilde{N}_i	number of voice users in the active (on) state or the number of voice packets for transmission in the i th TDMA frame
\bar{N}_{data}	mean number of information slots used by data users
\bar{N}_{video}	mean number of information slots used by MMPP video users
\bar{N}_{voice}	mean number of information slots used by voice users
N_i	number of cells in the VCT that allows the mobile user to move out of a VCT

with i ways

N_{phase}	number of MMPP video slots in phase i
N_A	number of available request slots in a TDMA frame
N_I	number of information slots in a TDMA frame
N_R	number of request slots in a TDMA frame
M	number of phases in a MMPP video process or total buffer size of a leaky bucket or number of mobile users in a VCT
M_{data}	number of data users
M_i	number of class i traffic users that can be supported at a single base station
M_v	number of voice users
M_{vb}	number of voice users who are in the silence states at the beginning of the frame
M_{vd}	number of voice users who become silent during the frame interval
M_{video}	number of MMPP video users
$M_{video.MMPP}$	number of MMPP video users
$M_{video.MPEG}$	number of MPEG video users
M_{voice}	number of voice users
p	probability of migrating to adjacent/surrounding base stations
P_o	probability that the equivalent capacity used in the test base station exceeds the allocated capacity
P_u	probability that the equivalent capacity used in the test base station is less than or equal to the allocated capacity
\tilde{Q}	number of video packets for transmission in the $(i-1)$ th TDMA frame with y_{i-1}

	number of video users including the tagged video user as the last user to transmit in this group of video users
$r(v)$	maximum number of successful reservations given that v requests have been transmitted in N_A slots
\tilde{R}	number of video packets for transmission in the i th TDMA frame with (y_i-1) number of video users excluding the tagged video user who transmits after this group of video users
\tilde{R}_1	number of tagged MMPP video packets that are transmitted in the i th frame for 1 MMPP video user or number of tagged MMPP video packets that arrive in the $(i-2)$ th frame for the tagged video user
R_b	bit rate
R_{MMPP}	mean MMPP code rate
R_{MPEG}	mean MPEG code rate
τ_b	time between bits
τ_d	die-out time of the tail of the pulsed signal which depends on the amplitude and phase response of the filters
τ_g	guard time
τ_p	propagation delay related to distance
$\Delta\tau_g$	error tolerance in guard time due to the instability of the clock
$\Delta\tau_p$	delay spread at the receiver
\bar{t}_1	mean voice talkspurt period
\bar{t}_2	mean voice silence period

\bar{t}_3	mean interarrival time between consecutive data message arrivals
\tilde{T}_{video}	MMPP video packet queueing delay at the portable terminal
\tilde{T}_{voice}	voice packet queueing delay at the portable terminal
T_{in}	time spent by a mobile user in a cell
T_C	size of a control slot in the downlink
T_I	size of an information slot in the uplink
T_R	size of a request slot in the uplink
T_{TDMA}	size of a TDMA frame
\tilde{U}	number of information slots between the end of the video packet transmission of the tagged video user in the $(i-1)$ th TDMA frame to the end of the last information slot in same frame
\tilde{V}	“off” period to the leaky bucket for the tagged MMPP video user
\tilde{W}	“on” period to the leaky bucket for the tagged MMPP video user
X	number of mobile users which handoffs to adjacent/surrounding base stations
\tilde{Y}_i	transmission order for the tagged video user among the M_{video} video users in the i th TDMA frame

List of Acronyms

AAL	ATM adaptation layer
ATM	asynchronous transfer mode
ARQ	automatic repeat request
BER	bit error rate
BISDN	broadband integrated services digital network
CAC	connection admission control
CBR	constant bit rate
CDMA	code division multiple access
CLP	cell loss priority
CPCS	common part convergence sublayer
CRC	cyclic redundancy check
DS-CDMA	direct sequence code division multiple access
FDMA	frequency division multiple access
FEC	forward error correction
GCRA	generic cell rate algorithm
GFC	generic flow control
HEC	header error control
MAC	medium access control
MMPP	Markov modulated Poisson processes
MPEG	motion picture experts group
MSC	mobile switching centre

PCN	personal communication networks
PDU	protocol data unit
QoS	quality of service
TDMA	time division multiple access
TDMA/DR	time division multiple access with dynamic reservation
UNI	user network interface
UPC	usage parameter control
VBR	variable bit rate
VCI	virtual channel identifier
VCN	virtual circuit number
VCT	virtual connection tree
VPI	virtual path identifier

Chapter 1

Introduction

1.1 Introduction

Wireless Asynchronous Transfer Mode (ATM) networks are attractive because they can provide a wide variety of new wireless broadband services providing true portability and support for personal, integrated broadband services currently envisioned for wired ATM systems only. A wireless ATM access network has to provide a reasonable user-transparent Quality of Service (QoS) for different service classes as well as seamless integration across an interconnection of wireless and wired ATM networks. In the present development of wired ATM networks and wireless personal communication networks, there are already some papers that address some of the issues in wireless ATM-based networks [1-12].

This thesis describes our work on the design of a cellular wireless ATM access network, the configuration of which is shown in Fig. 1.1. The network comprises a number of wireless access segments, each supporting a base station and a number of multimedia portable terminals. A base station acts as the central communication hub and wireless bandwidth controller in its wireless segment, and is connected to the wired ATM network via a multiplexer/demultiplexer. The multiplexer is required because of the bit rate mismatch between the wireless segments and the wired ATM network; specifically, each wireless segment has been designed to support an aggregate bit rate of only 20 Mb/s. An enhanced Medium Access Control (MAC) protocol, designed to allow seamless integration of the wireless access segments to the wired ATM network and to take into

consideration the characteristics of the various classes of services to provide satisfactory QoS, is proposed. This protocol is based on the Time Division Multiple Access with Dynamic Reservation (TDMA/DR) protocol described in [1-4].

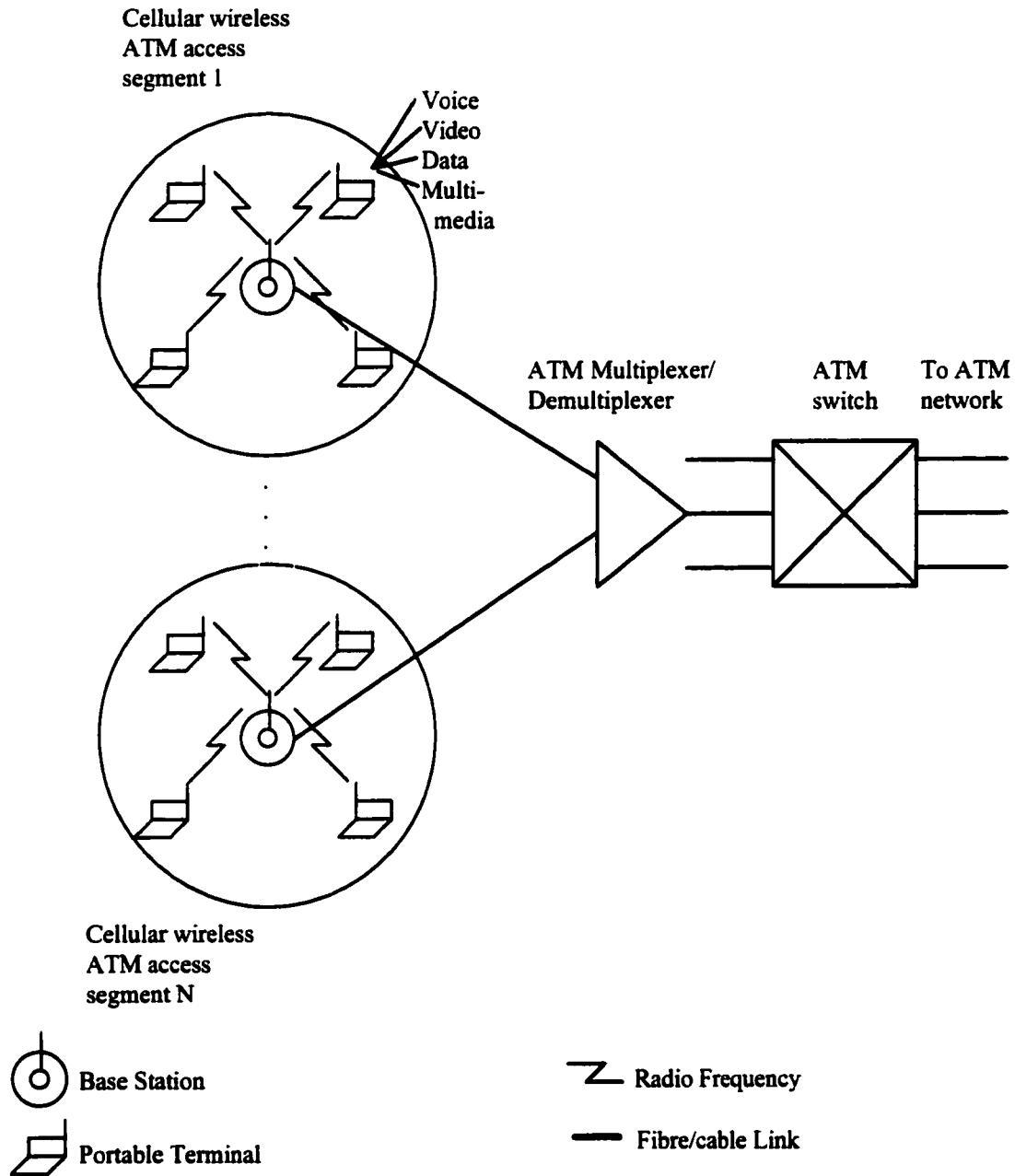


Fig. 1.1. Network Configuration of cellular wireless ATM access segments connected to a ATM switch through a propriety ATM multiplexer/demultiplexer

The uplink MAC protocol used in this network, which allows voice, video and data transmissions, is described. This protocol is designed to allow seamless integration from the wireless domain to the wired ATM network taking into account the various QoS for voice, video and data traffic. An algorithm for allocation and defragmentation of voice information slots which used the MAC protocol to improve bandwidth efficiency by taking advantage of the silence period of voice traffic is also described in [11].

The research described in this thesis is concerned with issues above the physical layer in the protocol stack. However, we recognize that the physical layer, particularly with respect to error performance, imposes limits on the Quality of Service (QoS) provisioning. Therefore, upper layer buffer dimensioning only needs to ensure all cell loss rate are slightly better or matching that provided by the physical layer processors.

This work is also concerned with Connection Admission Control (CAC) and Usage Parameter Control (UPC) issues in a cellular wireless ATM access network.

1.2 Literature Review

There are a number of papers in the literature that address some of the issues in wireless ATM-based networks. Wilson et al. [1] compare dynamic TDMA and spread-spectrum packet Code Division Multiple Access (CDMA) as multiple access strategies in an integrated voice/data Personal Communication Networks (PCN) environment. Voice and data users only are considered in the simulation. Simulation results show that while CDMA typically provide a 2:1 or greater capacity advantage over TDMA, the gains are generally associated with higher data delay for long messages generated by file transfer and multimedia application. Furthermore, practically achievable CDMA efficiencies may

be somewhat lower than these results because of thermal noise effects, imperfect power control, etc.

Raychaudhuri and Wilson in [2] present a discussion of issues related to the support of multimedia traffic in next-generation PCN. An example of demand assigned TDMA protocol is considered in detail, with a particular focus on a traffic mix consisting of Constant Bit Rate (CBR) voice and Variable Bit Rate (VBR) data with real-time constraints. Simulation models are used for performance evaluation. Time-of-expire (TOE) based queue service disciplines are introduced as a mechanism for improving the cell loss rate experienced by time-critical data, and simulation results investigating the effect of TOE processing are presented.

Raychaudhuri and Wilson in [3] present a discussion of system design issues related to the development of next-generation multimedia PCN. It is proposed that the baseline definition of emerging PCN systems be broadened to provide multimedia transport capabilities qualitatively similar to those offered by BISDN/ATM. A number of system-level design and technology selection issues are discussed. An outline of a dynamic TDMA based multimedia PCN system architecture is presented. Simulation based performance evaluation results are given for a mixed voice/data traffic scenario.

In [4], Raychaudhuri presents an ATM based transport architecture for next-generation multiservices PCN. An ATM based wireless network concept capable of supporting a mixture of Broadband Integrated Services Digital Networks (BISDN) services including CBR, VBR and packet data transport, is explored from an architecture viewpoint. Design issues related to the physical, MAC and data link layers of the ATM-

based radio link are discussed, and preliminary technical approaches are identified in each case.

McTiffin et al. [5] present an integrated system concept for a Direct Sequence Spread Spectrum CDMA radio access suitable for third-generation mobile radio. The system has been conceived to take account of such diverse services as low bit rate voice and quasi-broadband services of up to 256 kbps. Broadband services imply the use of ATM transmission technique, and particular attention is paid to the mutual impact of CDMA and ATM. An efficient Automatic Repeat Request technique is described which gives a suitable low overall error rate and a soft capacity limit.

In [6], Raghvendra discusses issues for mobile multimedia using ATM and microcellular technologies. Wyrwas et al. [7] discuss alternative access strategies for multi-media wireless systems. FDMA, TDMA, CDMA and random packet access schemes are considered. A number of possible strategies are presented and the major performance issues are discussed. In [8], Leslie et al. discuss some issues in local wireless ATM networks. Eng et al. [9] describe the theory, design and prototyping of a wireless ATM LAN/PBX capable of supporting mobile users with multi-Mb/s access rates and multi-Gb/s aggregate capacities. Karol et al. propose and study a demand-assignment channel access protocol for wireless packet (ATM) network in [10]. Based on the assumption of homogeneous traffic, their simulation results show that even with the 'worst possible' traffic characteristics, the delay-throughput performance of their protocol is close to the best possible with any access protocol.

Next, we consider the comparison of TDMA/DR with DS-CDMA. Channel congestion in TDMA/DR leads to higher probability of voice blocking, while increasing

traffic load in DS-CDMA will have the effect of degrading packet loss rate [1]. For TDMA/DR, the key user-level performance measures are voice call blocking probability, voice call delay and data delay. On the other hand, for DS-CDMA, there is no explicit voice call blocking, and degraded channel performance for high traffic loads will manifest itself in the form of increased voice packet loss rate [1].

In [1], results show that CDMA-based PCN does have a higher capacity than that of TDMA/DR, but practically achievable CDMA efficiencies may be somewhat lower than that indicated by these results because of thermal noise effects, imperfect power control, etc. [1]. Furthermore, CDMA requires accurate power control to avoid the “near-far” problem, adding to remote cost/complexity [3]. However, CDMA has the advantage of potentially supporting overlay operation when new frequencies are not available [3]. In addition, CDMA enjoys the advantage in not requiring time slots (bandwidth allocation) to be reserved in response to the demand from users or terminals as in the case of TDMA/DR. As long as the total interference does not exceed a design threshold, service quality is maintained in CDMA [34]. Furthermore, CDMA has no access delay as compared to a one TDMA frame delay in TDMA/DR.

For multimedia applications, DS-CDMA has the disadvantage of relatively low peak transmission bit-rate when compared with TDMA/DR [2-3]. DS-CDMA does not support high transmission bit-rates, making it less suitable for multimedia applications requiring relatively high transfer rate [3]. This problem may be ameliorated via multiple code transmissions per user or multirate CDMA operation at the cost of complexity [3]. For example, DS-CDMA may support low bit-rate VBR video (video conferencing), but not high bit rate VBR video (video-on-demand). On the other hand, TDMA/DR support

high burst transmission bit-rate and can actually be configured to operate with adaptively selected higher efficiency modulation modes to certain classes of applications [3], for example, high VBR video application.

In [55], a leaky bucket with a data buffer is studied under the assumption of Poisson arrivals. The tradeoff between the smoothness of the departure process and the waiting times is studied. Results consider both finite and infinite data buffer sizes. A leaky bucket with finite data buffer is analysed assuming a Markovian Arrival Process in [56]. In [57], Elwalid et al. analyse a generalized leaky bucket with a fluid model. Butto et al. consider the effectiveness of the leaky bucket by an exact analysis for an on-off traffic and also by a fluid flow model [58]. In [59], Bala et al. consider a leaky bucket with a spacer. This leaky bucket is analysed with a Poisson arrival process. Wu et al. present and study a discrete-time analysis of a leaky bucket with the arrivals being a Poisson process or Markov Modulated Poisson Process (MMPP) [60]. In [61], Sohraby et al. analyse a leaky bucket with data buffer under the assumption of a discrete-time Markovian Arrival Process. As a special case, the detail analysis of the binary Markov source throttled by the leaky bucket is presented.

A virtual connection tree concept has been proposed to avoid the need to involve the network call processor for every cell handoff attempt in cellular ATM networks [47]. The model for connection admission control to the virtual connection tree is for a homogeneous system.

The application of equivalent capacity to connection admission control in high speed network is proposed and discussed in [27,48].

1.3 Motivation

The objective of this research is to develop a better understanding of the performance expected from a wireless ATM access system by concurrently designing and modeling a wireless ATM access system. This work is concerned with the convergence of new technologies to realize a global communication system that will provide true portability and support for personal, integrated broadband services currently envisioned for wired ATM systems only. The proposed work will study issues related to the provision of user-transparent QoS across a wireless ATM access technology interworked with a wired backbone ATM network.

The proposed work is to design and study new access protocols for wireless ATM network to allow seamless integration between the wireless domain and the wired ATM networks for various types of traffic with different quality of service. As standards for ATM networking become more established and deployment of ATM networks become more widespread, the interconnection of wireless (radio) networks to wired ATM networks will be a natural development in the near future. With a good understanding and insights for the various issues concerning wireless ATM networks, the knowledge of these wireless ATM networks is of commercial value as a wide variety of new wireless broadband services can then be provided with such networks. Thus, only wireless ATM networks are needed to transmit heterogeneous traffic instead of having separate wireless networks each for transmitting voice, video or data only.

We expect future applications in the wireless ATM network to have high bit-rate traffic like high bit-rate VBR video. From Section 1.2, we know TDMA with dynamic

reservation (TDMA/DR) is able to support such a high bit-rate. Therefore, we are pursuing our research along the direction using the TDMA/DR protocol.

1.4 Overview of Thesis

This thesis describes and studies a cellular wireless ATM access network. In this introductory chapter, a review of the research literature relevant to the design issues of wireless ATM networks is presented. We consider the salient features of CDMA and TDMA/DR MAC protocols and choose the TDMA/DR protocol as the MAC protocol in our work.

In Chapter 2, we first present the research objectives of this thesis. The proposed integration of our wireless ATM access network to a wired ATM network is described. We also describe and discuss our transmission frame and our MAC protocol. The enhanced MAC protocol is designed to take into consideration the traffic characteristics of different service classes to provide bandwidth efficiency, good QoS for real-time traffic, and reasonable QoS for non-time-critical traffic. In the second part of this chapter, we propose to study a usage parameter control based on the leaky bucket in a cellular wireless ATM access network. We also propose a connection admission control to a virtual connection tree based on equivalent capacity for heterogeneous traffic in the latter part of this chapter.

In Chapter 3, a MAC simulation model for the cellular wireless ATM access network is developed and described in terms of some basic process models. In Section 3.3, some simulation results are presented. In the latter part of Chapter 3, approximate analyses of delay-sensitive traffic for voice and MMPP video under light load are presented. The mean packet queuing delay and the distribution for voice and MMPP

video traffic are derived. In Section 3.5, some numerical results which show that the approximate analytical results are quite close to the simulation results are presented.

In the first part of Chapter 4, simulation models for usage parameter control based on the leaky bucket are described. Some simulation results are presented Section 4.3. In the latter part of Chapter 4, an approximate analysis of the leaky bucket for voice traffic and a loose lower bound for the cell loss probability of the leaky bucket for MMPP video traffic are presented. In Section 4.5, numerical results and simulation results are presented.

In Chapter 5, simulation results are presented for the performance of MAC and UPC for MPEG video traffic.

In the first part of Chapter 6, a performance analysis for connection admission control to the virtual connection tree based on equivalent capacity for heterogeneous traffic in the cellular wireless ATM access network is developed. In the latter part of Chapter 6, numerical and simulation results are presented.

Finally, the research work in this thesis is concluded in Chapter 7.

Chapter 2

Wireless ATM Network Design

2.1 Introduction

In this chapter, the research objectives of this thesis are first presented. The integration of our wireless ATM access network to the wired ATM network, together with the transmission format and Medium Access Control (MAC) protocol, is then described. It is assumed that the radio transmission employs a Time-Division Multiple Access (TDMA) scheme for multiple access. The uplink MAC protocol is reservation-based, with delay-sensitive traffic being given a higher access priority. The resultant protocol is referred to as TDMA with dynamic reservation (TDMA/DR). In the latter part of this chapter, we propose to study a Usage Parameter Control (UPC) based on the leaky bucket in a cellular wireless ATM access network. The output processes of the heterogeneous traffic from the uplink MAC protocol are fed to the leaky buckets at the base station for each of the connections. Each leaky bucket will police its traffic through its token generation rate which is set at the connection's equivalent capacity. This equivalent capacity is determined during its CAC setup. We also propose a Connection Admission Control (CAC) to a Virtual Connection Tree (VCT) based on equivalent capacity for heterogeneous traffic in the second part of this chapter. The equivalent capacities for the heterogeneous traffic are assumed to be between the mean rate and the peak rate for each of the heterogeneous traffic transmitted by the uplink MAC protocol. Section 2.6 describes our CAC model to the VCT with overload probability in a base station as a performance measure. The size of a VCT, i.e., the number of base stations

contained in a VCT, is a key parameter that impacts the amount of standby capacity required and the frequency of handoff to adjacent VCTs. The standby capacity requirement and frequency of handoff to adjacent VCTs will be assessed with respect to the number of base stations in a VCT in Chapter 6.

The major design objectives of this research are to investigate and study a new enhanced MAC protocol, CAC and UPC which allow seamless integration of a cellular wireless ATM network to wireline ATM networks such that new broadband services can be provided.

The major goals are:

- To develop a better understanding of the performance expected from a wireless ATM access system by designing and modelling a cellular wireless ATM access network.
- To consider the implications of the access performance on how QoS can be delivered across a hybrid wireless/wireline ATM network.
- To propose a new enhanced wireless MAC protocol which can provide the required QoS for heterogeneous traffic.
- To propose UPCs which can provide the required QoS for heterogeneous traffic across a hybrid wireless/wireline ATM network.
- To propose new CACs to the Virtual Connection Tree (VCT) for heterogeneous traffic.
- To study the performance of these MAC protocol, UPCs and CACs by computer simulations and by mathematical analyses.

2.2 Integration of Wireless ATM Access Network to Wireline ATM network

For the design of a cellular wireless ATM access network, the following points have to be considered:

- Flexible allocation of bandwidth for heterogeneous traffic as is in the case of a wireline ATM network and not simply catering for one type of service class.
- Should satisfy the QoS of different service classes.
- Should have centralized control to allocate bandwidth to satisfy the different QoS.
- Should have minimal protocol conversion processing from the wireless domain to the wireline domain and vice versa.
- Should have seamless integration from the wireless domain to the wireline domain and vice versa.
- Must have in sequence delivery of ATM packets.

The general concept of integrating the cellular wireless ATM network to the wired ATM network with a minimal of protocol conversion is shown in Fig. 2.1 (similar to [1-4]). In this setup, minimal protocol conversion processing is required at the base station which simply strips off the wireless protocol header and trailer from, and inserts the wired ATM header to a packet moving from the wireless segment to the wired network, and performs the reverse for a packet moving in the reverse direction. The uplink MAC protocol handles the allocation of the information slots (wireless bandwidth) to the portable terminals in the wireless segment according to requests for these terminals. The base station also performs CAC and UPC functions.

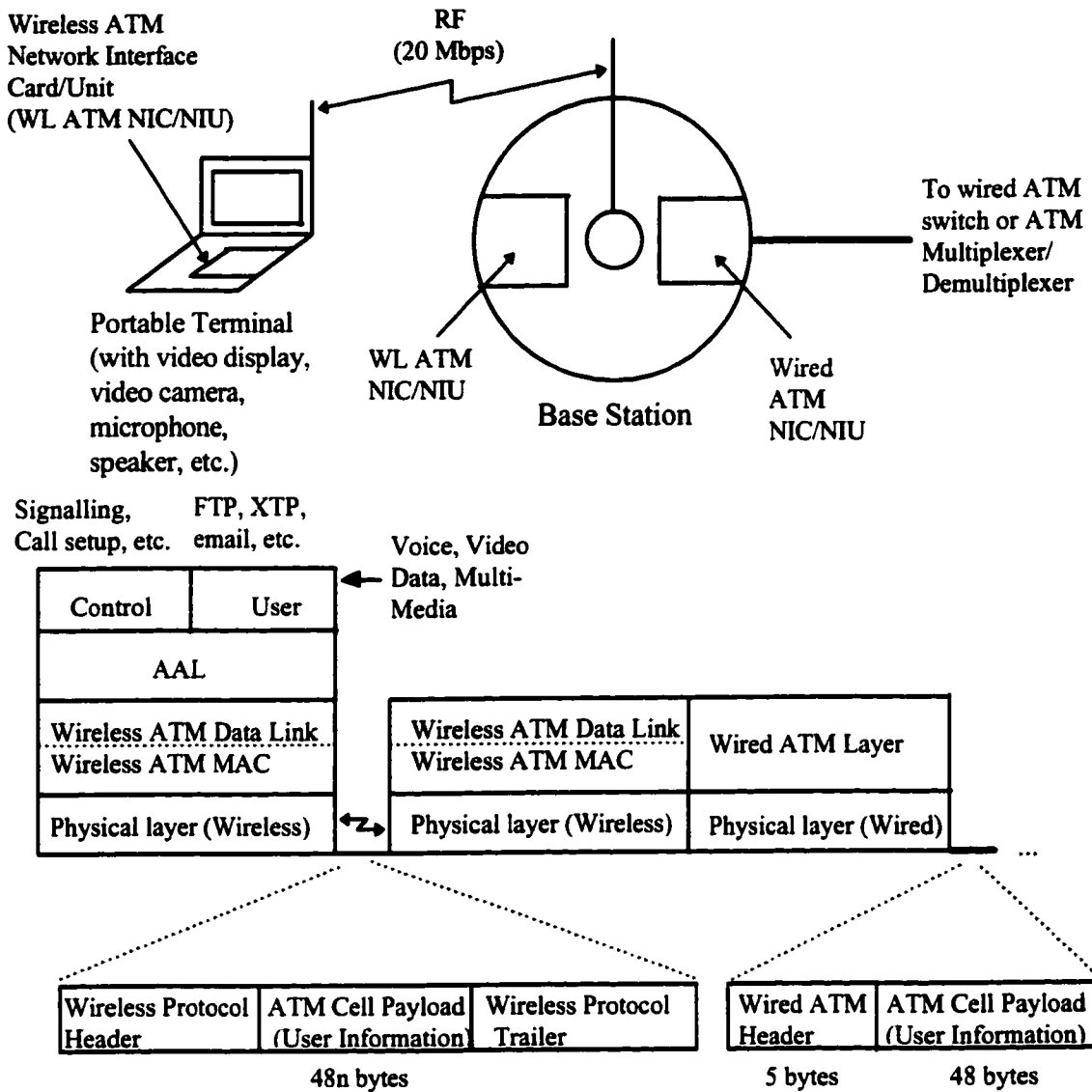
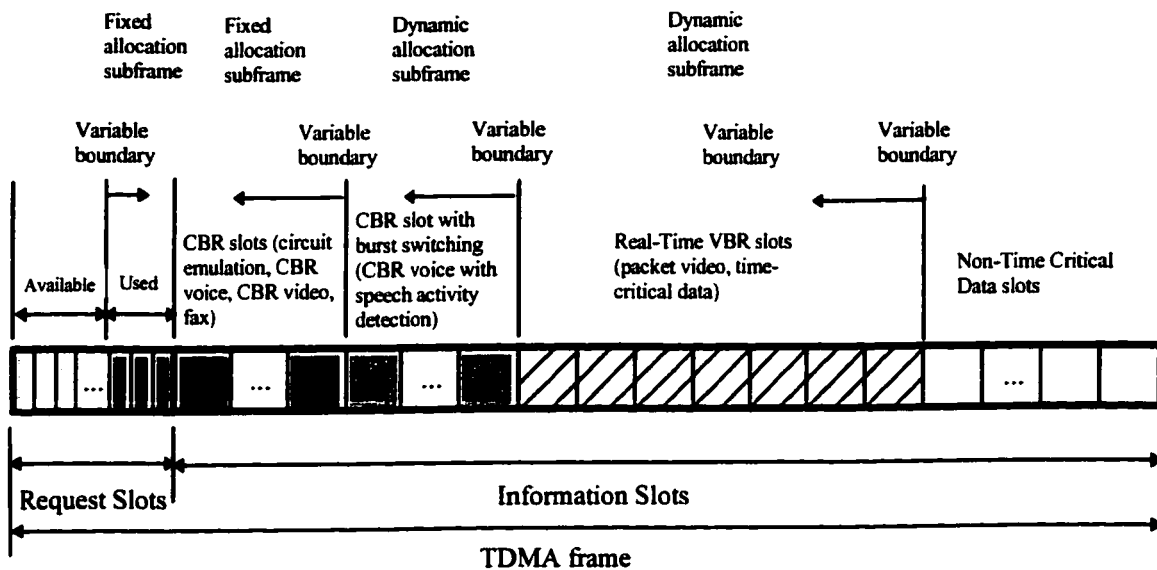


Fig. 2.1. General concept of integrating the cellular wireless ATM network to the wired ATM network

2.3 Transmission Frames

Information interchange between the base station and portable terminals in a wireless segment is via 2 frequency bands, a downlink for transmissions from the base station to the terminals, and an uplink in the reverse direction. The multiple access problem is confined to the uplink, where the TDMA frame format is as shown in Fig. 2.2.









-  Request packet in used request slot for real-time VBR traffic
-  Request packet in available request slot
-  CBR packet
-  CBR packet with burst switching
-  Real-Time VBR packet
-  Non-Time-Critical Data packet

Fig. 2.2. Uplink TDMA/DR frame format

The frame comprises *request slots* and *information slots*, and is synchronised to the voice packetisation time such that each active voice user will have exactly 1 packet for transmission in each frame. *Request slots* are classified as *available* or *used* in that *available* request slots are employed for initial access in slotted ALOHA (contention) mode for all traffic types from the portable terminals while *used* request slots are reserved for use by real-time VBR traffic types (like real-time VBR packet video, time-critical data or any real-time traffic that needs a request slot every TDMA frame) after having successfully gained access previously (via an *available* request slot). Note that the purpose of providing the *used* request slots is to exempt the real-time VBR traffic from

where τ_p is the propagation delay related to distance, $\Delta\tau_p$ is the delay spread at the receiver, $\Delta\tau_g$ is the error tolerance in guard time due to the instability of the clock and it is usually negligible, and τ_d is the die-out time of the tail of the pulsed signal which depends on the amplitude and phase response of the filters.

$$\tau_p = \frac{D}{C}, \quad (2.2)$$

where D is the maximum propagation distance in the cell and C is the speed of propagation in radio domain. The mean delay spread, $\Delta\tau_p$, for various types of environment is shown in Table 2.1 [24].

Table 2.1. Mean delay spread for various type of environment

S/No.	Type of Environment	Delay Spread, $\Delta\tau_p$	Delay Spread, $\Delta\tau_p$ for 20 Mbps
1	In-building	<0.1 μs	<2 bits
2	Open area	<0.2 μs	<4 bits
3	Suburban area	0.5 μs	10 bits
4	Urban area	3 μs	60 bits

From [24], the bit rate, R_b , is given by

$$R_b \leq \frac{1}{\tau_b}, \quad (2.3)$$

where τ_b is the time between bits and it is given by

$$\begin{aligned} \tau_b &= \Delta\tau_p + \tau_d + \Delta\tau_g \\ &\approx \Delta\tau_p + \tau_d \end{aligned} \quad (2.4)$$

If we consider a bit rate, R_b , of 20 Mbps, then from (2.3), $\tau_b \leq 50 \text{ ns}$, that is,

$(\Delta\tau_p + \tau_d) \leq 50 \text{ ns} \equiv 1 \text{ bit}$, $\Rightarrow \Delta\tau_p < 50 \text{ ns}$ and $\tau_d < 50 \text{ ns}$. If we consider the

maximum propagation distance, $D = 100 \text{ m}$, then $\tau_p = \frac{100}{3 \times 10^8} = 0.33 \mu\text{s} \equiv 6.67 \text{ bits}$. So the

guard time, $\tau_g = 6.67 + 1 \approx 8 \text{ bits} = 1 \text{ byte}$.

2.3.1.2 Service Type Field

The service type field is used to indicate the service type, for example, control/supervisory, voice, CBR traffic, CBR traffic with burst switching, real-time VBR/time-critical data traffic, non-time-critical data traffic, etc. This field simplifies processing of protocol conversion and bandwidth allocation at the base station by freeing the base station from the need to keep track of all information. For real-time VBR services, this field is also used to indicate the end of transmission. This is done by encoding the field to four 1's in the *used* request slot that has been assigned to the real-time VBR service. Note that this is possible because the service type of such a real-time VBR service is known to the base station through its assigned *used* request slot.

2.3.1.3 QoS parameter Field

The QoS parameter field contains the information that allows the bandwidth allocator at the base station to decide who should have access priority to the information slots in the next TDMA frame. The information in this field may include a packet's time of expiration, a packet's age (time spent in its local queue at the portable terminal), the length of a message queue, the number of slots required in the next TDMA frame by a real-time VBR service, and the status of the local queue at a portable terminal (i.e., whether it exceeds a given threshold). This information can be used for scheduling.

2.3.1.4 Cyclic Redundant Check Field

The 2-byte Cyclic Redundant Check (CRC) is used for bit error detection. In the present design, error correction can be carried out either by means of go-back-n automatic repeat request (ARQ) or Forward Error Correction (FEC) coding. The use of FEC however, incurs additional bandwidth wastage since part of the information payload will be used to transmit the redundant bits needed to correct errors. Nevertheless, the long

delays normally associated with go-back-n ARQ may make it necessary for some traffic types to sacrifice bandwidth efficiency and utilise FEC for error correction.

2.3.1.5 Packet Sequence Number Field

The Packet Sequence Number is used to detect lost packets. In this case, recovery, if necessary, will also utilise the go-back-n ARQ. In addition, this field is used by a voice user to indicate the end of its talkspurt to the base station. In this case, the field is encoded with a bit pattern of all 1's. Note that this end-of-talkspurt indication allows the base station to immediately reallocate the information slot used by this user to another user in the next frame.

2.3.1.6 Handoff Indicator Field

This 2-bit field is reserved for further development.

2.3.1.7 ATM Fields

The ATM fields have the similar functions to those in the wired ATM Cell field. The wireless ATM VCI is determined at call setup and it is mapped to the wired ATM VPI/VCI. It is assumed that the mapping is done during the connection setup by the control plane with the translation table updated at the base station interface. Note that there are no Generic Flow Control (GFC) and Header Error Control (HEC) fields in the wireless ATM packet. The GFC field is only significant at the User Network Interface (UNI) where it is used to control access from a number of terminals [5]. This function is already provided in the wireless segment by the bandwidth allocator in the base station. The HEC field is also not necessary since the error detection and correction provided within the wireless segment will generally be more powerful. In addition, the cell delineation function of the HEC field in the wired ATM network is also taken care of in

the wireless segment by the TDMA frame structure. Another reason why HEC should not be included is that the error probability in the wireless domain is much higher than that in the wired domain, causing header corruption leading to misrouted or lost packets. Thus, it is better to have the HEC computed in the base station for protocol conversion for *outbound inter-domain* traffic.

2.3.1.8 Uplink TDMA Frame Size

Assuming that the payload in the wireless ATM packet is 48 bytes ($n=1$), then the total uplink information slot size is 23.2 μ s, which is long enough to transmit one packet of 58 bytes ($2 \times 1 + 2 + 2 + 2 + 48 + 2$) or 464 bits. The total uplink request slot size is 12 or 14 bytes ($2 \times 1 + 2 + 2 + 4 + 2$ or $2 \times 1 + 2 + 2 + 6 + 2$), that is, 96 or 112 bits which are equivalent 4.8 μ s and 5.6 μ s, respectively. Note that one information slot is equivalent to 4.833 or 4.1428 request slots. Assuming that voice traffic of 32 Kbps and it is packetized using AAL type 1 with 47 bytes of payload, one voice packet needs 11.75 ms to be packetized. Thus, the TDMA frame size, T_{TDMA} is also 11.75 ms ($\frac{47 \times 8}{32 \times 10^3}$). Table 2.2 shows the TDMA frame size and the number of information slots for various voice bit rate. The lower the bit rate for voice makes the situation worse. Thus, echo cancellation is required.

Table 2.2. TDMA frame size for various voice bit rate

S/No.	Voice Bit Rate (Kbps)	TDMA frame (ms)	Equivalent no. of information slots in each TDMA frame
1	64	5.875	253
2	32	11.75	506
3	16	23.5	1012
4	8	47.0	2025

Let T_R and T_I be the slot size of one request slot and one information slot, respectively. Let N_R be the number of request slots in a TDMA frame. Then, the number

of information slots in a TDMA frame, $N_I = \lceil (T_{TDMA} - N_R T_R) / T_I \rceil$, where $\lceil x \rceil$ is the smallest integer greater than or equal to x . The overhead ratio is simply $(N_R T_R) / T_{TDMA}$.

Table 2.3. Overhead ratio due to the number of request slots in a TDMA frame of size 11.75 ms with request slot size of (a) 4.8 μ s and (b) 5.6 μ s

S/No.	No. of request slots	No. of information slots	Overhead ratio (%)
1	50	496	2.043
2	100	485	4.085
3	150	475	6.128
4	200	465	8.170

(a)

S/No.	No. of request slots	No. of information slots	Overhead ratio (%)
1	50	494	2.383
2	100	482	4.766
3	150	470	7.149
4	200	458	9.532

(b)

Table 2.3 shows the tradeoff between the number of request slots and the number of information slots, and the overhead ratio due the number of request slots in a TDMA frame of size 11.75 ms.

2.3.2 Downlink Slots

The downlink request slot format is shown in Fig. 2.5, while the downlink information slot format is shown in Fig. 2.6.

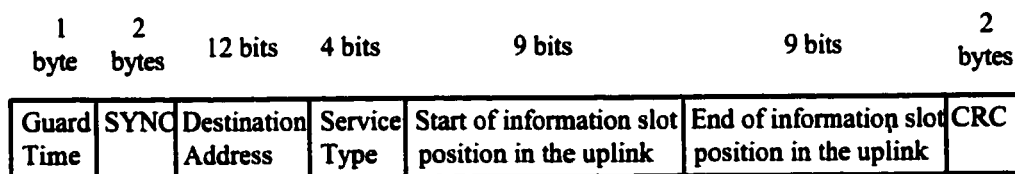


Fig. 2.5. Downlink control slot format

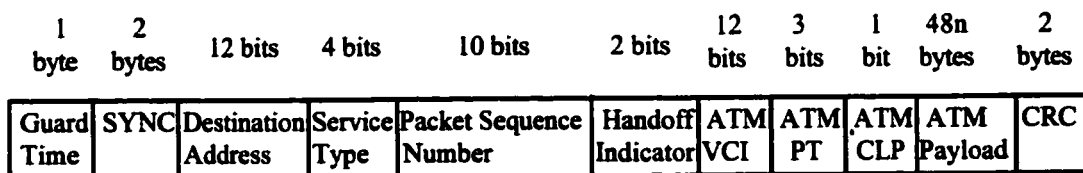


Fig. 2.6. Downlink information slot format

2.3.2.1 Destination Address

This field identifies the portable terminal for which a downlink packet is destined.

A broadcast address is defined with a bit pattern of all 1's.

2.3.2.2 Service Type Field

The service type field is used to indicate the service type. As with the case of the uplink, inclusion of this field simplifies protocol processing at the portable terminals. The control/supervisory packets in the downlink perform the following functions:

- broadcast the highest numbered *available* request slot in the next frame,
- broadcast the numbers of all collided requests and information slots in the last frame,
- inform portable terminals of their success or failure in gaining access to either request or information slots
- inform active voice users of changes in their allocation of information slots (this is due to a packing algorithm [11] which groups all voice information slots together and which is invoked whenever a talkspurt ends)
- carry out other signalling functions.

2.3.2.3 Start of Information Slot Position in the Uplink Field

Depending on the type of control packets, this field is used to indicate to a traffic type the starting position of its allocated information slot(s) in the next uplink frame, collided request slots in the last frame, collided information slots in the last frame, or the highest numbered *available* request slot in the next frame.

2.3.2.4 End of Information Slot Position in the Uplink Field

Similarly, this field is used to indicate to a traffic type the ending position of its allocated information slot(s) in the next uplink frame, collided request slots in the last

frame, collided information slots in the last frame, or the highest numbered *available* request slot. The information in this frame field may be the same as that in the start of information slot position. For examples, voice packets, data or video packets requiring only one information slot, highest position of the available request slot, etc.

2.3.3 Slot Timing for Uplink and Downlink

Fig. 2.7 shows the slot timing for the uplink and the downlink. The Frame SYNC is used to provide synchronization information at the beginning of each frame to the mobile users in the cell of each base station.

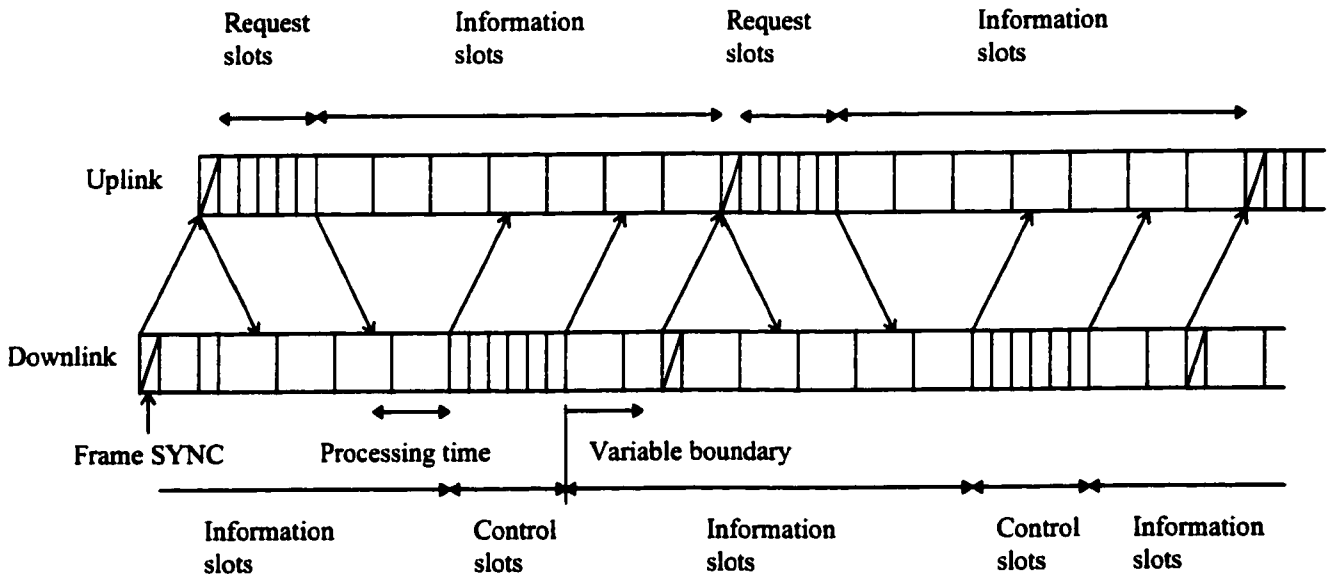


Fig. 2.7. Slot timing for the uplink and the downlink

2.4 Medium Access Control Protocol

The TDMA/DR MAC protocol designed here (and in [12]) is similar to that described in [1-4] except for the following enhancements:

- The MAC protocol allocates uplink information slots to CBR voice users dynamically on a burst switching basis. Thus, silent voice users are not allocated uplink information slots, and must contend for access at the start of each talkspurt. This allows statistical

multiplexing of active voice users. Thus, the bandwidth is more efficiently allocated and more voice users can be accommodated.

- The request slots are classified into *available* and *used* request slots, and the *available* request slots are used for all traffic types to contend for access to the uplink initially using the slotted Aloha protocol. The *used* request slots are dynamically allocated to real-time VBR traffic that have successfully gained access to the uplink through the use of an *available* request slot previously. The *used* request slots relieve the real-time VBR traffic of the need to contend for request slots at every frame. The rationale is that such traffic types, e.g., VBR video, will have data to transmit over many TDMA frames. This gives better performance with less delay for real-time VBR traffic. An exception here is an active voice user. Since each active voice user will have only 1 packet to transmit per TDMA frame, *used* request slots are not assigned to voice traffic.
- Receiver capture is exploited to provide voice users higher priority access to request slots by allowing them to transmit their request packets at a higher power level than non time-critical data users. The reason for this is that voice traffic is real-time, while non time-critical data traffic can be delayed. (Note that because request packets of real-time VBR traffic are generally transmitted through *used* request slots, and if such traffic are represented by VBR video of which there will not be many owing to the relatively low aggregate bit rate of a wireless segment, contention for the *available* request slots will typically be between the numerous voice and non time-critical data users.)

- A packing algorithm which packs up gaps in information slots caused by the ending of voice talkspurts and the algorithm drops voice packets in a 'round robin' manner during temporary video overload is developed [11]. This helps to spread voice clippings during this period to as many voice users as possible and bandwidth is used more efficiently by taking advantage of the silent periods of voice traffic.

How the MAC protocol handles 4 representative traffic types is now considered in greater detail.

Class 0 - CBR traffic: A class 0 user contends for initial access using the slotted ALOHA protocol in an *available* request slot. If it is unsuccessful, it tries again in the next frame. If it is successful, it is assigned a fixed number of information slots for the whole duration of its connection. The last packet of the connection will inform the base station that it is the last packet through the packet sequence number in the information slot using a pattern of ten 1's (see Section 2.3).

Class 1 - Real-time VBR and time-critical data traffic: A class 1 user also contends for initial access using the slotted ALOHA protocol in an *available* request slot. If it is unsuccessful, it tries again in the next frame. However, if it is successful, it will be assigned a *used* request slot in all subsequent frames for the whole duration of its connection. The class 1 user transmits its request for the number of information slots it needs in the next frame in its assigned *used* request slot in the current frame. At the end of the transmission, the portable terminal will inform the base station that the packet in the next TDMA frame is the last packet in the transmission through the 'service type' field (by setting to four 1's, see Section 2.3.1) in the *used* request slot. The 'service type' in the request slot for real-time VBR traffic is only significant for its first successful request slot

as the base station will know that the subsequent packets are for real-time VBR traffic due to the location of the assigned *used* request slots.

Class 2 - CBR voice with burst switching: A class 2 user contends for access in an *available* request slot using the slotted Aloha protocol at the start of each talkspurt. If it is unsuccessful, it tries again in the next frame. Because of real-time constraints of voice traffic, class 2 packets that are not transmitted after a given delay (two request slot contentions) are discarded, giving rise to speech clipping. However, if the class 2 user is successful, it is assigned a single information slot in each frame (and hence, need not contend for a request slot anymore) for the whole duration of the talkspurt. The assigned information slot may vary from frame to frame as other class 2 users end their talkspurts and are not assigned any more information slots (this is due to a packing algorithm which we describe in [11]). The last packet in the talkspurt will inform the base station that it is the last packet through the packet sequence number in the information slot using a pattern of ten 1's (see Section 2.3).

Class 3 - Non time-critical data: A class 3 user contends for access using the slotted Aloha protocol in an *available* request slot for each message in its buffer. If the request is unsuccessful, the user backs off for a random number of frames before trying again. Otherwise, the user is assigned a number of information slots in which to transmit the message. Note that the number of information slots assigned may be insufficient to transmit the entire message of the user. In this case, the user will need to contend for access anew after a random number of frames later to transmit the remaining portion of its message.

2.4.1 Bandwidth Allocation

To ensure reasonably good QoS is provided to every class of service, it is imperative that an efficient bandwidth allocation scheme is implemented at the base station. Nevertheless, because of the possibility of temporary overloads, it is necessary to have some form of priority structure among the different classes of services that will be supported. In this respect, we assume that service class j will always have priority over class k , when $j < k$, and $j, k = \{0, 1, 2, 3\}$. Within the individual classes, other priority schemes can be used to decide which user is given bandwidth and which is not during temporary overloads. Some examples of these priority schemes include random select, earliest due time, etc.

2.5 Usage Parameter Control

The aim of a policing function is to detect a nonconforming source as quickly as possible and to minimize the potentially negative effect of the excess traffic generated by such sources to the conforming ones. UPC in wireless/wireline ATM networks have not been proposed nor studied in the literature until recently. In [86], the effects of user mobility on the Generic Cell Rate Algorithm (GCRA) as the UPC is studied. No uplink MAC protocol is specified in [86]. A transit time is assumed in the wireless domain.

Our model of the UPC in a wireless/wireline ATM access network is shown in Fig.

2.8.

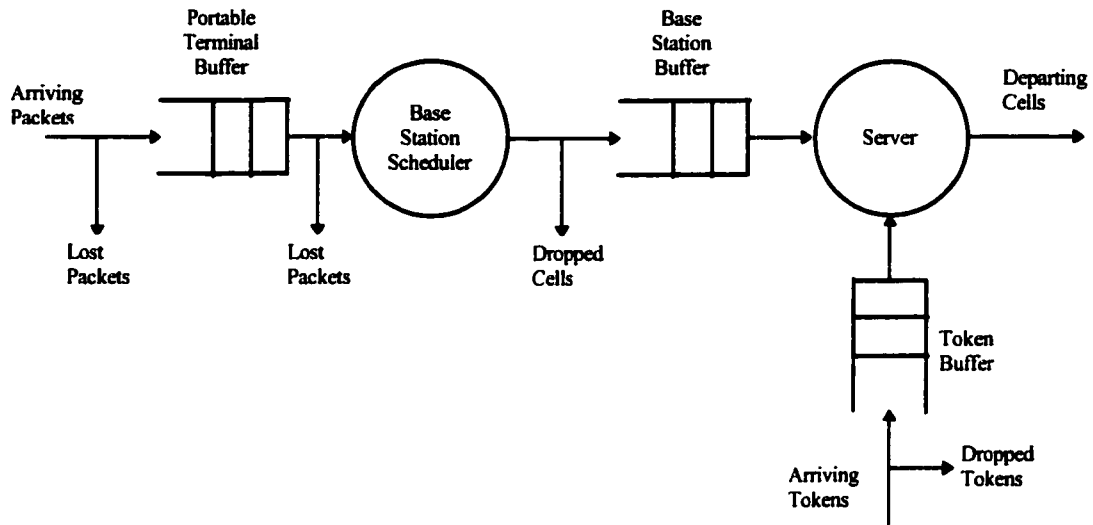


Fig. 2.8 Model of an arrival process to a portable terminal passing through the base station scheduler and a leaky bucket at the base station

A leaky bucket as the UPC is used at the base station to perform rate based control. There is a new problem here where the traffic characteristics are changed after passing through the wireless domain before entering the leaky bucket in the base station. The arrival process at the portable terminal buffer can be voice, video, data or multimedia traffic. Considering a particular connection, the arriving packets to the portable terminal buffer are transmitted to the base station buffer by the base station scheduler (uplink MAC). Packets at the portable terminal buffer can be lost due to 'late packet' for voice traffic. Packets can also be lost due to insufficient information slots in the uplink MAC protocol for voice traffic. Departed packets from the base station scheduler or uplink MAC protocol then become the arriving cells to the leaky bucket at the base station. The base station buffer is finite and cells arriving at a time when the buffer is full are discarded.

The main idea of the leaky bucket is that a cell, before entering the ATM multiplexer or network, must obtain a token from the token buffer. An arriving cell will

get one token and leave the leaky bucket if there is at least one token in the token buffer. Tokens arrive to the token buffer at a constant rate. The token generation rate is set at the equivalent capacity of a connection during CAC to the Virtual Connection Tree (VCT). With a finite token buffer, tokens arriving at a time when the token buffer is full are discarded. The size of the token buffer determines the number of cells that can be transmitted consecutively, controlling the burst length. The maximum number of cells that can leave the leaky bucket can be greater than the token buffer size since, while cells arrive and obtain tokens from the token buffer, new tokens arrive at a constant rate to the token buffer.

2.6 Connection Admission Control

The capacity of wireless ATM networks is related to cell size of a base station. Smaller cells tend to provide higher capacity. However, small sized cells, e.g., micro and pico cells, tend to incur more frequent handoffs due to user mobility. The network call processor for connection handoffs becomes the bottleneck. In [47], Acampora and Naghshineh propose the virtual connection tree (VCT) as a means to circumvent the need to involve the network call processor for every cell handoff attempt in cellular ATM networks. Fig. 2.9 shows a virtual connection tree that supports mobile cellular connections.

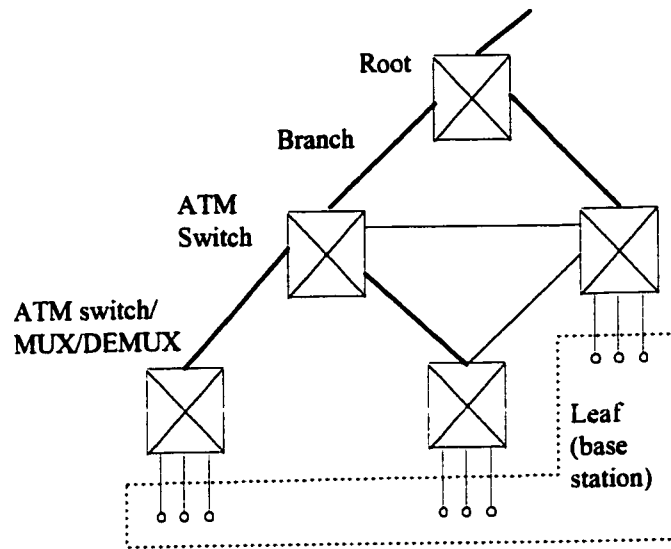


Fig. 2.9. A virtual connection tree

A VCT is a region containing B interconnected base stations. Sufficient resources are provided so that movements of mobile users from one base station to another within the VCT do not incur handoff. Specifically, at the time that a mobile connection is admitted to a VCT, a collection of virtual circuit numbers (VCNs) are assigned to the call. These VCNs enable the mobile to hand off between base stations in a geographical region covered by the VCT without involving the network call processor. The network call processor is only involved for handoffs between base stations belonging to different regions. In [47], the performance of the VCT has been evaluated by exploiting the statistical nature of the mobile environments such that overload is possible but unlikely. A homogeneous CAC (connection admission control) model for the VCT is considered in [47]. With wireless ATM perceived for supporting multimedia services, it is necessary to consider heterogeneous traffic models. In this thesis, we propose two CAC approaches for connection admission to the VCT based on equivalent capacity for heterogeneous traffic. The concept of equivalent capacity has been used for CAC for individual connections

between source and destination pairs [27,48,73-78]. The same metric of equivalent capacity can be used for resource allocation in the CAC problem under consideration.

Fig. 2.10 shows the CAC model to a VCT. When a mobile requests for a new connection, the network call processor will compute the equivalent capacity of the new request. If the sum of the equivalent capacities of the existing connections in the VCT and the equivalent capacity of the new requesting mobile to the VCT exceeds the maximum equivalent capacity of the VCT, then the new request is rejected. Otherwise, the new request is accepted. The network call processor will set up one connection for each base station in the VCT for the newly accepted mobile and the VCNs will also be assigned to the mobile. The VCNs will enable the mobile to roam in the base stations in a geographical region covered by the VCT without involving the network call processor. The call processor will also update the sum of equivalent capacities for all existing connections including the equivalent capacity of the new connection.

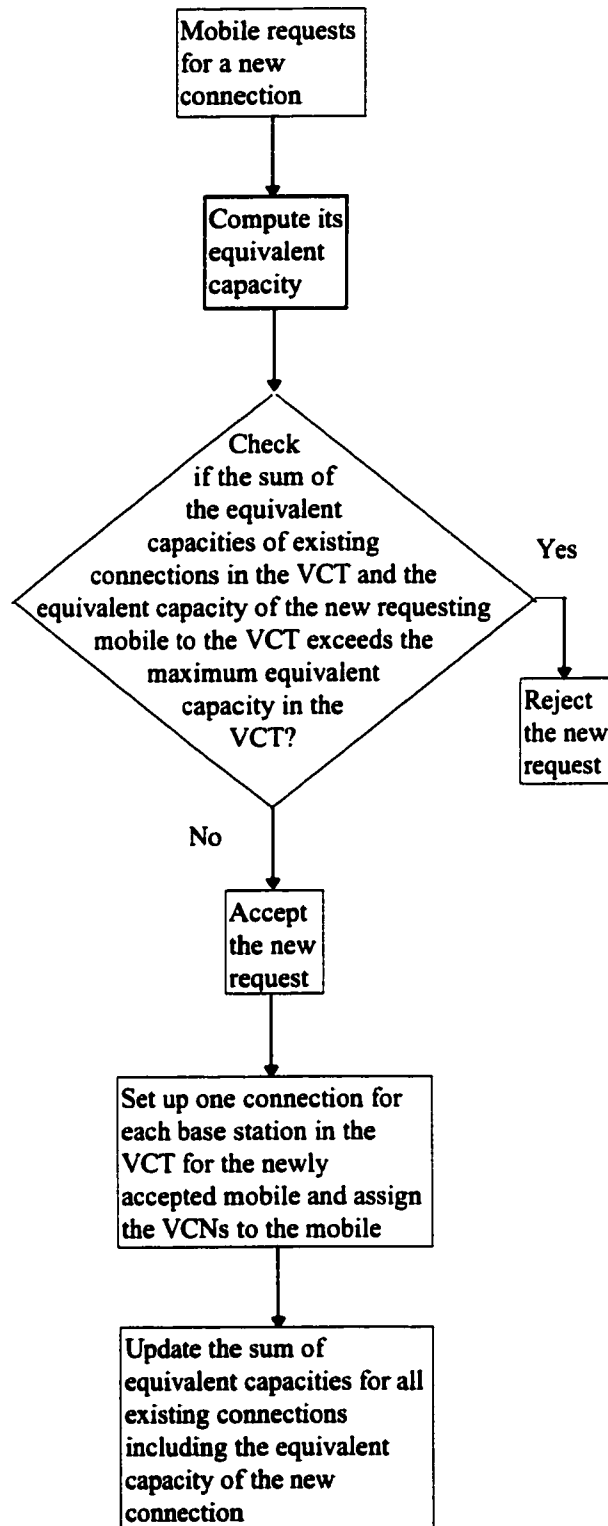


Fig. 2.10. CAC model for a virtual connection tree

Chapter 3

Medium Access Control

3.1 Introduction

Medium Access Control (MAC) protocols using TDMA/DR have been proposed and studied by computer simulation in [1-4]. In Section 2.4, we have proposed an enhanced TDMA/DR MAC protocol. In this Chapter, we will study and analyse the performance of this protocol by computer simulation and approximate analysis.

The first part of this chapter studies the performance of a cellular wireless ATM network using computer simulation. The uplink MAC protocol, used in this network which allows transmissions for heterogeneous traffic, is described in Chapter 2. In this simulation study, front end voice clipping and voice clippings within a voice talkspurt are considered. Some simulation results for the uplink MAC protocol are discussed. In the simulation model, only voice losses are considered but not video and data losses. All video and data packets are buffered. The simulation model is described in Section 3.2 while the simulation results are shown Section 3.3.

In the latter part of this chapter, an approximate analysis of delay-sensitive traffic of voice and MMPP video traffic is provided for the MAC protocol described in Chapter 2. The mean delays and the distributions of the voice and MMPP video traffic are obtained under light load in Section 3.4. To the best of our knowledge, there is no delay analysis of delay-sensitive traffic of voice and video in a cellular wireless ATM access network with heterogeneous traffic reported in the literature. Here, we present an approximate analysis

of the delay-sensitive traffic of voice and MMPP video under light loads as we believe most networks will operate in. The numerical results are shown in Section 3.5.

3.2 Simulation Model

3.2.1 Simulation Model Processes

Fig. 3.1 shows the simulation model for the proposed cellular wireless ATM uplink MAC protocol. There are four major components in the simulation model: (1) arrival processes of voice, video and data traffic, (2) request contentions in the request slot subframe, (3) allocation of bandwidth in the information slot subframe, and (4) voice, video and data uplink transmission in the information slot subframe. The arrival processes for voice, video and data are described in Section 3.2.2, while the request contention processes are described in Section 3.2.3. Information slots allocation and information slot transmissions are described in Sections 3.2.4 and 3.2.5, respectively.

As discussed in Chapter 2, video, voice and data traffic represent the class 1, class 2 and class 3 traffic, respectively. From the media access control point of view, video service is given the highest access priority. Each video source is assigned a *used* request slot for the duration of its connection. A voice source must contend for an *available* request slot on a per talkspurt basis, i.e., once the front-end packet of a voice source acquires access rights, that information slot becomes owned by the voice source for the duration of the talkspurt unless another information slot is allocated to the voice user during the talkspurt. On the other hand, data must contend for an *available* request slot on a per message basis.

Flow diagrams for the algorithms followed by each portable terminal for video, voice and data traffic are shown in Appendix A. Appendix A also contains the flow diagrams for the algorithm followed by the base station for information slots allocation.

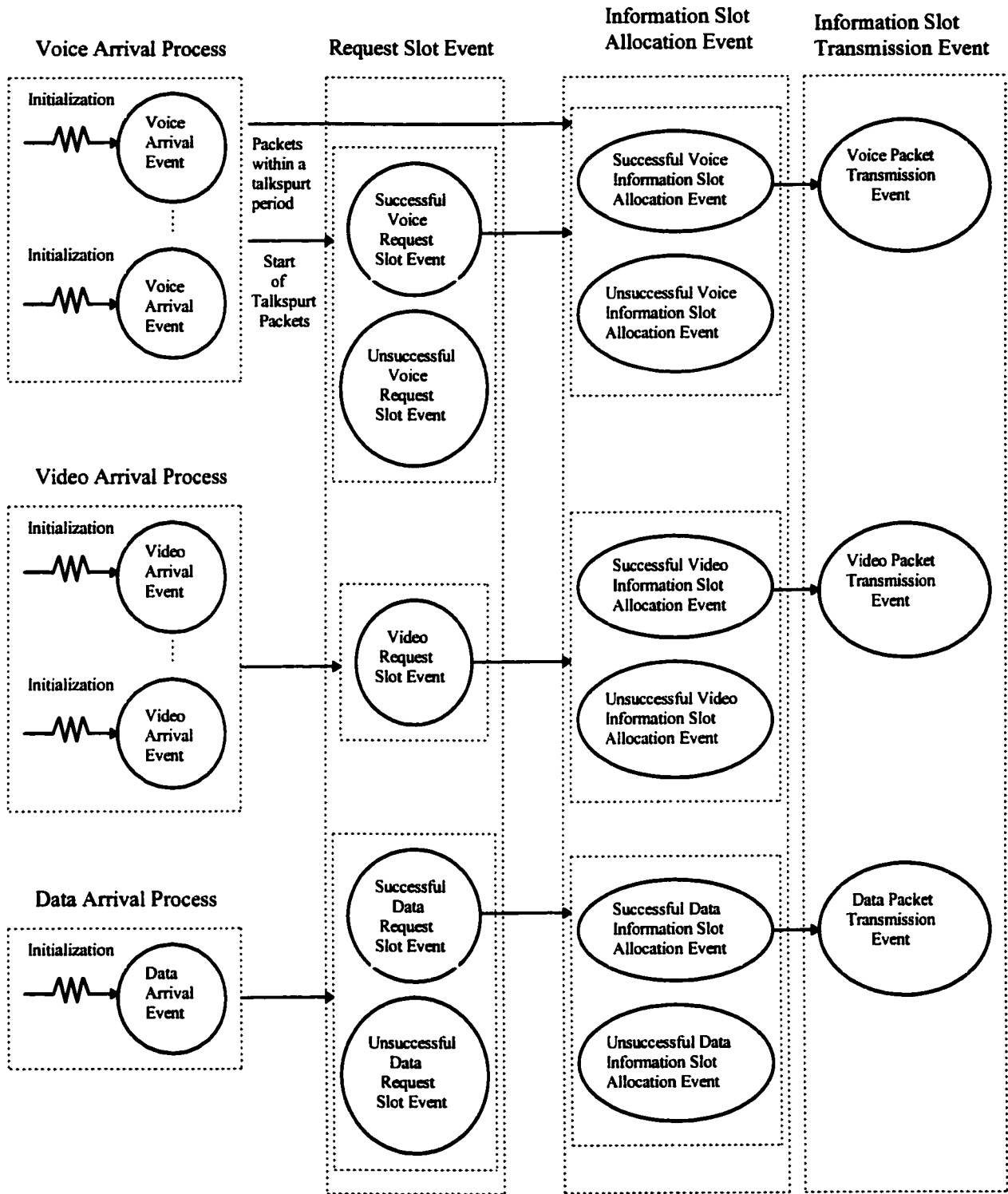


Fig. 3.1. Simulation model for the cellular wireless ATM uplink MAC protocol

3.2.2 Arrival Processes

Each of the heterogeneous traffic requires a different QoS. Table 3.1 shows the QoS requirements for voice, video and data traffic [33,34]. For data, ARQ can always be

used for retransmission if there is an error. However, for video traffic such stringent requirement of 10^{-12} BER cannot be met by the BER of 10^{-4} to 10^{-5} BER in the physical layer. So we will assume that a robust video traffic with a less stringent BER requirement of say 10^{-4} will be available for the wireless domain.

Table 3.1. Traffic types and their QoS requirements

Traffic Type	Data Rate	Bit Error Rate	Cell Loss Ratio	Maximum Delay
Voice	32/16/8 kbps	10^{-3}	5×10^{-3}	30-200 msec
	64 kbps	10^{-4}	10^{-3}	
Video	Mbps	10^{-10}	10^{-12}	100 msec
Data	kbps-Mbps	-	-	minutes

Traffic models for voice, video and data can be found in [25-28]. Models for voice and data are quite established, while models for video are still not well established.

3.2.2.1 Voice Arrival Process

A voice process is modeled as an On-Off process [29-30]. Fig. 3.2 shows the voice arrival process for a voice user. The “On” state (talkspurt period) is exponentially distributed with a mean value of \bar{t}_1 , while the “Off” state (silence period) is exponentially distributed with a mean value of \bar{t}_2 . During the talkspurt period, voice packets are generated after a packetization time of $T_{TDMA} = 11.75$ ms, where T_{TDMA} is the uplink TDMA frame time. From [29], the mean talkspurt period, $\bar{t}_1 = 0.352$ seconds, while the mean silence period, $\bar{t}_2 = 0.650$ seconds. Whereas from [30], the mean talkspurt period, $\bar{t}_1 = 1.0$ seconds, while the mean silence period, $\bar{t}_2 = 1.35$ seconds. Thus, the mean period between consecutive start of talkspurts is 1.002 seconds and 2.35 seconds for [29] and [30], respectively. Since we are considering the worst case performance for this wireless network, the former will result in higher probability for outstanding voice request collisions in the request slot subframe.

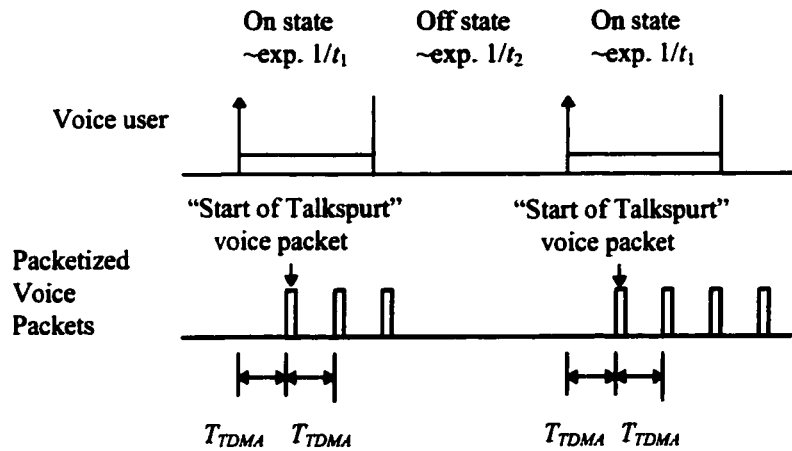


Fig. 3.2. On-Off source model for voice arrival process

Fig. 3.3 shows the packetized voice process for the case where the start of the next talkspurt period falls within the last packetization period for the last voice packet in the previous talkspurt. Thus, in this case, voice packets are packetized as though there is no silence period between the two talkspurt periods. Otherwise, considering many consecutive small silence and talkspurt periods being generated within a packetization time and a voice packet is generated at each start of talkspurt, many voice packets can be produced in a packetization time. In other words, such silence periods are disregarded (filled in).

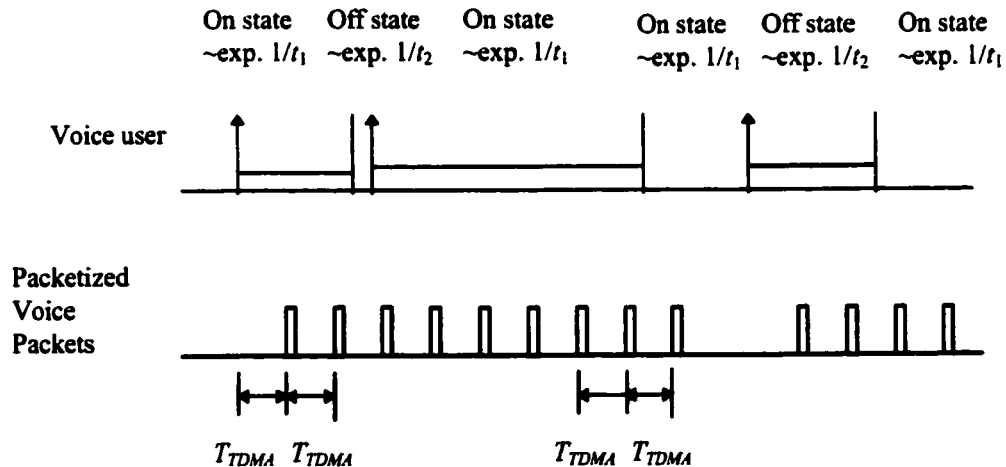


Fig. 3.3. Packetized voice process for the case where the start of the next talkspurt period falls within the last packetization period for the last voice packet in the previous talkspurt

Assuming that the number of voice users, $M_{\text{voice}} = 100$ and no voice loss, and the mean number of information slots used by voice users, \bar{N}_{voice} , is given by

$$\bar{N}_{\text{voice}} = \frac{0.352}{0.352 + 0.650} \times 100 = 35.1. \quad (3.1)$$

3.2.2.2 Video Arrival Process

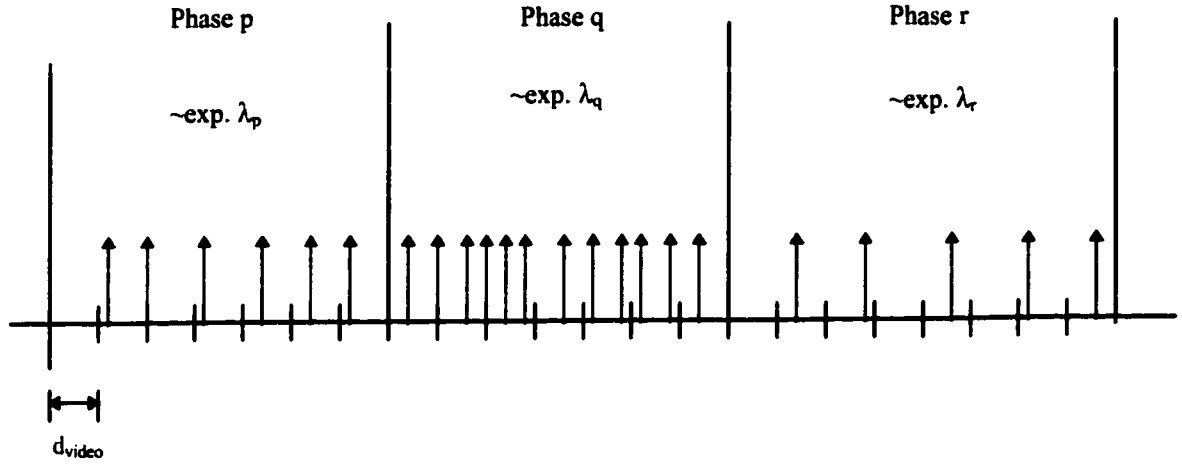


Fig. 3.4. 8-state MMPP for video arrival process

The video arrival process is modeled as a 8-state Markov-Modulated Poisson Processes (MMPP) [31-32]. The number of phases, $M = 8$, while the slot time, $d_{\text{video}} = 16.96 \mu\text{s}$. The

$M \times M$ phase transition probability matrix in a slot time, $\mathbf{H} = [h_{ij}]$, ($1 \leq i, j \leq M$), is given by

$$\mathbf{H} = \begin{bmatrix} 9.998 \cdot 10^{-1} & 9.848 \cdot 10^{-5} & 5.820 \cdot 10^{-9} & 2.675 \cdot 10^{-13} & 1.054 \cdot 10^{-17} & 3.738 \cdot 10^{-22} & 1.227 \cdot 10^{-26} & 1.929 \cdot 10^{-31} \\ 1.688 \cdot 10^{-4} & 9.997 \cdot 10^{-1} & 1.182 \cdot 10^{-4} & 8.148 \cdot 10^{-9} & 4.280 \cdot 10^{-13} & 1.897 \cdot 10^{-17} & 7.475 \cdot 10^{-22} & 1.371 \cdot 10^{-26} \\ 1.694 \cdot 10^{-8} & 2.007 \cdot 10^{-4} & 9.997 \cdot 10^{-1} & 1.379 \cdot 10^{-4} & 1.086 \cdot 10^{-8} & 6.420 \cdot 10^{-13} & 3.162 \cdot 10^{-17} & 6.959 \cdot 10^{-22} \\ 1.039 \cdot 10^{-12} & 1.847 \cdot 10^{-8} & 1.840 \cdot 10^{-4} & 9.997 \cdot 10^{-1} & 1.576 \cdot 10^{-4} & 1.397 \cdot 10^{-8} & 9.172 \cdot 10^{-13} & 2.523 \cdot 10^{-17} \\ 4.346 \cdot 10^{-17} & 1.030 \cdot 10^{-12} & 1.539 \cdot 10^{-8} & 1.673 \cdot 10^{-4} & 9.997 \cdot 10^{-1} & 1.772 \cdot 10^{-4} & 1.746 \cdot 10^{-8} & 6.403 \cdot 10^{-13} \\ 1.309 \cdot 10^{-21} & 3.877 \cdot 10^{-17} & 7.724 \cdot 10^{-13} & 1.259 \cdot 10^{-8} & 1.505 \cdot 10^{-4} & 9.997 \cdot 10^{-1} & 1.969 \cdot 10^{-4} & 1.083 \cdot 10^{-8} \\ 2.920 \cdot 10^{-26} & 1.038 \cdot 10^{-21} & 2.585 \cdot 10^{-17} & 5.618 \cdot 10^{-13} & 1.007 \cdot 10^{-8} & 1.338 \cdot 10^{-4} & 9.997 \cdot 10^{-1} & 1.100 \cdot 10^{-4} \\ 4.885 \cdot 10^{-31} & 2.026 \cdot 10^{-26} & 6.059 \cdot 10^{-22} & 1.645 \cdot 10^{-17} & 3.932 \cdot 10^{-13} & 7.835 \cdot 10^{-9} & 1.171 \cdot 10^{-4} & 9.999 \cdot 10^{-1} \end{bmatrix}. \quad (3.2)$$

Equation (3.2) is obtained from [31,32] which describe the MMPP characterization of the video model in [89]. In the simulation model, h_{ii} is calculated as $(1 - \sum_{j=1, j \neq i}^M h_{ij})$ to make the sum

of probability equal to 1.0. The video cell generation rate while in phase i is denoted by λ_i , ($1 \leq i \leq M$). The arrival rate matrix is given by

$$\lambda = \begin{bmatrix} 8.531 \times 10^{-2} \\ 1.175 \times 10^{-1} \\ 1.410 \times 10^{-1} \\ 1.645 \times 10^{-1} \\ 1.880 \times 10^{-1} \\ 2.115 \times 10^{-1} \\ 2.350 \times 10^{-1} \\ 2.700 \times 10^{-1} \end{bmatrix}, \quad (3.3)$$

The interarrival time between consecutive arrivals in phase i is assumed to be exponentially distributed with an arrival rate of λ_i , $i=1,2,\dots,M$. The number of slots in phase i , $N_{phase} = (1-p)^{k-1}p$, where $p = 1 - h_{ij}$. Thus, the length of each phase is geometrically distributed. Assuming that the number of video users, $M_{video}=3$, the mean number of information slots used by video users, \bar{N}_{video} , is given by

$$\bar{N}_{video} = \frac{4.643 \times 10^6}{48 \times 8} \times 11.75 \times 10^{-3} \times 3 = 426.2 \text{ for AAL type 5.} \quad (3.4).$$

Assuming that the number of video users, $M_{video}=2$, the mean number of information slots used by video users, \bar{N}_{video} , is given by

$$\bar{N}_{video} = \frac{4.643 \times 10^6}{48 \times 8} \times 11.75 \times 10^{-3} \times 3 = 284.1 \text{ for AAL type 5.} \quad (3.5)$$

3.2.2.3 Data Arrival Process

The data arrival process is modeled as a Poisson process with a mean arrival rate of $1/\bar{t}_3$. At each arrival, a data message is generated with a geometric number of packets. Thus, the interarrival time between consecutive message arrivals is exponentially distributed with a rate of $\lambda_{data,i}$ for data user i . The mean interarrival time between consecutive message arrivals, $\bar{t}_3 = 1.0$ s.

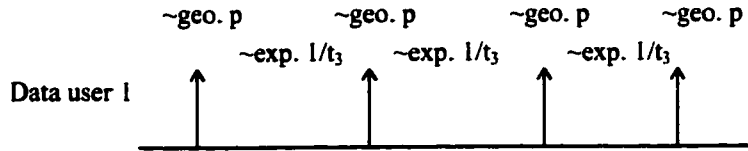


Fig. 3.5. Poisson process for data message arrival with a geometric number of packets for data arrival process

Assuming a mean of 5.12 kbits per message, the mean number of packets in a message is calculated as $\lceil 5.12 \times 10^3 / (48 \times 8) \rceil$ considering using AAL type 5. The number of data packets in each message is assumed to be geometrically distributed with the mean of 14 packets in each message. Thus, the number of packets, k , in a message has a geometric distribution as follows:

$$\Pr[k \text{ packets in a message}] = (1-p)^{k-1} p, \text{ where } p = 1/E[k], k \in [0, \dots, 1336]. \quad (3.6)$$

For AAL type 5, maximum payload of Common Part Convergence Sublayer-Protocol Data Unit (CPCS-PDU) = 65535 octets, the CPCS-PDU trailer = 8 octets, we need another 25 octets in PAD to provide 48 octet alignment of CPCS-PDU trailer. So, $65535 + 25 + 8 = 65568$ octets. Thus $65568 / 48 = 1366$ ATM cell payload. Assuming that the number of data users, $M_{data} = 100$, the mean number of information slots used by data users, \bar{N}_{data} , is given by

$$\bar{N}_{data} = 14 \times 11.75 \times 10^{-3} \times 100 = 16.45. \quad (3.7)$$

3.2.3 Request Slot Contention Processes

In the request slot subframe, there are seven type of contention requests in current available request slots: (1) new “start of talkspurt” voice requests, (2) unsuccessful “start of talkspurt” voice requests in the previous request slot subframe, (3) successful “start of talkspurt” voice requests but unsuccessful information slot allocation, (4) new head of line

(HOL) data message requests, (5) unsuccessful HOL data message requests in their previous requests in the request slot subframe, (6) long data messages which were not completely transmitted in the previous transmission frame due to insufficient information slots for data, and (7) voice control request packet for releasing information slot for the last voice packet in a talkspurt which is discarded due to insufficient voice information slot.

Unsuccessful voice requests will retry in the next TDMA frame, while unsuccessful data message requests will retry after a random number of TDMA frames. This number is equally distributed from 0 to *max*. In the simulation model, *max* is set to 11.

3.2.4 Information Slot Allocation Process

In the information slot allocation, video traffic has a higher access priority than that for voice traffic, while voice traffic has a higher access priority than that for data traffic. Video traffic has more stringent real-time requirements than that for voice traffic. For data traffic, some delay can be tolerated but not packet loss.

A random select scheme is used for selecting the active data users' packets to be transmitted in the information slots when there is sufficient information slots for data users and when there is insufficient information slots. For the case when there is insufficient information slots for data users, those data users that are not selected and the data user which can only transmit part of its message will retry after a random number of TDMA frames. Other possible schemes are: (1) select message with least (most) number of packets, (2) select message whose packet queue length in the portable terminal is the longest, etc.

In the uplink MAC protocol for a cellular wireless ATM network with heterogeneous traffic described in Chapter 2, each voice user is allocated an information

slot only during its talkspurt period (burst switching). In order to ease the implementation at the portable terminals such that the allocation of information slots to other traffic (data and video) can be made in a contiguous block, the allocation of voice information slots must also be made in a block with contiguous voice information slots (variable length voice block). Due to 'end of talkspurt' voice packets, gap or gaps will appear in the variable length voice block when such information slots become available in the next TDMA frame. These gaps in the variable length voice block need to be 'defragmented' with minimum changes in the positions of the voice information slots so that the base station will only have to inform those voice users with changes in location for their voice information slots. For voice users, an algorithm has been proposed in [11] for allocation and defragmentization of voice information slots when there is sufficient information slots and when there is insufficient information slots. This algorithm takes into account of (1) 'end of talkspurt' packets or gaps in the variable length voice block, (2) minimum changes in the positions of the voice information slots, (3) sufficient and insufficient information slots, as well as (4) new successful voice requests.

For video users, a random select scheme is used for selecting which video users' packets to be transmitted first when there is sufficient information slots and when there is insufficient information slots. No video packet loss is considered.

The minimum time starting from the end of the request slot subframe for processing the requests to the time that the first downlink control packet is transmitted is assumed to be 400 information slots. This assumption will enable the last downlink control packet to be broadcasted before the end of the current TDMA frame.

3.3 Simulation Results

In this simulation results, we consider only voice losses but no video and data losses. The simulation parameters are as follows:

- TDMA frame, $T_{TDMA} = 11.75$ ms (voice of 32 kbps with AAL type 1 (47 bytes payload)),
- Request slot time, $T_R = 4.8$ μ s,
- Information slot time, $T_I = 23.2$ μ s,
- Control slot time in the downlink, $T_C = 3.7$ μ s,
- Number of voice users, $M_{voice} = 100$,
- Number of data users, $M_{data} = 100$,
- Number of video users, $M_{video} = 2$ or 3 ,
- Video generation slot length, $d_{video} = 16.96$ μ s,

The other simulation parameters for the data, voice and video arrival processes are as described in the previous section.

Before looking at the simulation results, let us define some of the performance measures.

- *Mean queueing delay* (voice, video or data) is defined as the time interval between the time of arrival of a packet to the time of departure of the packet from the queue (voice, video or data) to the uplink channel. In the case where voice loss is considered, the mean voice queueing delay does not include those voice packets that are discarded at the portable terminals.
- *Voice (video) packet delay variation* or *jitter* is defined as the difference between the queueing delays of two consecutive voice (video) packets which are transmitted from the portable terminals. The latter queueing delay is used to subtract from the previous queueing delay.

- *Voice losses* is defined as the ratio of the voice packets which are discarded due to (1) unsuccessful requests in the request slot subframe (front end voice clippings) and (2) insufficient information slots in the information slot subframe (voice clippings within a talkspurt) to the total number of voice packets that are discarded and transmitted.
- *Channel utilization* is defined as the percentage usage of the information slot subframe by voice, video and data users.

3.3.1 Voice Performance

Fig. 3.10 shows the probability of more than zero outstanding voice request collisions. Note that the knee of this probability for 2 video users is about 60 request slots. Beyond this point, any further increase in the number of request slots will not have a significant decrease in this probability.

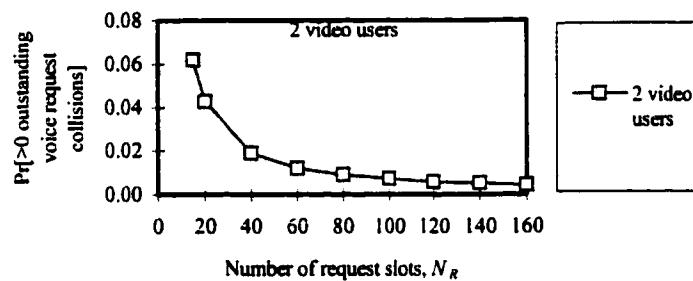


Fig. 3.10 Probability of more than zero outstanding voice request collisions

Voice traffic is handled on a loss basis in the sense that voice packets that are not transmitted after a given queueing delay (2 request slot contentions) are dropped. This results in front-end clipping of talkspurts. In addition, because video traffic has a higher access priority to information slots than voice traffic, during temporary video overloads, some voice talkspurts can be deprived of information slots. This results in mid-talkspurt clippings. Fig. 3.11 shows that for the simulated configuration, mid-talkspurt clippings are negligible compared to front-end clippings. With at least 15 request slots, the total

percentage of voice clippings falls to less than 0.4%. Note that for telephony speech quality, loss of voice information not exceeding 0.5% is generally acceptable. Again, the knee of the curve in Fig. 3.11 is at about 60 request slots.

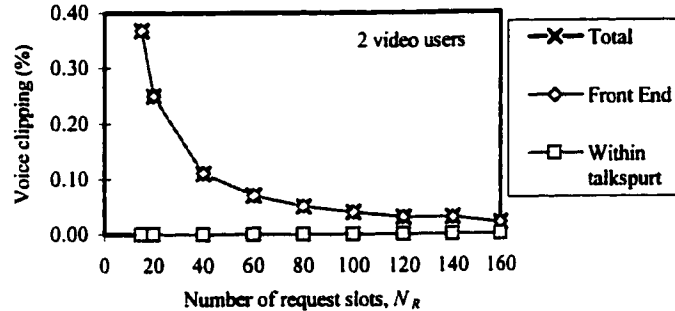


Fig. 3.11. Percentage voice clippings

For those voice packets that have not been dropped, the distributions of queueing delay and queueing delay variations, for 60 request slots, are shown in Figs. 3.12 and 3.13, respectively. Observe that all the voice packets are transmitted within 2 TDMA frames (which is to be expected). In fact, 99.5% of the voice packets experience queueing delays not exceeding 24.2 ms (i.e., $1045T_I$). The distribution of queueing delay variation shows a high probability (0.95) for a talkspurt to transmit through the same information slot in every frame. Again, this is to be expected from the MAC protocol. The non-zero delay variations are clearly caused by the MAC protocol's packing algorithm which packs up gaps in information slots caused by the ending of talkspurts, and its 'round-robin' manner of dropping voice packets during temporary video overloads.

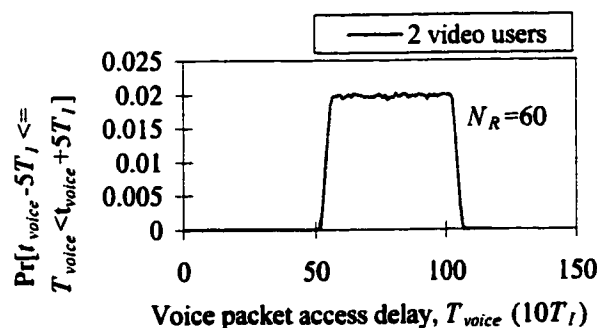


Fig. 3.12. Distribution of voice packet access delay with 60 request slots

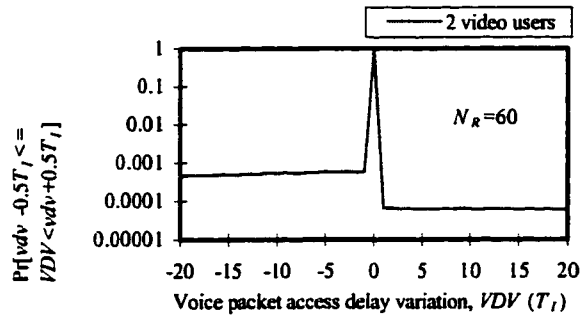


Fig. 3.13. Distribution of voice packet access delay variation with 60 request slots

3.3.2 MMPP Video Performance

Video traffic is accorded the highest priority, and since in the simulation study no video traffic is ever dropped, we consider only its delay performance. From simulation results for the video model used, 3 video users are not supportable as the resulting voice packet loss is unacceptably high. Therefore, we consider only 2 video users. Fig. 3.14 shows that the mean queueing delay of video remains at a relatively constant value of 21 ms for various numbers of request slots. Figs. 3.15 and 3.16 show the distributions of video packet queueing delay and delay variation assuming each frame has 60 request slots (this number of request slots yields an acceptable probability of request collisions from simulation). Observe that most video packets are transmitted within 2.5 TDMA frames (i.e., 29.3 ms), where $T_f = 23.2 \mu s$. In [33] it is stated that compressed video can tolerate a maximum delay of 100 ms while preserving good interactivity. As for queueing delay variation, for most video packets this does not exceed a value equal to the length of 1 information slot. This is attributable to the high priority of video traffic and that blocks of contiguous information slots within a frame are normally allocated to the 2 video users. The simulation results indicate that queueing delay variation is bounded between -2.32 ms and 16.24 ms, with 99.08% of the packets having delay variations between -2.32 ms and 2.32 ms with 2 video users. Note that the negative values of queueing delay variation are

caused by the video packet interarrival time being longer than the information slot duration.

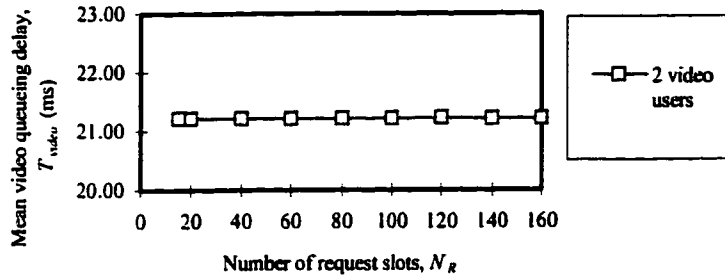


Fig. 3.14. Mean MMPP video packet access delay

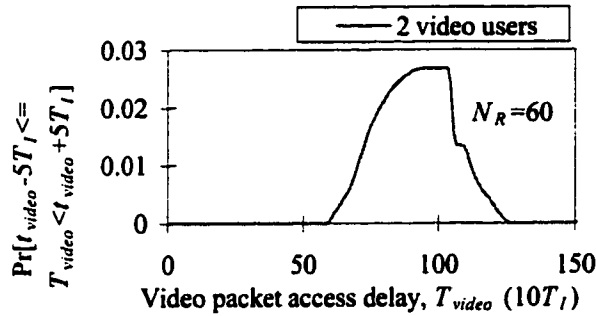


Fig. 3.15. Distribution of MMPP video packet access delay with 60 request slots

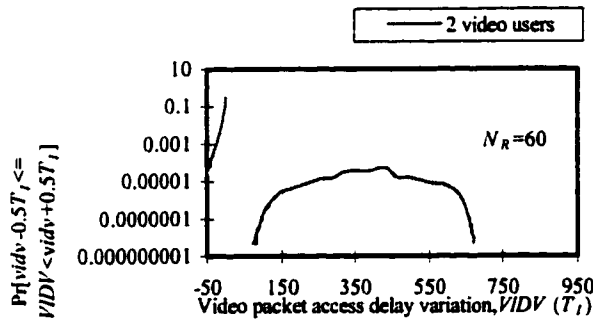


Fig. 3.16. Distribution of MMPP video packet access delay variation with 60 request slots

3.3.3 Data Performance and Overall Channel Utilization

Finally, Figs. 3.17 and 3.18 show the mean queuing delay experienced by data traffic and the overall percentage utilisation of the information slots, respectively. The mean data packet queuing delay in this case does not exceed 50 ms which is well within acceptable limits. The corresponding information slot utilization level is below 60%. This, and the results presented for voice and data performance, suggests that more voice and

data users can be supported by the wireless segment under consideration. Alternatively, if a lower rate video codec is used, the number of video users that can be supported may be increased.

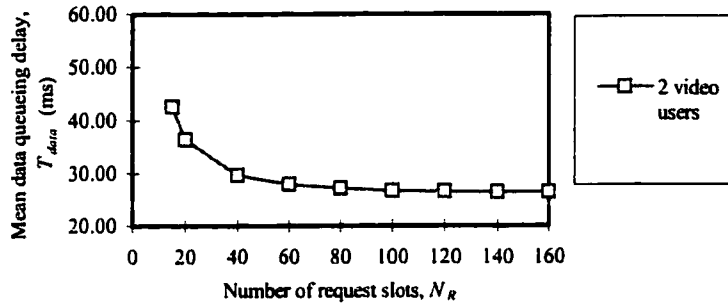


Fig. 3.17. Mean data packet access delay

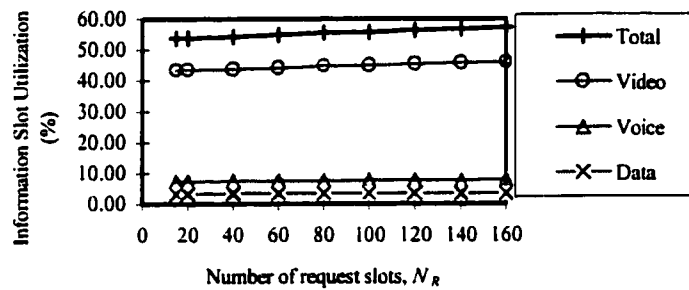


Fig. 3.18. Total information slot utilization

3.4 Performance Analyses

3.4.1 Voice Traffic

Assuming only classes 1, 2 and 3 services in the wireless segment under consideration, there are at least 6 types of requests that may contend for the *available* request slots in a frame. These are (a) voice (class 2) requests due to (i) a new voice talkspurt, (ii) an existing voice talkspurt that has not successfully gained access to a request slot, and (iii) an existing voice talkspurt that has not successfully gained access to an information slot, and (b) data (class 3) request due to (iv) a new data message, (v) an existing data message that has not successfully gained access to a request slot, and (vi) a long data message that has not been completely transmitted. To aid in the design of the

uplink frame composition (i.e., the numbers of request and information slots) we can carry out an approximate analysis to relate the number of *available* request slots in a frame to the probability of collision between contending requests. In the following, we adopt the analysis from [80] assuming light load conditions and that voice has higher power level than that of data requests, i.e., *priority for voice requests over data requests*. However, we consider a finite population for voice requests instead of an infinite population [80]. With voice traffic having higher priority (as is the case in our MAC protocol), the probability of collision between contending voice requests can be obtained simply by assuming no data traffic is present.

Since a *used* request slot is assigned to a class 1 (video) user for the whole duration of its connection, we can consider collisions in request slots to be caused only by voice and data arrivals if we assume that the connection duration of a video user is much longer than those of voice and data users. Further, the number of *available* request slots is $N_A = N_R - M_{\text{video}}$, where N_R is the total number of request slots and M_{video} is the number of video users. Consider the arrival processes for voice, video and data traffics to be as described in Section 3.2. Then, the probability that m requests arrive to the *available* request slots in the i th TDMA frame, $\Pr[A_i = m]$, consists of two types of arrivals. These arrivals are those coming from the voice users who are in the silent states at the beginning of the frame and those coming from the voice users who become silent during the frame, denoted by A_{i1} and A_{i2} , respectively. Let M_{vb} be the number of voice users who are in the silent states at the beginning of the frame and M_{vd} be the number of voice users who become silent during the frame interval. On the assumption that the arrival processes are independent, the probability of the former arrival type is given by

$$\Pr[A_{i1} = m_1] = \binom{M_{vb}}{m_1} p_1^{m_1} (1-p_1)^{M_{vb}-m_1} \quad (3.8)$$

where $p_1 = 1 - e^{-\lambda T_{TDMA}}$, T_{TDMA} is the TDMA frame length, $\lambda = 1/(\bar{t}_1 + \bar{t}_2)$ is the request arrival rate of one voice user, M_v is the number of voice users, \bar{t}_1 is the mean talkspurt period and \bar{t}_2 is the mean silence period.

Next, given that there is one ‘‘arrival’’ for the case of an end of talkspurt in an TDMA frame, the pdf of this ‘‘arrival’’ is uniformly distributed between zero and T_{TDMA} . Therefore, the pdf of the duration of the residual lifetime, in which a new voice request can arrive, is also uniformly distributed. The pdf of the second type of voice request arrival, is given by

$$\Pr[A_{i2} = m_2] = \binom{M_{vd}}{m_2} p_2^{m_2} (1-p_2)^{M_{vd}-m_2}, \quad (3.9)$$

where $p_2 = \int_0^{T_{TDMA}} (1 - \exp[-t_R / \bar{t}_2]) (1 / T_{TDMA}) dt_R = 1 - \bar{t}_2 [1 - \exp(-T_{TDMA} / \bar{t}_2)] / T_{TDMA}$. The pdf of the number of voice users who become dormant during the frame interval, is given by

$$\Pr[M_{vd} = d] = \binom{M_{vd}}{d} p_1^d (1-p_1)^{M_{vd}-d}. \quad (3.10)$$

Let C_i be the number of outstanding collisions in the i th TDMA frame. The sequence $\{C_i; i=0,1,2,\dots\}$ constitutes a first order homogeneous Markov Chain whose transition probabilities are obtained as follows:

$$\begin{aligned}
P_{jk} &= \Pr[C_{i+i} = k | C_i = j], \quad i, j = 0, 1, 2, \dots, M_v \quad (m+j-d-k) \geq 0, \\
&= \sum_{d=0}^j \Pr[M_{vd} = d | C_i = j] \sum_{m=0}^{M_v-j+d} \Pr[A = m | M_{vb} = M_v - j, M_{vd} = d] B(m+j-d-k, m+j-d; N_A) \\
&= \sum_{d=0}^j \Pr[M_{vd} = d | C_i = j] \sum_{m=0}^{M_v-j+d} \sum_{m_1=\max(0, m-d)}^{\min(M_v-j, m)} \Pr[A_{i1} = m_1 | M_{vb} = M_v - j] \Pr[A_{i2} = m - m_1 | M_{vd} = d] \\
&\quad \times B(m+j-d-k, m+j-d; N_A) \tag{3.11} \\
&= \sum_{d=0}^j \binom{j}{d} p_1^d (1-p_1)^{j-d} \sum_{m=0}^{M_v-j+d} B(m+j-d-k, m+j-d; N_A) \sum_{m_1=\max(0, m-d)}^{\min(M_v-j, m)} \binom{M_v-j}{m_1} p_1^{m_1} (1-p_1)^{M_v-j-m_1} \\
&\quad \times \binom{d}{m-m_1} p_2^{m-m_1} (1-p_2)^{d-m+m_1}
\end{aligned}$$

where $B(u, v; N_A) = \Pr[u \text{ successful requests} | v \text{ requests were transmitted in } N_A \text{ slots}]$ and it can be computed recursively as follows. Define $\eta(u, v) =$ number of combinations that u requests are successful given that v requests have been transmitted randomly in N_A slots.

Then

$$B(u, v; N_A) = \frac{\eta(u, v)}{N_A^v} \tag{3.12}$$

and

$$\eta(u, v) = \binom{N_A}{u} \binom{v}{u} u! (N_A - u)^{v-u} - \sum_{i=1}^{r(v)-u} \binom{u+i}{i} \eta(u+i, v), \tag{3.13}$$

where $r(v) =$ maximum number of successful reservations given that v requests have been transmitted in N_A slots,

$$r(v) = \begin{cases} v, & v \leq N_A \\ N_A - 1, & v > N_A. \end{cases} \tag{3.14}$$

At steady state, we have

$$\boldsymbol{\pi} = \boldsymbol{\pi} \boldsymbol{\psi} \tag{3.15}$$

where $\boldsymbol{\pi} = [\pi_0 \ \pi_1 \ \pi_2 \ \dots \ \pi_{M_v}]$, $\pi_k = \lim_{i \rightarrow \infty} \Pr[C_i = k]$ and $\boldsymbol{\psi} = [P_{jk}]$. The expected number

of request collisions, $E[C]$, is given by

$$E[C] = \sum_{k=0}^{M_v} k\pi_k \quad (3.16)$$

Since $\pi_1 = 0$, $\Pr[2 \text{ or more outstanding request collisions}] = 1 - \pi_0$.

Let us consider the delay in terms of the number of TDMA frame(s) incurred by the voice requests due to contention for the request slot subframe, F . Voice packets delayed for more than two TDMA frames are discarded. Consider a tagged voice request. Let $K_{D,i}$ be the number of voice requests transmitting in slots that are *different* from that of the tagged voice request in the i th TDMA frame, and $K_{S,i}$ be the number of voice requests transmitting in the *same slot* as the tagged voice request in the i th TDMA frame.

Consider the case where $F=0$, we have

$$\Pr[F=0] = \sum_{\substack{c_{i-1}=0 \\ c_{i-1} \neq 1}}^{M_v} \Pr[C_{i-1} = c_{i-1}] \sum_{a_i=1}^{M_v} P[A_i = a_i] / (1 - \Pr[A_i = 0]) \Pr[K_{D,i} = a_i + c_{i-1} - 1]. \quad (3.17)$$

For the case where $F=1$, we have

$$\begin{aligned} \Pr[F=1] = & \sum_{\substack{c_{i-1}=0 \\ c_{i-1} \neq 1}}^{M_v} \Pr[C_{i-1} = c_{i-1}] \sum_{\substack{a_i=2 \text{ for } c_{i-1}=0 \\ a_i=1 \text{ for } c_{i-1} \geq 2}}^{M_v} P[A_i = a_i] / \begin{cases} 1 - \Pr[A_i = 0] - \Pr[A_i = 1], & \text{for } c_{i-1} = 0 \\ 1 - \Pr[A_i = 0], & \text{for } c_{i-1} \geq 2 \end{cases} \\ & \times \sum_{s_i=1}^{a_i-1} \Pr[K_{S,i} = s_i] \sum_{c_i=s_i+1}^{a_i} \Pr[C_i = c_i | C_{i-1} = c_{i-1}] \sum_{a_{i+1}=0}^{M_v-1} \Pr[A_{i+1} = a_{i+1}] \Pr[K_{D,i+1} = a_{i+1} + c_i - 1] \end{aligned} \quad (3.18)$$

Note that equation (3.18) has many nested summations. These summations can only be computed for a small number of voice users. For a large number of voice users, the amount of computations is simply too large to be computed. Therefore, in order to reduce equation (3.18) to a computable and tractable form, we assume a Poisson distribution for the number of voice request arrivals. With this assumption, we have

$$\Pr[F=0] = \frac{e^{-\lambda T_{TDMA}}}{1 - e^{-\lambda T_{TDMA}}} \left(\frac{N_A}{N_A - 1} \right) \left[e^{\lambda T_{TDMA} \left(\frac{N_A - 1}{N_A} \right)} - 1 \right] \sum_{\substack{c_{i-1}=0 \\ c_{i-1} \neq 1}}^{M_v} \Pr[C_{i-1} = c_{i-1}] \left(\frac{N_A - 1}{N_A} \right)^{c_{i-1}}, \quad (3.19)$$

and

$$\begin{aligned} \Pr[F=1] &= \frac{e^{-\lambda T_{TDMA} \left(\frac{N_A + 1}{N_A} \right)}}{1 - e^{-\lambda T_{TDMA}} - \lambda T_{TDMA} e^{-\lambda T_{TDMA}}} \left(\frac{N_A}{N_A - 1} \right) \Pr[C_i = 0] \\ &\times \sum_{a_i=2}^{M_v} \frac{(\lambda T_{TDMA})^{a_i}}{a_i!} \sum_{s_i=1}^{a_i-1} \binom{a_i-1}{s_i} \left(\frac{1}{N_A} \right)^{s_i} \sum_{c_i=s_i+1}^{a_i} \Pr[C_i = c_i | C_{i-1} = 0] \left(\frac{N_A - 1}{N_A} \right)^{c_i} \\ &+ \frac{e^{-\lambda T_{TDMA} \left(\frac{N_A + 1}{N_A} \right)}}{1 - e^{-\lambda T_{TDMA}}} \left(\frac{N_A}{N_A - 1} \right) \sum_{c_i=2}^{M_v} \Pr[C_i = c_i] \sum_{a_i=1}^{M_v} \frac{(\lambda T_{TDMA})^{a_i}}{a_i!} \\ &\times \sum_{s_i=1}^{\min(a_i + c_{i-1} - 1, M_v - 1)} \binom{\min(a_i + c_{i-1} - 1, M_v - 1)}{s_i} \left(\frac{1}{N_A} \right)^{s_i} \sum_{c_i=s_i+1}^{\min(a_i + c_{i-1}, M_v)} \Pr[C_i = c_i | C_{i-1} = c_{i-1}] \left(\frac{N_A - 1}{N_A} \right)^{c_i} \end{aligned} \quad (3.20)$$

where $\lambda = M_v / (\bar{t}_1 + \bar{t}_2)$. The derivations for equations (3.19) and (3.20) are shown in the Appendix B.

To calculate the mean voice delay, let us first define some variables. Let \tilde{D}_1 denote the time interval from the time the tagged voice packet arrives in a TDMA frame to the “beginning” of the next TDMA frame, \tilde{D}_2 denote the single TDMA frame that the voice packet has to wait if $F=0$ as it can only be transmitted in the next TDMA frame, or two TDMA frame time if $F=1$, \tilde{D}_3 denote the request slot subframe that the tagged voice packet has to wait, \tilde{D}_4 denote the time interval that the tagged voice packet has to wait before it can be transmitted in the information slot assigned to it by the base station scheduler in the previous frame, and \tilde{T}_{voice} denote the voice packet queueing delay. The voice packet queueing delay, \tilde{T}_{voice} , is given by

$$\tilde{T}_{voice} = \tilde{D}_1 + \tilde{D}_2 + \tilde{D}_3 + \tilde{D}_4 \quad (3.21)$$

Let us assume that \tilde{D}_1 is uniformly distributed between the “beginning” of two consecutive TDMA frames, i.e., between zero and T_{TDMA} . Its pdf is given by

$$f_{\tilde{D}_1}(t) = \begin{cases} \frac{1}{T_{TDMA}}, & \text{if } 0 \leq t < T_{TDMA}, \\ 0, & \text{otherwise} \end{cases}, \quad (3.22)$$

That is, the mean of \tilde{D}_1 is

$$E[\tilde{D}_1] = \frac{1}{2} T_{TDMA}. \quad (3.23)$$

The pdf of \tilde{D}_2 is given by

$$f_{\tilde{D}_2}(t) = \begin{cases} \frac{\Pr[F=0]}{\Pr[F=0] + \Pr[F=1]}, & \text{if } 0 \leq t < T_{TDMA} \text{ and } F=0 \\ \frac{\Pr[F=1]}{\Pr[F=0] + \Pr[F=1]}, & \text{if } 0 \leq t < T_{TDMA} \text{ and } F=1, \\ 0, & \text{otherwise} \end{cases}, \quad (3.24)$$

while the pdf of \tilde{D}_3 is given by

$$f_{\tilde{D}_3}(t) = \begin{cases} 1, & \text{if } t = N_R T_R, \\ 0, & \text{otherwise} \end{cases}, \quad (3.25)$$

where N_R is the number of request slots in the request slot subframe and T_R is the time duration of one request slot. That is, the means of \tilde{D}_2 and \tilde{D}_3 are respectively, given by

$$E[\tilde{D}_2] = \frac{\Pr[F=0] + 2 \Pr[F=1]}{\Pr[F=0] + \Pr[F=1]} T_{TDMA}, \quad (3.26)$$

and

$$E[\tilde{D}_3] = N_R T_R. \quad (3.27)$$

Let \tilde{N} be the number of voice users in the active (on) state or the number of voice packets for transmission in a TDMA frame. Assuming that the number of voice users is less than or equal to the number of information slots under light load ($M_v \leq N_i$), the pdf of N is given by

$$\Pr[\tilde{N} = n] = \binom{M_v}{n} P_{on}^n (1 - P_{on})^{M_v - n}, \quad (3.28)$$

where $P_{on} \approx \frac{\bar{t}_1}{\bar{t}_1 + \bar{t}_2}$. To calculate the pdf of \tilde{D}_i , let us assume that voice packets are transmitted at the “beginning” of their information slots and each of the n active voice packets have equal probability of transmitting in each of the n consecutive information slots starting from the information slot subframe. Therefore, its pdf is given by

$$f_{\tilde{D}_i}(t = (i-1)T_i) = \sum_{n=i}^{M_v} \frac{1}{n} \Pr[\tilde{N} = n] \delta[t - (i-1)T_i], \quad i = 1, 2, \dots, M_v, \quad (3.29)$$

where $\delta(\cdot)$ is an impulse function. Thus, the mean of \tilde{D}_i is

$$\begin{aligned} E[\tilde{D}_i] &= \sum_{n=1}^{M_v} \sum_{i=1}^n \frac{1}{n} \Pr[\tilde{N} = n] (i-1)T_i \\ &= T_i \sum_{n=1}^{M_v} \frac{1}{n} \Pr[\tilde{N} = n] \sum_{j=0}^{n-1} j \\ &= \frac{T_i}{2} \sum_{n=1}^{M_v} (n-1) \Pr[\tilde{N} = n] \\ &= \frac{T_i}{2} [M_v P_{on} - 1 + (1 - P_{on})^{M_v}] \end{aligned} \quad (3.30)$$

Therefore, the mean voice delay is given by

$$E[\tilde{T}_{voice}] = E[\tilde{D}_1] + E[\tilde{D}_2] + E[\tilde{D}_3] + E[\tilde{D}_4] \quad (3.31)$$

Next, let us consider the distribution of the voice packets. First let us define

$$f_0 = \frac{\Pr[F = 0]}{\Pr[F = 0] + \Pr[F = 1]} \quad (3.32)$$

and

$$f_1 = \frac{\Pr[F = 1]}{\Pr[F = 0] + \Pr[F = 1]}. \quad (3.33)$$

From equations (3.21) and (3.25), the voice packet delay is given by

$$\tilde{T}_{voice} = \bar{T} + \tilde{D}_1 + \tilde{D}_2 + \tilde{D}_4, \quad (3.34)$$

and its pdf is given by

$$\begin{aligned} f_{\tilde{T}_{voice}}(t) &= f_0 \int_{-\infty}^{\infty} f_{\tilde{D}_1}(t - \bar{T} - T_{TDMA} - D_4) f_{\tilde{D}_4}(D_4) dD_4 \\ &\quad + f_1 \int_{-\infty}^{\infty} f_{\tilde{D}_1}(t - \bar{T} - 2T_{TDMA} - D_4) f_{\tilde{D}_4}(D_4) dD_4, \end{aligned} \quad (3.35)$$

where $\bar{T} = N_R T_R$. Considering each discrete point of $f_{\bar{D}_k}(D_k)$ and multiplying $f_{\bar{D}_k}(t - \bar{T} - D_2 - D_k)$ for all possible range of values, we have 5 main intervals.

For $(\bar{T} + T_{TDMA} + (i-1)T_l) \leq t < (\bar{T} + T_{TDMA} + iT_l)$, for $i = 1, 2, \dots, M_v$,

$$f_{\bar{T}_{\text{voice}}}(t) = \frac{f_0 T_l}{T_{TDMA}} \left[\sum_{j=1}^i \sum_{n=j}^{M_v} \frac{1}{n} \Pr[\tilde{N} = n] \right]. \quad (3.36)$$

For $(\bar{T} + T_{TDMA} + (M_v - 1)T_l) \leq t < (\bar{T} + 2T_{TDMA})$,

$$\begin{aligned} f_{\bar{T}_{\text{voice}}}(t) &= \frac{f_0 T_l}{T_{TDMA}} \left[\sum_{j=1}^{M_v} \sum_{n=j}^{M_v} \frac{1}{n} \Pr[\tilde{N} = n] \right] \\ &= \frac{f_0 T_l}{T_{TDMA}} [1 - (1 - P_{on})^{M_v}] \end{aligned} \quad (3.37)$$

For $(\bar{T} + 2T_{TDMA} + (i-1)T_l) \leq t < (\bar{T} + 2T_{TDMA} + iT_l)$, for $i = 1, 2, \dots, M_v$,

$$f_{\bar{T}_{\text{voice}}}(t) = \frac{f_0 T_l}{T_{TDMA}} \left[\sum_{j=i+1}^{M_v} \sum_{n=j}^{M_v} \frac{1}{n} \Pr[\tilde{N} = n] \right] + \frac{f_1 T_l}{T_{TDMA}} \left[\sum_{j=1}^i \sum_{n=j}^{M_v} \frac{1}{n} \Pr[\tilde{N} = n] \right]. \quad (3.38)$$

For $(\bar{T} + 2T_{TDMA} + (M_v - 1)T_l) \leq t < (\bar{T} + 3T_{TDMA})$,

$$\begin{aligned} f_{\bar{T}_{\text{voice}}}(t) &= \frac{f_1 T_l}{T_{TDMA}} \left[\sum_{j=1}^{M_v} \sum_{n=j}^{M_v} \frac{1}{n} \Pr[\tilde{N} = n] \right] \\ &= \frac{f_1 T_l}{T_{TDMA}} [1 - (1 - P_{on})^{M_v}] \end{aligned} \quad (3.39)$$

For $(\bar{T} + 3T_{TDMA} + (i-1)T_l) \leq t < (\bar{T} + 3T_{TDMA} + iT_l)$, for $i = 1, 2, \dots, M_v$,

$$f_{\bar{T}_{\text{voice}}}(t) = \frac{f_1 T_l}{T_{TDMA}} \left[\sum_{j=i+1}^{M_v} \sum_{n=j}^{M_v} \frac{1}{n} \Pr[\tilde{N} = n] \right]. \quad (3.40)$$

3.4.2 MMPP Video Traffic

We assume that there is no overload in the information slot subframe. The video arrival process is modelled as an M -state MMPP. Let h_i be the probability of being in phase i in steady state. Then, we have

$$[h_1 h_2 \dots h_M] = [h_1 h_2 \dots h_M] \mathbf{H}. \quad (3.41)$$

In each phase, the video arrival process is Poisson distributed with a mean video arrival rate, λ_i , in a video slot, d_{video} . For a Poisson arrival process with a mean rate λ , the probability of \tilde{G} arrivals in any interval of length t is given by

$$\Pr[\tilde{G} = g] = \frac{(\lambda t)^g e^{-\lambda t}}{g!}. \quad (3.42)$$

Let \tilde{D} be the number of video packets arriving during an interval of length t . For 1 video user, \tilde{D} is the weighted sum of the Poisson arrival processes in each of the M phases. Its pdf is given by

$$\Pr[\tilde{D} = d] = \sum_{v=1}^M \frac{\left[\frac{\lambda_v}{d_{video}} t \right]^d e^{-\frac{\lambda_v}{d_{video}} t}}{d!} h_v. \quad (3.43)$$

For 2 video users, \tilde{D} is the weighted sum of the Poisson arrival processes in each of the M phases for user 1 and user 2. From the property of Poisson processes, the sum of 2 Poisson processes with mean arrival rate λ_x and λ_y is also a Poisson process with a mean rate $(\lambda_x + \lambda_y)$. Then, for 2 video users, the pdf of \tilde{D} is given by

$$\Pr[\tilde{D} = d] = \sum_{u=1}^M \sum_{v=1}^M \frac{\left[\frac{\lambda_u + \lambda_v}{d_{video}} t \right]^d e^{-\frac{\lambda_u + \lambda_v}{d_{video}} t}}{d!} h_u h_v. \quad (3.44)$$

For M_{video} video users, \tilde{D} is the weighted sum of the Poisson arrival processes in each of the M phases for user 1 to user M_{video} . From the property of Poisson processes, the sum of M_{video} Poisson processes with mean rates λ_{x_1} , λ_{x_2} , ..., and $\lambda_{x_{M_{video}}}$ is also a Poisson process with a mean arrival rate, $\sum_{i=1}^{M_{video}} \lambda_{x_i}$. Generalizing for M_{video} video users, the pdf of \tilde{D} is given

by

$$\Pr[\tilde{D}=d]=\sum_{i_1=1}^M \sum_{i_2=1}^M \dots \sum_{i_{M_{\text{video}}}=1}^M \left[\frac{\sum_{i=1}^{M_{\text{video}}} \lambda_{i_i}}{d_{\text{video}}} t \right]^d e^{-\frac{\sum_{i=1}^{M_{\text{video}}} \lambda_{i_i}}{d_{\text{video}}} t} / d! \times \prod_{i=1}^{M_{\text{video}}} h_{i_i}. \quad (3.45)$$

Let \tilde{B} be the number of video packets arriving during a TDMA frame and T_{TDMA} be the time interval for a TDMA frame. For M_{video} video users, the pdf of \tilde{B} is given by

$$\Pr[\tilde{B}=b]=\sum_{i_1=1}^M \sum_{i_2=1}^M \dots \sum_{i_{M_{\text{video}}}=1}^M \left[\frac{\sum_{i=1}^{M_{\text{video}}} \lambda_{i_i}}{d_{\text{video}}} T_{\text{TDMA}} \right]^b e^{-\frac{\sum_{i=1}^{M_{\text{video}}} \lambda_{i_i}}{d_{\text{video}}} T_{\text{TDMA}}} / b! \times \prod_{i=1}^{M_{\text{video}}} h_{i_i}. \quad (3.46)$$

To calculate the mean video delay, let us first define some variables. Let \tilde{D}_5 denote the time interval from the time that a tagged video packet arrives (j th arrival) in a TDMA frame to the beginning of the next TDMA frame in the i th frame, \tilde{D}_6 denote the one TDMA frame that the tagged video packet has to wait in the $(i+1)$ th frame, \tilde{D}_7 denote the request slot subframe that the tagged video packet has to wait in the $(i+2)$ th frame, \tilde{D}_8 denote the delay due to voice packet being transmitted before the video packets and the time interval the tagged video packet has to wait for other video packets to be transmitted first in the $(i+2)$ th frame, \tilde{D}_9 denote the delay due to voice packets being transmitted before the video packets in the $(i+2)$ th frame, \tilde{D}_{10} denote the time interval that the tagged video packet has to wait for other video packets to be transmitted first in the $(i+2)$ th frame and \tilde{T}_{video} denote the video packet queuing delay. The video packet queuing delay, \tilde{T}_{video} , is given by

$$\tilde{T}_{\text{video}} = \tilde{D}_5 + \tilde{D}_6 + \tilde{D}_7 + \tilde{D}_8. \quad (3.47)$$

Let us assume that \tilde{D}_5 is triangularly distributed between the beginning of two consecutive TDMA frames, i.e., between zero and T_{TDMA} . Its pdf is given by

$$f_{\tilde{D}_5}(t) = \begin{cases} \frac{4t}{T_{TDMA}^2}, & 0 < t < \frac{T_{TDMA}}{2} \\ \frac{4(T_{TDMA} - t)}{T_{TDMA}^2}, & \frac{T_{TDMA}}{2} < t < T_{TDMA} \\ 0, & \text{otherwise} \end{cases} \quad (3.48)$$

while its cdf is given by

$$F_{\tilde{D}_5}(t) = \begin{cases} \frac{2t^2}{T_{TDMA}^2}, & 0 < t < \frac{T_{TDMA}}{2} \\ 1 - \frac{2(T_{TDMA} - t)^2}{T_{TDMA}^2}, & \frac{T_{TDMA}}{2} < t < T_{TDMA} \\ 1, & T_{TDMA} < t < \infty \end{cases} \quad (3.49)$$

The mean of \tilde{D}_5 is

$$E[\tilde{D}_5] = \frac{1}{2} T_{TDMA} \quad (3.50)$$

The pdf of \tilde{D}_6 is given by

$$f_{\tilde{D}_6}(t) = \begin{cases} 1, & \text{if } t = T_{TDMA} \\ 0, & \text{otherwise} \end{cases} \quad (3.51)$$

while the pdf of \tilde{D}_7 is given by

$$f_{\tilde{D}_7}(t) = \begin{cases} 1, & \text{if } t = N_R T_R \\ 0, & \text{otherwise} \end{cases} \quad (3.52)$$

where N_R is the number of request slots in the request slot subframe and T_R is the time duration of one request slot. That is, the means of \tilde{D}_6 and \tilde{D}_7 are respectively, given by

$$E[\tilde{D}_6] = T_{TDMA}, \quad (3.53)$$

and

$$E[\tilde{D}_7] = N_R T_R. \quad (3.54)$$

Let \tilde{N} denote the number of voice users in the active (on) state or the number of voice packets for transmission in a TDMA frame. Assuming that the number of voice users is less than or equal to the number of information slots under light load ($M_v \leq N_I$), where M_v ,

is the number of voice users and N_I is the number of information slots in the information slots subframe, the pdf of \tilde{N} is given by

$$\Pr[\tilde{N} = n] = \binom{M_v}{n} P_{on}^n (1 - P_{on})^{M_v - n}, \quad (3.55)$$

where $P_{on} = \frac{\bar{t}_1}{\bar{t}_1 + \bar{t}_2}$, \bar{t}_1 is the mean talkspurt (on) period and \bar{t}_2 is the mean silence period.

The pdf of \tilde{D}_0 is given by

$$f_{\tilde{D}_0}(t) = \begin{cases} \Pr[\tilde{N} = n], & \text{if } t = nT_I \\ 0 & , \text{otherwise} \end{cases}, \quad (3.56)$$

where T_I is the size of an information slot in the information slot subframe. The video packets are transmitted at the end of the voice information slots block. Each of the k video packets is assumed to have equal probability of transmitting in each of the k consecutive information slots. Assuming that the tail distribution of \tilde{B} is small under light load, the pdf of \tilde{D}_{10} is given by

$$f_{\tilde{D}_{10}}(t = (j-1)T_I) = \sum_{k=j}^{N_I - M_v} \frac{1}{k} \Pr[\tilde{B} = k] \delta[t - (j-1)T_I], \quad (3.57)$$

where $\delta(\cdot)$ is an impulse function. The pdf of \tilde{D}_8 is given by

$$f_{\tilde{D}_8}(t = (n+j-1)T_I) = \Pr[\tilde{N} = n] \sum_{k=j}^{N_I - M_v} \frac{1}{k} \Pr[\tilde{B} = k] \delta[t - (n+j-1)T_I], \quad (3.58)$$

and its mean is given by

$$\begin{aligned} E[\tilde{D}_8] &= \sum_{n=0}^{M_v} \Pr[\tilde{N} = n] \sum_{k=1}^{N_I - M_v} \sum_{j=1}^k \frac{1}{k} \Pr[\tilde{B} = k] (n+j-1)T_I \\ &= \frac{T_I}{2} \sum_{n=0}^{M_v} \Pr[\tilde{N} = n] \sum_{k=1}^{N_I - M_v} (2n+k-1) \Pr[\tilde{B} = k] \end{aligned}, \quad (3.59)$$

where $\sum_{j=1}^k (n+j-1) = \frac{k}{2}(2n+k-1)$. Therefore, the mean video delay is given by

$$\begin{aligned} E[\tilde{T}_{video}] &= E[\tilde{D}_5] + E[\tilde{D}_6] + E[\tilde{D}_7] + E[\tilde{D}_8] \\ &= \bar{T}^* + E[\tilde{D}_8] \end{aligned} \quad (3.60)$$

where $\bar{T}^* = \frac{3}{2}T_{TDMA} + N_R T_R$.

Next, let us consider the distribution of the video packets. The video packet delay is given by

$$\begin{aligned} \tilde{T}_{video} &= \tilde{D}_5 + \tilde{D}_6 + \tilde{D}_7 + \tilde{D}_9 + \tilde{D}_{10} \\ &= \bar{T}^* + \tilde{D}_5 + \tilde{D}_9 + \tilde{D}_{10} \end{aligned} \quad (3.61)$$

where $\bar{T}^* = T_{TDMA} + N_R T_R$. Its pdf is given by

$$f_{\tilde{T}_{video}}(t) = \sum_{n=0}^{M_v} \Pr[\tilde{N} = n] \int_{-\infty}^{\infty} f_{\tilde{D}_5}(t - \bar{T}^* - nT_I - D_{10}) f_{\tilde{D}_{10}}(D_{10}) dD_{10}. \quad (3.62)$$

For ease of computation, we discretize the pdf of \tilde{D}_5 and its pdf is given by

$$f_{\tilde{D}_5}(t = wT_I) = F_{\tilde{D}_5}(t = (w+1)T_I) - F_{\tilde{D}_5}(t = wT_I), \quad (3.63)$$

where $0 \leq w \leq N_{TDMA}$, $0 \leq t \leq N_{TDMA} T_I$, $N_{TDMA} = \left\lceil \frac{T_{TDMA}}{T_I} \right\rceil$ and $\lceil x \rceil$ is the greatest integer smaller or equal to x . Considering each discrete point of $f_{\tilde{D}_{10}}(D_{10})$ and multiplying each discrete point of $f_{\tilde{D}_5}(t - \bar{T}^* - nT_I - D_{10})$ with probability $\Pr[\tilde{N} = n]$ for all possible range of values, we have

$$\begin{aligned} f_{\tilde{T}_{video}}(t) &\approx \sum_{n=0}^{M_v} \Pr[\tilde{N} = n] \sum_{w=0}^{N_{TDMA}} f_{\tilde{D}_5}(t = wT_I) \\ &\times \sum_{j=1}^{N_I - M_v} \sum_{k=j}^{N_I - M_v} \begin{cases} \frac{1}{k} \Pr[\tilde{B} = k], & \text{if } (\bar{T}^* + (n+j-1+w)T_I) \leq t < (\bar{T}^* + (n+j+w)T_I) \\ 0 & , \text{otherwise} \end{cases} \end{aligned} \quad (3.64)$$

3.5 Numerical Results

3.5.1 Voice Performance

Here, we consider the same parameters as in Section 3.3 and the number of video users is 2 (about 60% total channel utilization). Figs. 3.19 and 3.20 show the mean voice queuing delay and the distribution of the voice queuing delay, respectively. The

analytical results are very close to the simulation results. This shows that the assumptions made in Section 3.4.1 are reasonable. Voice can tolerate a maximum delay of 200 ms while preserving good real-time interactivity [33].

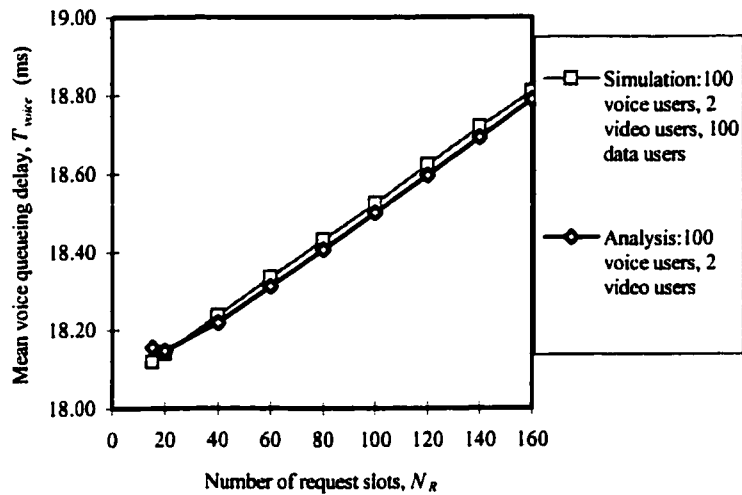


Fig. 3.19. Mean voice packet queuing delay

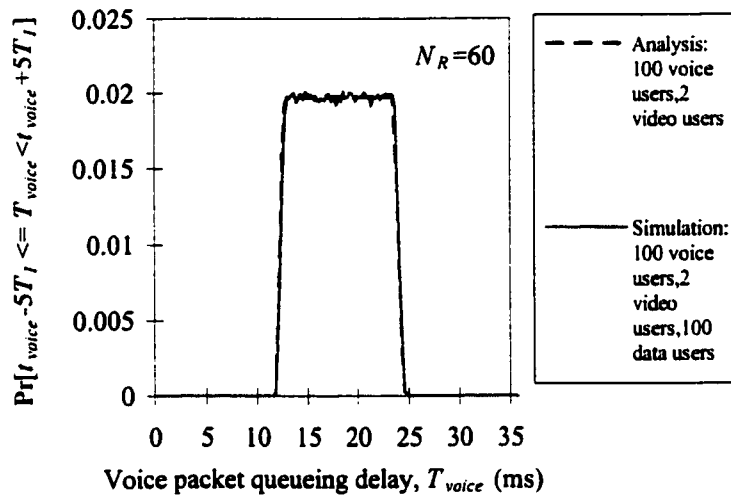


Fig. 3.20. Distribution of voice packet queuing delay

3.5.2 MMPP Video Performance

Figs. 3.21 and 3.22 show the mean video queuing delay and the distribution of the video queuing delay, respectively. The analytical results are quite close to the simulation results, without making use of the assumptions in Section 3.4.2. This shows that the assumptions are reasonable. Fig. 3.21 shows that the mean queuing delay of video

remains at about 21 ms for various numbers of request slots. Fig. 3.22 shows the distribution of queuing delay assuming each frame has 60 request slots (this number of request slots yields an acceptable probability of request collisions from simulation). Observe that most video packets are transmitted within 2.5 TDMA frames (i.e., 29.3 ms), where $T_f = 23.2 \mu\text{s}$. In [33] it is stated that compressed video can tolerate a maximum delay of 100 ms while preserving good real-time interactivity.

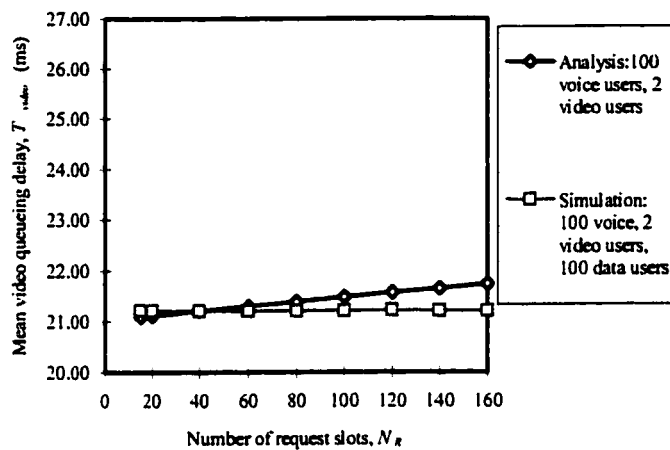


Fig. 3.21. Mean MMPP video packet queuing delay

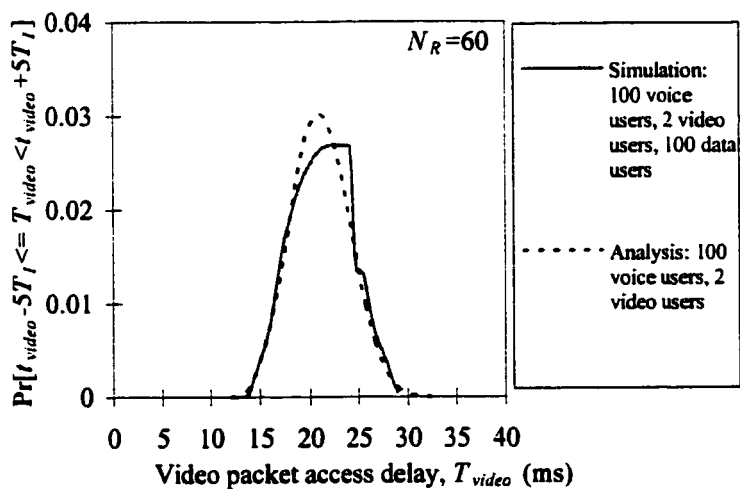


Fig. 3.22. Distribution of MMPP video packet queuing delay

3.6 Summary

The performance of our enhanced MAC protocol is evaluated in this chapter. The enhancements of our MAC protocol over the MAC protocol proposed in [1-4] is described in Section 2.4. In [1-4], an information slot is allocated to a voice user for the whole connection regardless of whether the voice traffic is in a talkspurt state or is in a silence state. That is, an information slot is allocated regardless of whether there is a packet to send or not. In our MAC protocol, an information slot is allocated only during the talkspurt state. This is similar in spirit to that of Packet Reservation Multiple Access (PRMA) in [13]. However, PRMA is first designed for voice users and if data users are added, they will be allocated information slots that are not used by the voice users. The information slots allocated to each data user can be excessive if the data slots are dispersed among the voice slots. In our MAC protocol, the voice users are grouped together using a voice packing algorithm in [11]. This allows the allocation of information slots to other users (like video and data) by simply specifying the starting and ending slot positions for these users. In other words, burst-switching is used for voice service.

Numerical results show that acceptable QoS for voice, MMPP video and data can be achieved in a wireless segment that supports up to 100 voice, 100 data and 2 MMPP video users. Mathematical analyses for the delay performance of voice and MMPP video traffic are presented. These analyses give insights to the components that constitute the mean delays and delay distributions. Numerical results show that the analytical results closely approximate the simulation results, indicating that the assumptions used in the analytical models are reasonable.

The analysis for computing the probability of collisions between contending voice requests consider finite population instead of infinite population [80]. For the actual

computation, the number of states with our analysis is just the number of voice users plus one instead of a large but finite number in the infinite population case. The distribution of the number of video packets arriving in a time interval for a MMPP video user (equation (3.43)) and the distribution of the number of video packet arriving in a time interval for the superposition of a number of MMPP video users (equation (3.45)) are presented in the analysis for MMPP video traffic. These results are also used in Chapter 4 to derive the output process from the uplink MAC protocol for a MMPP video traffic. This process is then fed to the input buffer of a leaky bucket in the base station.

Instead of using MMPP video traffic, we can also use Motion Picture Experts Group (MPEG) video traffic source sequence to study the performance of the uplink MAC protocol. Such a study is presented in Chapter 5 and it compares its simulation results with the results obtained in this Chapter.

Chapter 4

Usage Parameter Control

4.1 Introduction

The leaky bucket has been studied extensively in the literature [55-61] with different arrival processes. The arrival processes can be Poisson process, Markovian process, exponential On/Off process, MMPP, etc. (see Section 1.2). However, UPC in wireless/wireline ATM network have not been proposed nor studied in the literature until recently [86]. There are two stages: (1) uplink MAC protocol and (2) UPC at the base station. In [86], the effects of user mobility on the GCRA as the UPC is studied. However, no uplink MAC protocol is specified. A transit time in the wireless domain is assumed. The GCRA has been studied in [87-88]. In our study of the leaky bucket as the UPC, the arrival process to the leaky bucket at the base station is the output process from the uplink MAC protocol. The output process may or may not “match” the arrival processes of these leaky buckets studied in the literature such that analytical results can be obtained.

The first part of this chapter studies the performance of UPC by computer simulation, using leaky bucket at the base station to police heterogeneous traffic described in Chapter 3 according to their equivalent capacities discussed in Chapter 6. The simulation models are described in Section 4.2 while the simulation results are presented in Section 4.3.

In the latter part of this chapter, an approximate analysis of voice loss is provided and a loose lower bound is obtained for MMPP video loss in Section 4.4. The On/Off

video process to the leaky bucket at the base station is characterized. It is found that the On period and the Off period are not independent. Numerical results are shown in Section 4.5.

4.2 Simulation Models

Figs. 4.1, 4.2 and 4.3 show the simulation model for usage parameter control using a leaky bucket at the base station for a voice traffic, an MMPP video traffic and a data traffic, respectively. The first portion of Figs. 4.1, 4.2 and 4.3, before entering the leaky bucket, is due to the MAC protocol described in Chapter 3.

4.2.1 Voice Traffic

The front end voice loss and the voice loss within the talkspurt are results of the MAC protocol. At the leaky bucket, the voice loss due to the leaky bucket depends on the input voice buffer, B_{voice} , and the voice token buffer, $B_{voice.token}$. The sum of these two buffers is denoted by B_v .

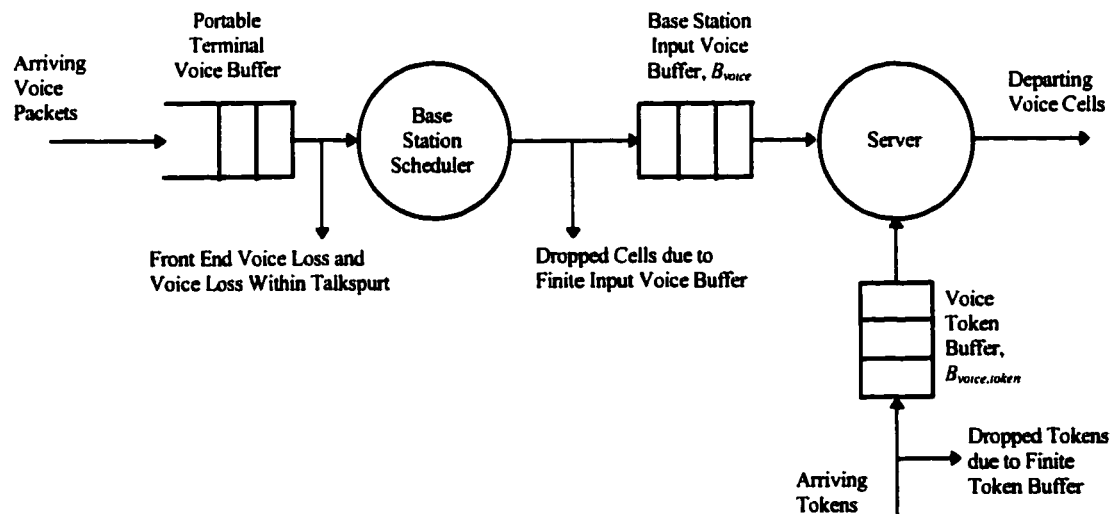


Fig. 4.1. Simulation model of a voice traffic arriving to a portable terminal passing through the base station scheduler and a leaky bucket at the base station

4.2.2 MMPP Video Traffic

There is no video loss at the MAC protocol. At the leaky bucket, the video loss due to the leaky bucket depends on the input video buffer, B_{video} , and the video token buffer, $B_{video,token}$. The sum of these two buffers is denoted by B_{vi} .

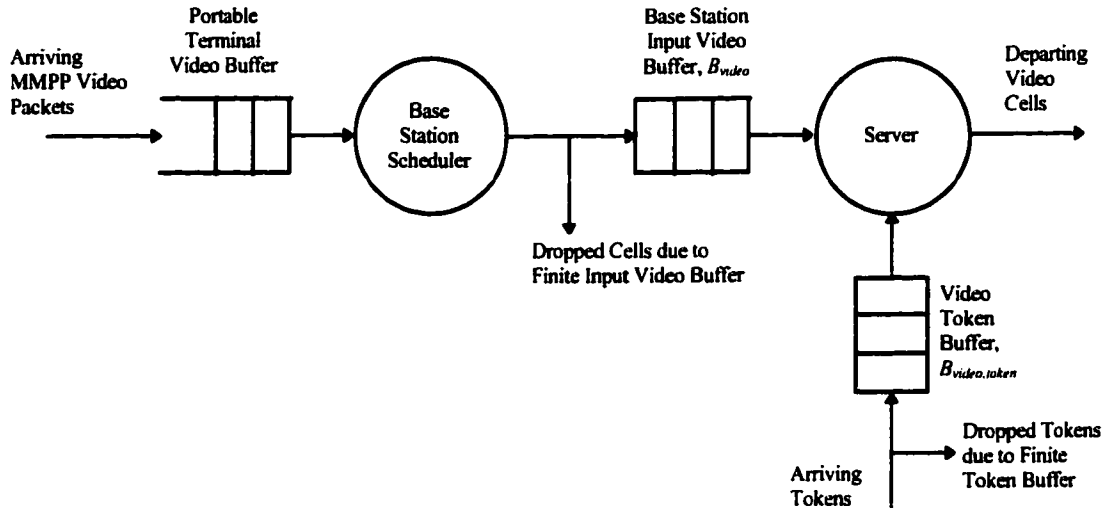


Fig. 4.2. Simulation model of a MMPP video traffic arriving to a portable terminal passing through the base station scheduler and a leaky bucket at the base station

4.2.3 Data Traffic

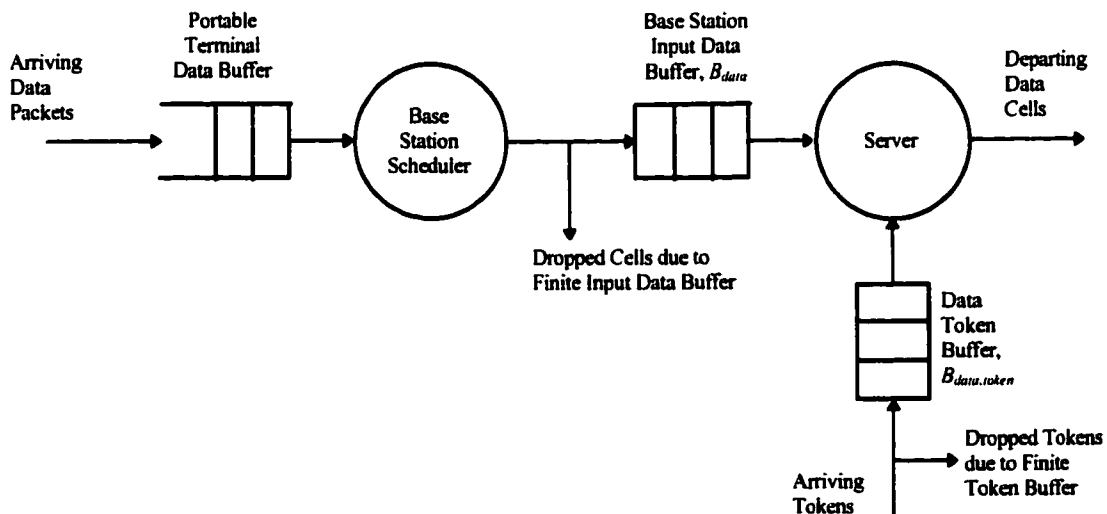


Fig. 4.3. Simulation model of a data traffic arriving to a portable terminal passing through the base station scheduler and a leaky bucket at the base station

There is no data loss at the MAC protocol. At the leaky bucket, the data loss due to the leaky bucket depends on the input data buffer, B_{data} , and the data token buffer, $B_{data,token}$. The sum of these two buffers is denoted by B_d .

4.3 Simulation Results

The results obtained here are from a simulation model of the MAC protocol and leaky buckets for voice, MMPP video and data traffic based on the SMPL simulation kernel described in [79]. Each simulation point has been obtained by running the simulation for a duration of 500000 TDMA frames with three simulation runs. The parameters are the same as those in Chapters 3 with the number of request slots set at 60. The leaky buckets has the following parameters: the voice token generation rate is $1000 T_f$ (20 kbps equivalent capacity in Chapter 6); the video token generation rate is $\frac{10}{3} T_f$ (6 Mbps equivalent capacity in Chapter 6); the data token generation rate is $2000 T_f$ (10 kbps equivalent capacity in Chapter 6). The number of video users is 2.

4.3.1 Voice Performance

Fig. 4.4 shows the voice packet/cell losses with respect to the number of voice buffer at the input buffer of a leaky bucket with the sum of the size of the voice buffer and the voice token buffer fixed at 100. The voice packet/cell losses consist of front end voice loss due to unsuccessful attempt in the request slot subframe, voice loss due to insufficient information slots for the voice user and the voice loss due to the finite voice buffer of the leaky bucket. The voice losses depend on the sum of the size of the voice buffer and the voice token buffer and not on their individual sizes.

Fig. 4.5 shows the mean voice transmission delay (from portable terminal to the base station), the mean voice queuing delay at the voice buffer of the leaky bucket and the mean total voice delay (which is the sum of the previous two delays) with respect to the number of voice buffer at the input buffer of the voice leaky bucket, with the sum of the size of the voice buffer and the voice token buffer fixed at 100. Since the voice losses remain constant (Fig. 4.4), the mean total voice delay is lowest when the size of the voice buffer is one. This voice delay is less than the 200 ms requirement for acceptable conversation. However, the total voice loss is greater than 1%. Therefore, we need to consider the trade-off between total voice loss and the total buffer size of the voice buffer and the voice token buffer. Note that the input voice buffer needs real memory spaces, while the voice token buffer can be implemented by a counter.

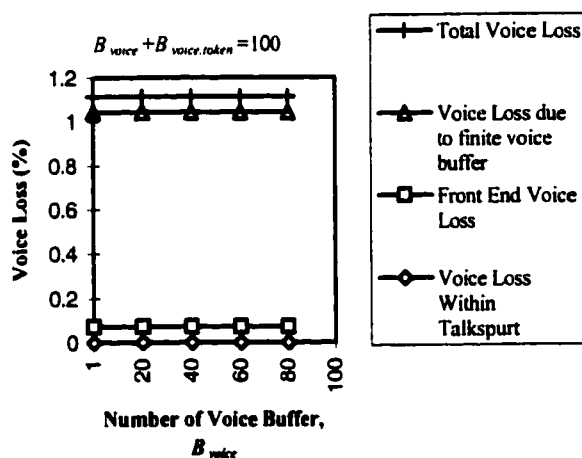


Fig. 4.4. Voice losses with respect to input voice buffer

Fig. 4.6 shows the voice packet/cell losses with respect to the total buffer size of the voice buffer and the voice token buffer, B_v . The number of voice buffer at the input

buffer of a leaky bucket is fixed at 1. For acceptable total voice loss of 0.5 % or better, the total buffer size must be greater than or equal to 130.

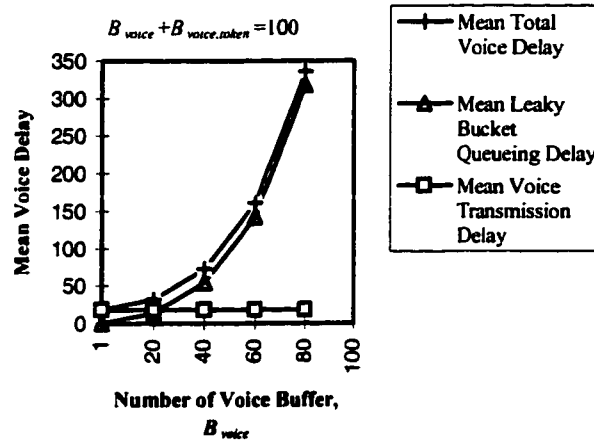


Fig. 4.5. Mean voice delays with respect to input voice buffer

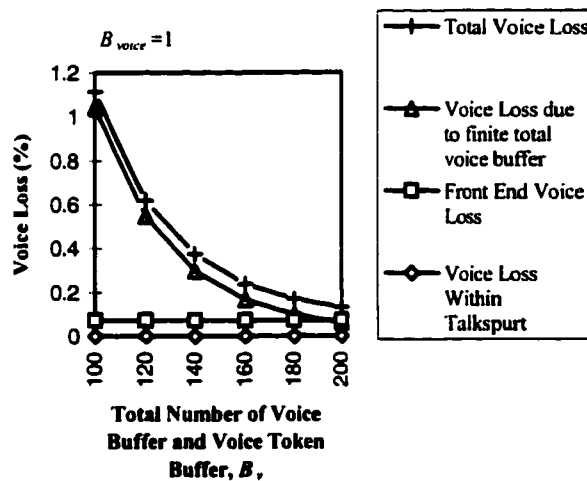


Fig. 4.6. Voice losses with respect to total buffer size

Fig. 4.7 shows the mean voice transmission delay, the mean voice queueing delay at the voice buffer of the leaky bucket and the mean total voice delay with respect to the total buffer size of the voice buffer and the voice token buffer, B . The number of voice

buffer at the input buffer of a leaky bucket is again fixed at 1. From Fig. 4.7, with the voice buffer size set to 1, the mean leaky bucket queuing delay is very small and the mean total voice delay is almost equal to the mean voice transmission delay. The mean voice transmission delay remains relatively constant as the total buffer size increases.

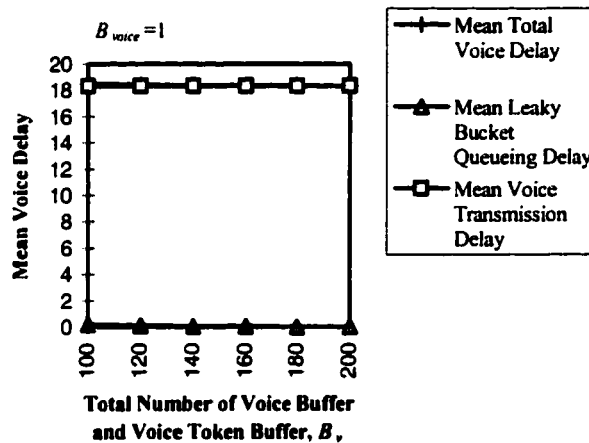


Fig. 4.7. Mean voice delays with respect to total buffer size

4.3.2 MMPP Video Performance

Fig. 4.8 shows the MMPP video cell losses with respect to the number of video buffer at the input buffer of a leaky bucket with the sum of the size of the video buffer and the video token buffer fixed at 2000. The MMPP video loss depends on the sum of the video buffer and the video token buffer and not on their individual sizes.

Fig. 4.9 shows the mean MMPP video transmission delay (from portable terminal to the base station), the mean MMPP video queueing delay at the video buffer of the leaky bucket and the mean total MMPP video delay (which is the sum of the previous two delays) with respect to the number of video buffer at the input buffer of the video leaky bucket, with the sum of the video buffer and the video token buffer fixed at 2000. Since

the MMPP video loss remains constant (Fig. 4.8), the mean total MMPP video delay is lowest when the size of the video buffer is one. This video delay is less than the 100 ms requirement for acceptable video transmission. However, the total MMPP video loss is greater than 2%. Therefore, we need to consider the trade-off between video loss and the total buffer size of the video buffer and the video token buffer. Note that the input video buffer requires real memory spaces, while the video buffer can be implemented by a counter.

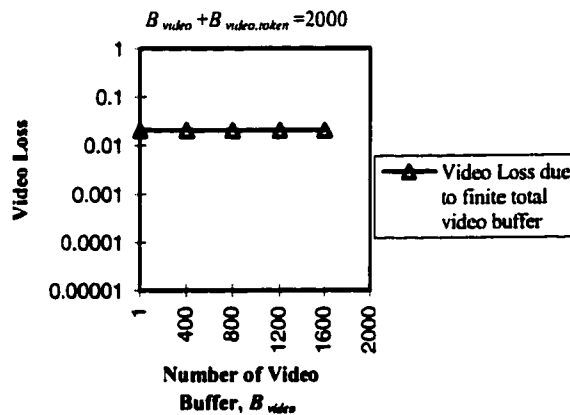


Fig. 4.8. MMPP video loss with respect to the input video buffer

Fig. 4.10 shows the MMPP video cell loss with respect to the total buffer size of the video buffer and the video token buffer, B_{vi} . The number of video buffer at the input buffer of a leaky bucket is fixed at 1. For acceptable video loss of 10^{-4} , the total buffer size must be approximately 14000.

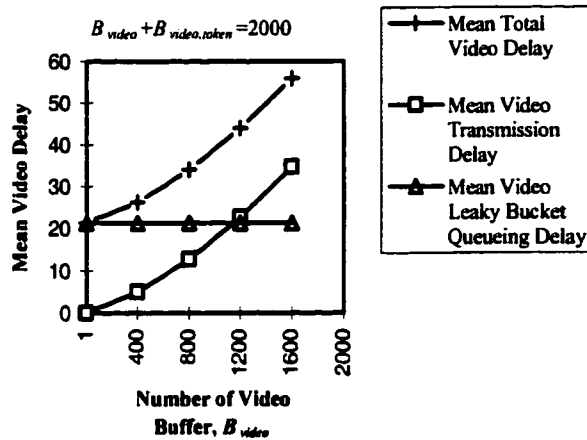


Fig. 4.9. Mean MMPP video delays with respect to the input video buffer

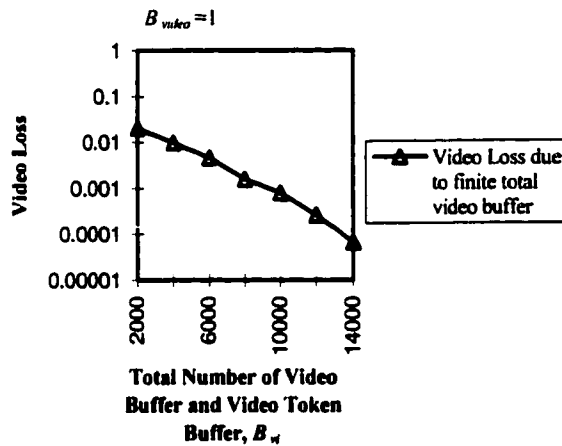


Fig. 4.10. MMPP video loss with respect to total buffer size

Fig. 4.11 shows the mean MMPP video transmission delay, the mean MMPP video queuing delay at the video buffer of the leaky bucket and the mean total MMPP video delay with respect to the total buffer size of the video buffer and the video token buffer, B_{vt} . The number of video buffer at the input buffer of a leaky bucket is again fixed at 1. From Fig. 4.11, with the video buffer size set to 1, the mean MMPP video leaky bucket

queueing delay is very small and the mean total MMPP video delay is almost equal to the mean MMPP video transmission delay. The mean MMPP video transmission delay remains relatively constant as the total buffer size increases.

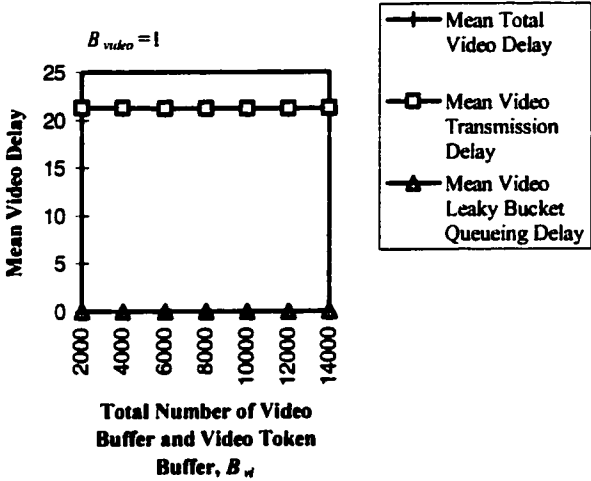


Fig. 4.11. Mean MMPP video delays with respect to total buffer size

4.3.3 Data Performance

Fig. 4.12 shows the data cell losses with respect to the number of data buffer at the input buffer of a leaky bucket with the sum of the size of the data buffer and the data token buffer fixed at 100. The data loss depends on the sum of the size of the data buffer and the data token buffer and not on their individual sizes.

Fig. 4.13 shows the mean data transmission delay (from portable terminal to the base station), the mean data queueing delay at the data buffer of the leaky bucket and the mean total data delay (which is the sum of the previous two delays) with respect to the number of data buffer at the input buffer of the data leaky bucket with the sum of the size of the data buffer and the data token buffer fixed at 100. Since the data loss remains constant (Fig. 4.12), the mean total data delay is lowest when the size of the data buffer is

one. This data delay is acceptable as data traffic is not time-critical. However, the total data loss is greater than 2%. Therefore, we need to consider the trade-off between data loss and the total buffer size of the data buffer and the data token buffer.

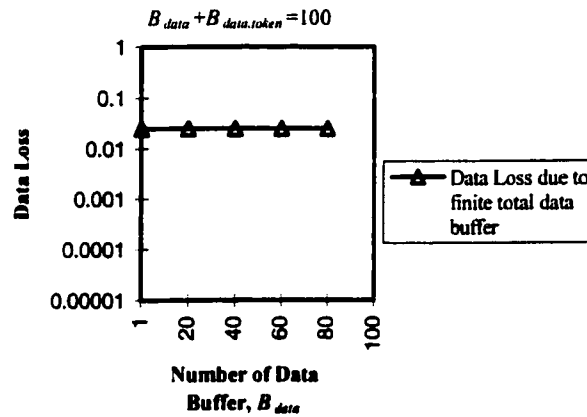


Fig. 4.12. Data loss with respect to the input data buffer

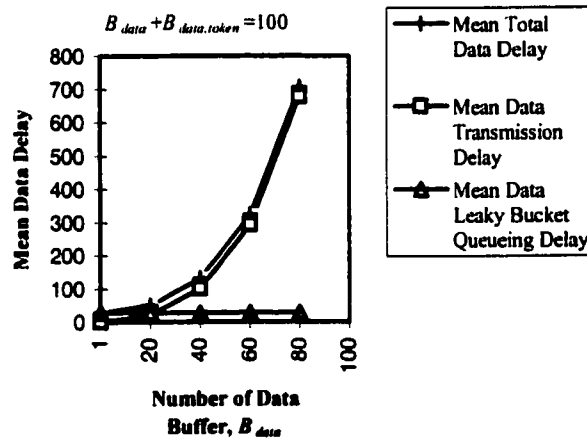


Fig. 4.13. Mean data delays with respect to the input data buffer

Fig. 4.14 shows the data cell loss with respect to the total buffer size of the data buffer and the data token buffer, B_d . The number of data buffer at the input buffer of a

leaky bucket is fixed at 1. For a data loss of 10^{-4} , the total buffer size must be approximately 280 (extrapolating the curve in Fig. 4.14). Assuming a physical transmission layer with BER of 10^{-4} , Forward Error Correction (FEC) or Automatic Repeat ReQuest (ARQ) must be used for retransmission if there is an error for data traffic. Data traffic needs a low BER of about 10^{-10} , while its delay is not time-critical.

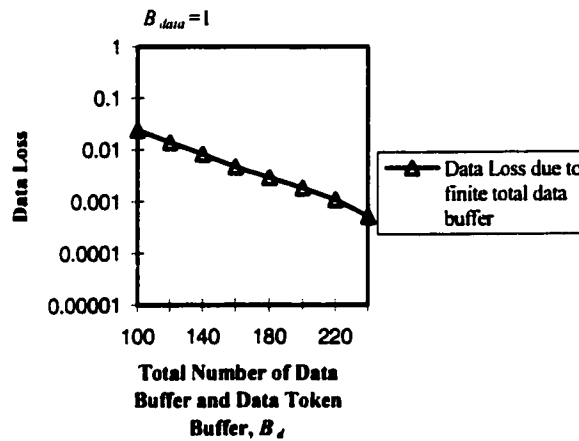


Fig. 4.14. Data loss with respect to total buffer size

Fig. 4.15 shows the mean data transmission delay, the mean data queueing delay at the data buffer of the leaky bucket and the mean total data delay with respect to the total buffer size of the data buffer and the data token buffer, B_d . The number of data buffer at the input buffer of a leaky bucket is again fixed at 1. From Fig. 4.15, with the data buffer size set to 1, the mean data leaky bucket queueing delay is very small and the mean total data delay is almost equal to the mean data transmission delay. The mean data transmission delay remains relatively constant as the total buffer size increases.

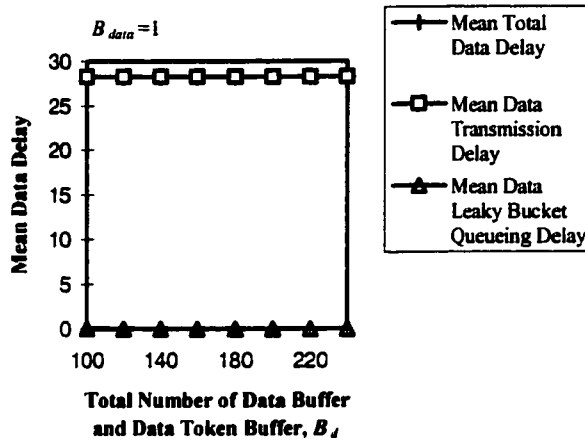


Fig. 4.15. Mean data delays with respect to total buffer size

4.4 Performance Analyses

4.4.1 Voice Traffic

Assuming the voice arrival process in Section 3.2.2.1 and light load condition, the voice loss due to front-end clippings of talkspurt and the mid-talkspurt voice loss due to insufficient information slots are almost zero. With these assumptions, the output voice process from the uplink MAC protocol is approximately equal to the input voice process to the uplink MAC protocol at the portable terminal. This input voice process is an On-Off process with an exponentially distributed “On” period and an exponentially distributed “Off” period. The output voice process from the uplink MAC protocol is the input voice process to the leaky bucket at the base station. Therefore, the input voice process to the leaky bucket can be approximated as the input voice process at the portable terminal. From [58], the probability of cell loss, P_{CL} , for such a leaky bucket model with exponentially distributed On/Off process, is given by

$$P_{CL} = \frac{b-a}{b} \frac{\lambda_1 - \lambda_2}{\lambda_1 e^{(\lambda_1 - \lambda_2)M} - \lambda_2}, \quad (4.1)$$

where a is the token generation rate in cells per second, b is the peak burst rate in cells per second, M is the buffer size of the input buffer and the token buffer, $\lambda_1 = 1/(b-a)h$, $\lambda_2 = 1/ak$, h is the mean “On” period in seconds and k is the mean “Off” period in seconds. For the voice traffic, $a = 1/1000T_l$, $b = 1/T_{TDMA}$, $M = B_v$, $h = \bar{t}_1$ and $k = \bar{t}_2$, where T_l is the size of an information slot, T_{TDMA} is the size of a TDMA frame, \bar{t}_1 is the mean talkspurt period and \bar{t}_2 is the mean silence period.

4.4.2 MMPP Video Traffic

The output video process from the uplink MAC protocol is an On/Off process. This process is also the input video process to the leaky bucket the base station. Assuming that there is no overload condition in the information slots, the number of tagged MMPP video packets that are transmitted in the i th frame for 1 MMPP video user, denoted by \tilde{R}_i , is equal to the number of tagged MMPP video packets user that arrive in the $(i-2)$ th frame for the tagged video. From equation (3.43), the pdf of \tilde{R}_i is given by

$$\Pr[\tilde{R}_i = r_i] = \sum_{v=1}^M \frac{\left[\frac{\lambda_v}{d_{video}} T_{TDMA} \right]^n e^{-\frac{\lambda_v}{d_{video}} T_{TDMA}}}{r_i!} h_v. \quad (4.2)$$

Let \tilde{W} denote the “On” period for the tagged video user. Its pdf is given by

$$\Pr[\tilde{W} = wT_l] = \Pr[\tilde{R}_i T_l = r_i T_l], \quad w = 1, 2, \dots, N_l, \quad (4.3)$$

where N_l is the number of information slots in a TDMA frame.

Next, let us find the pdf of the “Off” period for the tagged video user. Let \tilde{N}_i denote the number of voice users in the active (On) state or the number of voice packets for transmission in the i th TDMA frame. From equation (3.55), the pdf of \tilde{N}_i is given by

$$\Pr[\tilde{N}_i = n_i] = \binom{M_v}{n_i} P_{on}^{n_i} (1 - P_{on})^{M_v - n_i}. \quad (4.4)$$

Let \tilde{Y}_i denote the transmission order for the tagged video user among the M_{video} video users in the i th TDMA frame. Its pdf is given by

$$\Pr[\tilde{Y}_i = y_i] = \frac{1}{M_{video}}. \quad (4.5)$$

Let \tilde{Q} denote the number of video packets for transmission in the $(i-1)$ th TDMA frame with y_{i-1} number of video users including the tagged video user as the last user to transmit in this group of video users. Using the results of equation (3.46) and conditioning on \tilde{Y}_{i-1} , we have

$$\Pr[\tilde{Q} = q | \tilde{Y}_i = y_i] = \sum_{j_1=1}^M \sum_{j_2=1}^M \cdots \sum_{j_{y_{i-1}}=1}^M \frac{\left[\frac{\sum_{j=1}^{y_{i-1}} \lambda_{j_i}}{d_{video}} T_{TDMA} \right]^q}{q!} e^{-\frac{\sum_{j=1}^{y_{i-1}} \lambda_{j_i}}{d_{video}} T_{TDMA}} \prod_{j=1}^{y_{i-1}} h_{j_i}. \quad (4.6)$$

The number of information slots between the end of the video packet transmission of the tagged video user in the $(i-1)$ th TDMA frame to the end of the last information slot in same frame, \tilde{U} , is given by

$$\tilde{U} = N_i - \tilde{N}_{i-1} - \tilde{Q}. \quad (4.7)$$

Let \tilde{R} denote the number of video packets for transmission in the i th TDMA frame with (y_i-1) number of video users excluding the tagged video user who transmits after this group of video users. Using the results of equation (3.46) and conditioning on \tilde{Y}_i , we have

$$\Pr[\tilde{R} = r | \tilde{Y}_i = y_i] = \sum_{j_1=1}^M \sum_{j_2=1}^M \dots \sum_{j_{(y_i-1)}=1}^M \frac{\left[\frac{\sum_{l=1}^{y_i-1} \lambda_{j_l}}{d_{\text{video}}} T_{\text{TDMA}} \right]^r}{r!} e^{-\frac{\sum_{l=1}^{y_i-1} \lambda_{j_l}}{d_{\text{video}}} T_{\text{TDMA}}} \prod_{l=1}^{y_i-1} h_{j_l}. \quad (4.8)$$

The ‘‘Off’’ period of 1 MMPP video user, denoted by \tilde{V} , is the period between the last video packet that is transmitted by the tagged video user in the $(i-1)$ th TDMA frame and the first video packet that is transmitted by the tagged video user in the i th TDMA frame.

It is given by

$$\tilde{V} = \bar{T}''' + N_R T_R + (\tilde{U} + \tilde{N}_i + \tilde{R}) T_i, \quad (4.9)$$

where $\bar{T}''' = \left(\frac{T_{\text{TDMA}} - N_R T_R}{T_i} - \left\lfloor \frac{T_{\text{TDMA}} - N_R T_R}{T_i} \right\rfloor \right) T_i$, N_R is the number of request slots in a TDMA

frame, T_R is the size of a request slot and $\lfloor x \rfloor$ is the greatest integer smaller or equal to x .

Putting equation (4.7) into equation (4.9), we have

$$\tilde{V} = \bar{T}''' + N_R T_R + (N_i - \tilde{N}_{i-1} - \tilde{Q} + \tilde{N}_i + \tilde{R}) T_i. \quad (4.10)$$

Its pdf is given by

$$\Pr[\tilde{V} = \bar{T}''' + N_R T_R + \nu T_i] = \begin{cases} \sum_{n_{i-1}=0}^{M_\nu} \Pr[\tilde{N}_{i-1} = n_{i-1}] \sum_{y_{i-1}=1}^{M_{\text{video}}} \sum_{q=0}^{N_i - n_{i-1}} \Pr[\tilde{Q} = q | \tilde{Y}_{i-1} = y_{i-1}] \Pr[\tilde{Y}_{i-1} = y_{i-1}] \\ \times \sum_{n_i=0}^{M_\nu} \Pr[\tilde{N}_i = n_i] \sum_{y_i=1}^{M_{\text{video}}} \sum_{r=0}^{N_i - n_i} \Pr[\tilde{R} = r | \tilde{Y}_i = y_i] \Pr[\tilde{Y}_i = y_i], & \text{if } \nu = (N_i - n_{i-1} - q + n_i + r) \\ 0, & \text{otherwise} \end{cases}, \quad (4.11)$$

where $\nu = 0, 1, 2, \dots, 2N_i - 2$. Note that the ‘‘On’’ period and the ‘‘Off’’ period are not independent of each other. Thus, the analysis of the cell loss probability a leaky bucket with such a dependent On/Off process is difficult. Therefore, here, we try to get a lower bound, which may be very loose, for the cell loss probability of the leaky bucket.

Let α and β denote the mean “On” period and the mean “Off” period of the output video process from the uplink MAC protocol, respectively. From equations (4.3) and (4.11), α and β are given by

$$\alpha = T_I \sum_{w=1}^{N_I} w \Pr[\tilde{W} = wT_I], \quad (4.12)$$

and

$$\beta = T_I \sum_{v=1}^{2N_I-2} v \Pr[\tilde{V} = \bar{T}^{(v)} + N_R T_R + vT_I] + \bar{T}^{(N_I)} + N_R T_R. \quad (4.13)$$

To obtain a loose lower bound for the range of the total buffer size in Section 4.5.2, we use the analytical results in [58] to calculate the cell loss probability as in equation (4.1).

For the MMPP video user, $h = \alpha$ and $k = \beta$, $a = 1/(10/3T_I)$, $b = 1/T_I$ and $M = B_{vi}$.

4.5 Numerical Results

4.5.1 Voice Performance

Fig. 4.16 shows the voice loss with respect to the total buffer size, B_{vi} . The approximate analytical result is close to the simulation result. From Fig. 4.16, for a voice loss of 0.5%, the total buffer size is about 130.

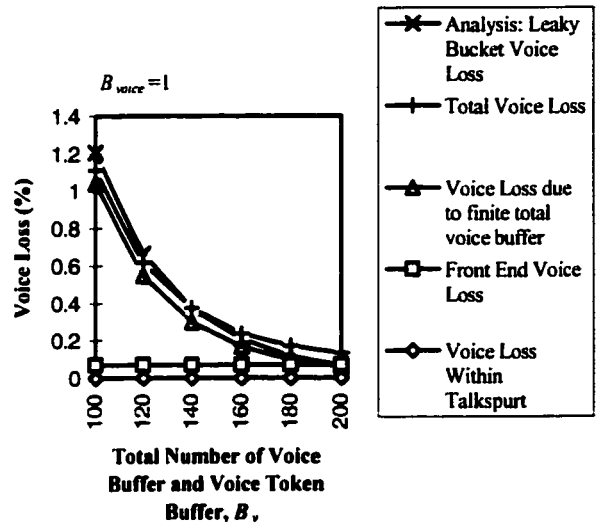


Fig. 4.16. Voice losses with respect to the total buffer size

4.5.2 MMPP Video Performance

Figs. 4.17 and 4.18 show the “On” period and “Off” period distributions to the leaky bucket. The analytical results are close to the simulation results.

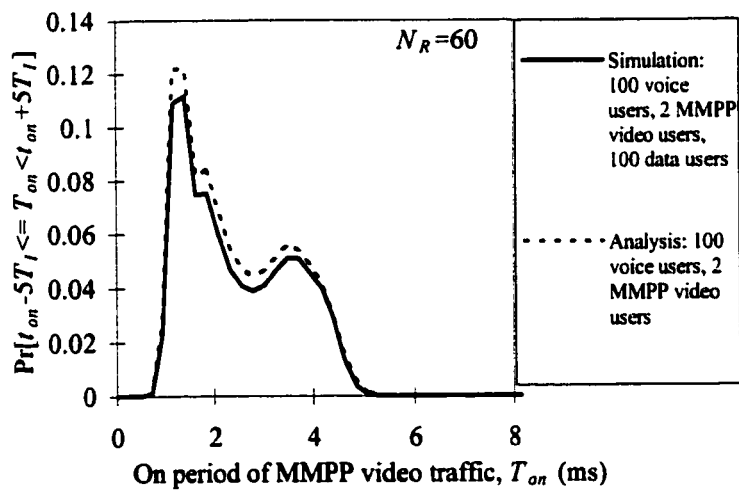


Fig. 4.17. “On” period distribution to the leaky bucket

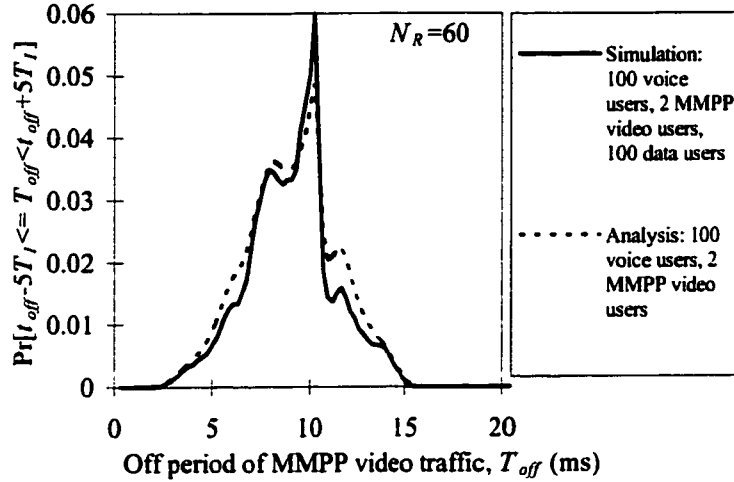


Fig. 4.18. “Off” period distribution to the leaky bucket

Table 4.1 shows the MMPP video loss in the leaky bucket from simulation results and from the loose lower bound. From the simulation results, for a video loss of 10^{-4} , the total buffer size is about 14000.

Table 4.1. MMPP video loss

Total Buffer Size, B_{vi}	MMPP Video Loss (Simulation)	MMPP Video Loss (Lower Bound)
2000	2.077×10^{-2}	2.112×10^{-5}
4000	9.893×10^{-3}	1.777×10^{-9}
6000	4.675×10^{-3}	1.495×10^{-13}
8000	1.587×10^{-3}	1.258×10^{-17}
10000	7.944×10^{-4}	1.059×10^{-21}
12000	2.587×10^{-4}	8.907×10^{-26}
14000	6.605×10^{-5}	7.494×10^{-30}

4.6 Summary

Our model of the UPC (leaky bucket) is described in Section 2.5. The leaky bucket is placed at the base station which is part of the network. The reasons why the leaky bucket is not placed in the portable terminal are (1) that users may cheat in their contract

made during connection setup by modifying the software used for traffic policing such that they can send more packets than that specified in the contract and (2) that the traffic characteristics are changed after passing through the uplink MAC protocol and may need to be policed again at the base station.

Considering the case where the total buffer size (input buffer size and token buffer size) is constant and the input buffer size is increased from 1 buffer size upwards, the traffic (voice, MMPP video or data) packet/cell loss remains constant while the leaky bucket queueing delay increases. Since the packet/cell loss is constant and leaking bucket queueing delay is increasing, we should keep the input buffer size at 1 for real-time traffic like voice and MMPP video so that their QoS for queueing delay at the leaky bucket are kept at a minimum. Note that the input buffers to the leaky buckets require memory spaces, while the token buffers can be implemented by counters.

With the QoS for queueing delay at the leaky bucket kept at a minimum, we should also consider the QoS for packet/cell loss. The traffic packet/cell loss decreases as the total buffer size increases. With the input buffer size kept at 1, this means that the token pool size is increased. To satisfy the QoS for packet/cell loss, we must increase the token pool size until the required packet/cell loss for the various traffic (voice, video or data) is met. For real-time voice traffic, the total packet/cell loss requirement is 0.5 percent which can be met with the total buffer size of about 130. For real-time MMPP video traffic, the cell loss requirement is assumed to be 10^{-4} which can be met with the total buffer size of about 14000. With these constraints, we can then determine the corresponding token pool sizes that can satisfy these requirements. For non-time critical

data traffic, the BER is about 10^{-10} . This cannot be met by a physical transmission layer with BER of 10^{-4} . FEC or ARQ must be used for retransmission if there is an error for data traffic.

The token generation rates for the traffic sources considered in this chapter are set according to their equivalent capacities in Chapter 6.

In this chapter, an approximate analysis of voice loss is provided and loose lower bound for the range consider in Section 4.5.2 is obtained for MMPP video loss. The On/Off video process to the leaky bucket at the base station is characterized. The pdfs of the On and Off periods are obtained using the analytical results in Section 3.4.2 (equations (3.43) and (3.45)). These results give the pdfs for the number of video packets arriving in a time duration for a MMPP video user and for a superposition of a number of MMPP video users.

The simulation models in this chapter is also used to evaluate the performance of MPEG video traffic in the next chapter.

Chapter 5

MPEG Video Traffic

5.1 Introduction

In Chapter 3 and Chapter 4, we have studied the performance of the uplink MAC protocol and the UPC with voice, MMPP video and data traffic. An MMPP video model allows its delay performance analysis for the uplink MAC protocol and also for characterizing the output process from this protocol. On the other hand, we can also study the performance of the uplink MAC protocol and the UPC with Motion Picture Experts Group (MPEG) source sequence using computer simulation.

The first part of this chapter describes the simulation model for MPEG video traffic. The uplink MAC protocols and the UPC are also described. In this simulation study, front end voice clippings and voice clippings within a voice talkspurt are considered. In the latter part of this chapter, some simulation results for the uplink MAC protocols and the UPC are discussed. In the simulation model for MAC protocols, only voice losses are considered but not video and data losses. All video and data packets are buffered at the portable terminals. But all traffic cell losses are considered at the leaky bucket.

5.2 Simulation Model

The simulation models are the same as those in Section 3.2 and Section 4.2 except that the MMPP video arrival process is replaced by MPEG video arrival process, two uplink MAC protocols are considered and the “equivalent” number of MPEG video users is calculated in Section 5.2.3.

5.2.1 MPEG Arrival Process

The MPEG source sequence used here is obtained from the internet via anonymous ftp from ftp.bellcore.com in directory pub/vbr.video.trace. There is a file in the directory called MPEG.data which contains 174136 integers giving the frame size in bits for the movie “Star Wars”. This data set represents the output bandwidth of a variable bit rate (VBR) video coder which conforms to the MPEG-1 standard. The frame rate is 24 frames per second. Each integer in the data file corresponds to the number of bits generated in each frame. This video data is packetized such that video packets are generated consecutively from the start of each frame with AAL type 5. Each video packet size corresponds to an information slot in the information slot subframe. Each video source has a mean rate of 374 kbps. Each of the starting frame in the other video sources are offset from that of the first video source by a multiple of 200 video frames.

5.2.2 MAC Protocols

5.2.2.1 Protocol 1

Protocol 1 is the same uplink MAC protocol, as described in Chapter 2, in which video traffic have priority over voice traffic in the information slot subframe.

5.2.2.2 Protocol 2

Protocol 2 is basically the same as Protocol 1 except that voice traffic have priority over video traffic in the information slot subframe.

5.2.3 “Equivalent” number of MPEG video sources

The MMPP video arrival process is modelled as an 8-state MMPP. The number of phases is $M = 8$, while the slot time, $d_{video} = 16.96 \mu\text{s}$. The $M \times M$ phase transition probability matrix in a slot time, $\mathbf{H} = [h_{ij}]$, ($1 \leq i, j \leq M$), is given by equation (3.2). In the

simulation model, h_{ii} is calculated as $(1 - \sum_{\substack{j=1 \\ i \neq j}}^M h_{ij})$ to ensure that the probabilities sum to unity. The steady state probability distribution that the video traffic is in state i , is denoted by h_i . The steady state probability matrix, $\mathbf{h} = [h_1, h_2, \dots, h_M]^T$, can be calculated iteratively by equation (3.41). The MMPP video cell generation rate per video slot while in phase i is denoted by $\lambda_{i,slot}$, ($1 \leq i \leq M$). The arrival rate matrix is given by equation (3.3). The MMPP video cell generation rate per second while in phase i is denoted by $\lambda_{i,sec}$, ($1 \leq i \leq M$) and is given by

$$\lambda_{i,sec} = \lambda_{i,slot} / d_{video} . \quad (6.1)$$

The mean number of MMPP cells generated per second, $\bar{\lambda}$, is given by

$$\bar{\lambda} = \sum_{i=1}^M h_i \lambda_{i,sec} . \quad (6.2)$$

Assuming AAL type 5, the mean MMPP code rate, R_{MMPP} , is given by

$$R_{MMPP} = 48 \times 8 \times \bar{\lambda} . \quad (6.3)$$

The mean MPEG code rate, R_{MPEG} , is 374 kbps. Therefore, mean “equivalent” number of MPEG video users, $M_{video,MPEG}$, is given by

$$M_{video,MPEG} = \frac{M_{video,MMPP} R_{MMPP}}{R_{MPEG}} = 19 , \quad (6.4)$$

where $M_{video,MMPP}$ is the number of MMPP video users which is equal to 2.

5.3 MAC Performance

5.3.1 Simulation Results

Each simulation point has been obtained by running the simulation for a duration of 100000 TDMA frames with five simulation runs. The parameters are the same as those

in Chapter 3. However, the 2 MMPP video sources in Chapter 3 are replaced by 19 MPEG video sources except otherwise stated.

5.3.1.1 Protocol 1

Fig. 5.1 shows the mean queueing delay of video for various numbers of request slots with Protocol 1. The MPEG video traffic has a higher mean video packet queueing delay than that of the MMPP video traffic under “equivalent” load. The MPEG video traffic has a mean video packet queueing delay of about 28 ms, while the MMPP video traffic has a delay of about 21 ms.

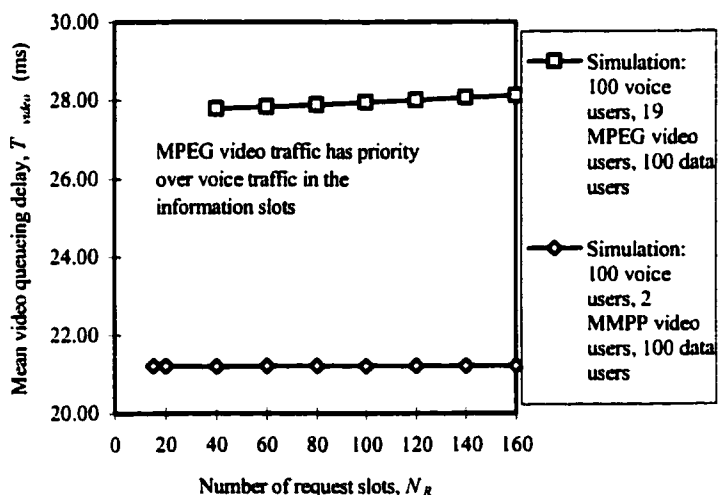


Fig. 5.1. Mean video packet queueing delay with Protocol 1

Fig. 5.2 shows the distribution of video packet queueing delay assuming each frame has 60 request slots. All MMPP video packets are transmitted within 30.16 m, while all MPEG video packets are transmitted within 79.81 ms. In [33], it is stated that compressed video can tolerate a maximum delay of 100 ms while preserving good real-time interactivity.

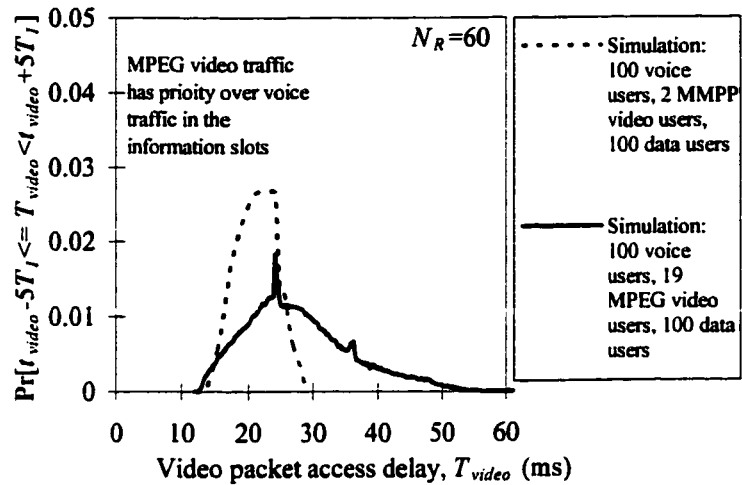


Fig. 5.2. Distribution of video packet queuing delay with 60 request slots with Protocol 1

Fig. 5.3 shows the front-end, mid-talkspurt and total voice clippings. Voice traffic is handled on a loss basis in the sense that voice packets that are not transmitted after a given queuing delay (2 request slot contentions) are dropped. This results in front-end clipping of talkspurt. In addition, because video traffic has higher priority access to information slots than voice traffic (Protocol 1), during temporary video overloads, some voice talkspurt can be deprived of the information slots. This results in mid-talkspurt clippings. Fig. 5.3 shows that the total voice clipping (with 19 MPEG video users) is more than 30 % which is not acceptable. Note that for telephony speech quality, loss of voice information exceeding 0.5 % is generally unacceptable.

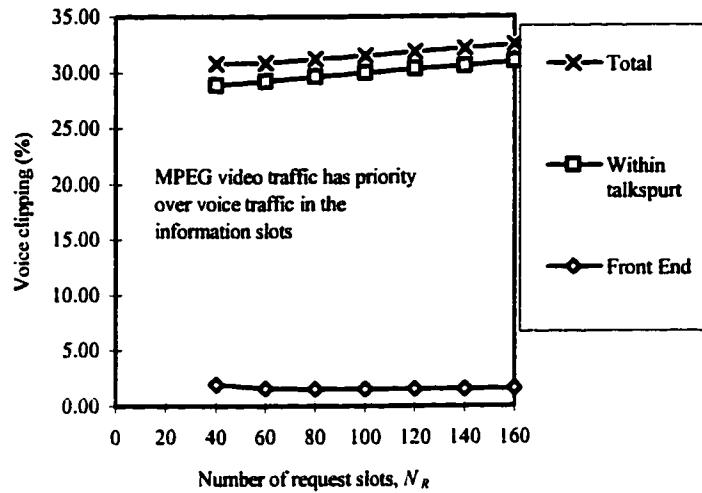


Fig. 5.3. Percentage voice clipping for 100 voice users, 19 MPEG video users and 100 data users with Protocol 1

Fig. 5.4 shows that the total voice clipping (with 2 MMPP video users) is less than 0.5 % which is acceptable. The mid-talkspurt clipping for the voice sources with 2 MMPP sources is zero. This implies that there is sufficient information slots for both the video and voice users. Therefore, all the results for the case with 2 MMPP video users are the same for both Protocol 1 and Protocol 2.

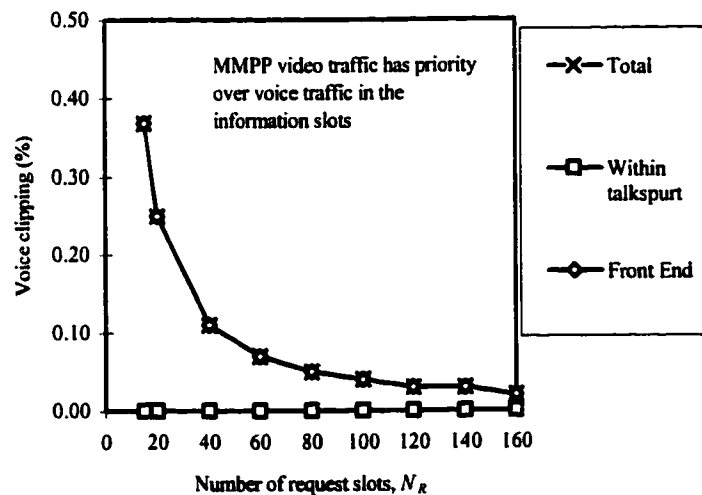


Fig. 5.4. Percentage voice clipping for 100 voice users, 2 MMPP video users and 100 data users with Protocol 1

Fig. 5.5 shows the front-end, mid-talkspurt and total voice clipping with respect to the number of MPEG video sources. The number of request slots is set at 60. For the total voice clipping to be below 0.5 %, the number of MPEG video sources must be 5 or less.

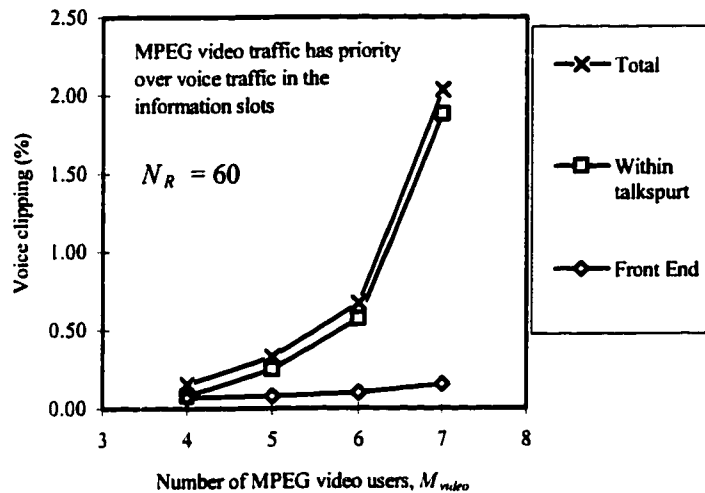


Fig. 5.5. Voice clippings with respect to the number of MPEG video users (with 100 voice users and 100 data users) for Protocol 1

5.3.1.2 Protocol 2

Fig. 5.6 shows the mean queueing delay of video for various numbers of request slots with Protocol 2. The MPEG video traffic has a higher mean video packet queueing delay than that of the MMPP video traffic under “equivalent” load. The MPEG video traffic has a mean video packet queueing delay of about 28.5 ms, while the MMPP video traffic has a delay of about 21 ms. Note that the mean MPEG video packet queueing delay for Protocol 2 is only slightly higher than that for Protocol 1 (compare Fig. 5.1 with Fig. 5.6).

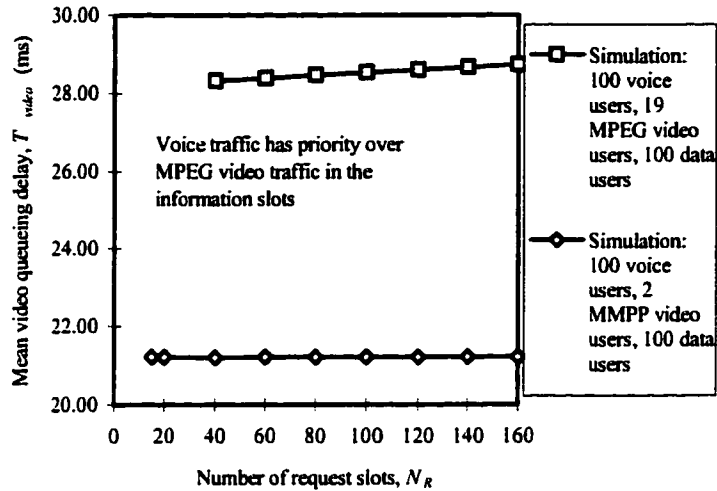


Fig. 5.6. Mean video packet queuing delay with Protocol 2

Fig. 5.7 shows the distribution of video packet queuing delay assuming each frame has 60 request slots. All MMPP video packets are transmitted within 30.16 m, while all MPEG video packets are transmitted within 83.29 ms (still less than the 100 ms QoS requirement for good real-time interactivity).

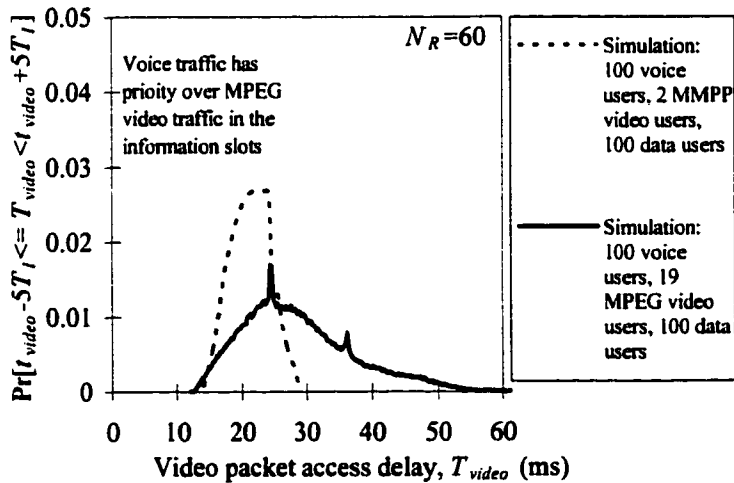


Fig. 5.7. Distribution of video packet queuing delay with 60 request slots for Protocol 2

Fig. 5.8 shows the front-end, mid-talkspurt and total voice clippings. Voice traffic is handled on a loss basis in the sense that voice packets that are not transmitted after a given

queueing delay (2 request slot contentions) are dropped. This results in front-end clipping of talkspurt. However, because voice traffic has higher priority access to information slots than video traffic (Protocol 2), during temporary video overloads, no voice talkspurt can be deprived of the information slots. This eliminates the mid-talkspurt clipping. Fig. 5.8 shows that the total voice clippings (with 19 MPEG video users) is not exceeding than 0.2 % for 40 or more request slots, which is acceptable. Note that for telephony speech quality, loss of voice information not exceeding 0.5 % is generally acceptable.

The mean MPEG video packet queueing delays for both Protocol 1 and Protocol 2 (about 28 ms and 28.5 ms, respectively) is higher than the mean MMPP video packet queueing delay (about 21 ms) under “equivalent” load.

Protocol 2 has a slightly higher mean MPEG video packet queueing delay than that of Protocol 1. However, Protocol 2 has an acceptable voice clipping loss with MPEG sources as compared to an unacceptable voice clipping in Protocol 1 with 19 MPEG sources. In both cases, the MPEG video satisfies the real-time QoS requirement of transmitting their packets within 100 ms for good interactivity. Otherwise, the “late” video packets would be discarded at the destination.

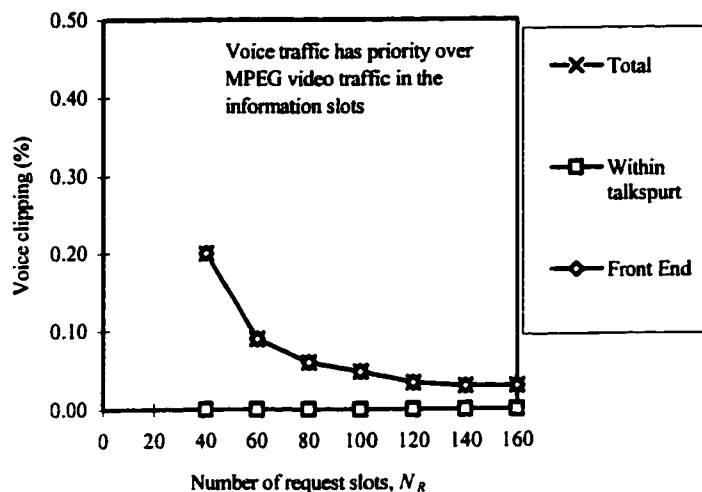


Fig. 5.8. Percentage voice clipping with 100 voice users, 19 MPEG video users and 100 data users for Protocol 2

5.4 UPC Performance

5.4.1 Simulation Results

Each simulation point has been obtained by running the simulation for a duration of 100000 TDMA frames with three simulation runs. The parameters are the same as those in Section 4.3. However, the 2 MMPP video sources in Chapter 4 are replaced by 5 MPEG video sources and 19 MPEG video sources for Protocol 1 and Protocol 2, respectively.

The equivalent capacity of 1 MMPP video source is set at 6 Mbps. The bandwidth of 1 MMPP video source is approximately 10 times that of 1 MPEG source. So, the equivalent capacity of 1 MPEG source is set at 600 kbps (above its mean rate of 374 kbps). The token generation rate of the leaky bucket is also set at this rate, i.e., 600 kbps.

5.4.1.1 Protocol 1

From simulation results in Section 5.3.1.1, Protocol 1 causes high voice packet droppings. Therefore, we will not consider the performance of the usage parameter

control for 19 MPEG video sources under Protocol 1. Instead, we will consider the performance for 5 MPEG video sources which allows the voice packet dropping to be below 0.5 %. Fig. 5.9 shows the MPEG video cell loss with respect to the total buffer size of the video buffer and the video token buffer, B_{vt} . The number of video buffer at the input buffer of a leaky bucket is fixed at 1. For acceptable video loss of 10^{-4} , the total buffer size must be approximately 190 (from Fig. 5.9).

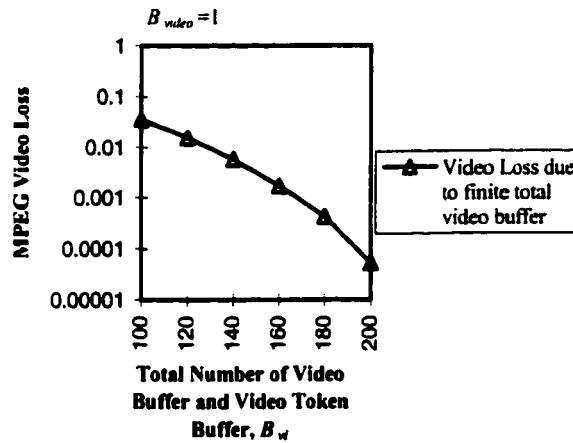


Fig. 5.9. MPEG video loss with respect to total buffer size (with 100 voice users, 5 MPEG video users and 100 data users) for Protocol 1

5.4.1.2 Protocol 2

Fig. 5.10 shows the MPEG video cell loss with respect to the total buffer size of the video buffer and the video token buffer, B_{vt} . The number of video buffer at the input buffer of a leaky bucket is fixed at 1. For acceptable video loss of 10^{-4} , the total buffer size must be approximately 8000 (extrapolating the curve in Fig. 5.10).

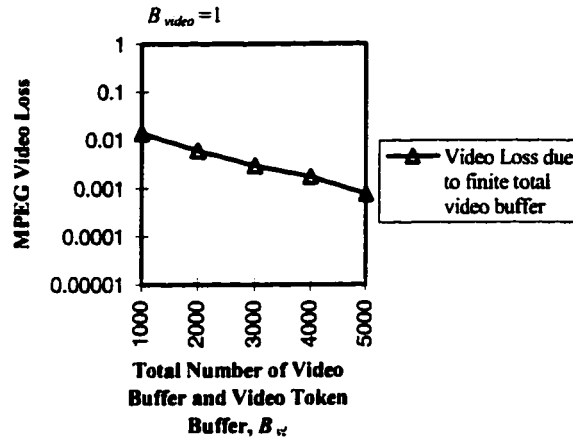


Fig. 5.10. MPEG video loss with respect to total buffer size (with 100 voice users, 19 MPEG video users and 100 data users) for Protocol 2

5.5 Summary

Models for video traffic are still not well established. Instead of using MMPP video model to obtain tractable analysis and some performance measures of the MAC and UPC in Chapter 3 and 4, we can also get such performance results by using MPEG video traces. The traces are also dependent on the type of video sources. For example, if the video source is capturing an action movie like “Starwars”, then the video source is very bursty as the scene changes a lot and if the video source is capturing a video conferencing where the scene does not change too much, then the video source is less bursty.

Simulation results show that acceptable QoS for voice, MPEG video and data can be achieved in the wireless segment that support 100 voice, 100 data and 5 or 19 MPEG video users for Protocols 1 and 2, respectively. The reason for being able to support only 5 MPEG video users for Protocol 1 may be that the source is very bursty as the video traces are from “Starwars”. For real-time MPEG video traffic with a cell loss of 10^{-4} , the

**total buffer size of the leaky bucket is about 190 for Protocol 1 with 5 MPEG video users
and about 8000 for Protocol 2 with 19 MPEG video users.**

Chapter 6

Connection Admission Control

6.1 Introduction

CAC to a VCT has been proposed and studied for a homogeneous traffic in [47]. However, for wireless ATM networks, the traffic is heterogeneous. Therefore, in this Chapter, the CAC to a VCT is extended to handle heterogeneous traffic based on equivalent capacity. New performance metrics are also modeled by mathematical analysis. Equivalent capacities for different traffic sources have been proposed in the literature [48,73-78]. In our study, we assume that the equivalent capacity for each connection is between its mean and peak capacity.

The VCT concept is employed to overcome the problem of frequent network call processor in a micro-cellular wireless ATM network. A number of virtual circuit numbers (VCNs) are given to the mobile user during connection setup. These VCNs enable the mobile users to move from one base station to another base station in the VCT without the involvement of the network call processor. Resources have to be allocated in each base station in the VCT for every connection of the mobile user.

In this chapter, we study the CAC model proposed in Chapter 2 for admission to the VCT. We propose two CAC approaches for admission to the VCT based on equivalent capacity for heterogeneous traffic. We study the performance of one of these approaches by mathematical analysis and the other approach by computer simulation. The quality of service performance are the overload probability in a base station and the %

overload period in a base station. The other new performance metrics are the reserved capacity, standby capacity, probability of migrating to adjacent or surrounding base stations and the mean frequency of handoffs to the adjacent or surrounding VCTs. In this study, we also consider both one-dimensional and two-dimensional mobility models.

6.2 Performance Analysis

For notational convenience, we list below the parameters used throughout this chapter:

B = the number of base stations supported by a given VCT.

C_0 = the allocated capacity of the test base station.

C_N = the equivalent capacity of the entire VCT.

C_i = the equivalent capacity used in the test base station.

P_o = the probability that the equivalent capacity used in the test base station exceeds the allocated capacity.

P_u = the probability that the equivalent capacity used in the test base station is less than or equal to the allocated capacity.

C_{ik} = the equivalent capacity of the i th connection belonging to the k th class.

n_{jk} = the number of class k connections in the j th base station.

K = the total number of traffic classes supported.

M_i = the number of class i traffic users that can be supported at a single base station.

C_R = the equivalent capacity that must be reserved at the root of the VCT.

C_S = the standby capacity.

Since mobile users can migrate from one base station to another within the VCT without incurring handoff, overload can occur if and only if the equivalent capacity of all the active mobiles in a test base station temporarily exceeds the base station capacity, i.e., if $C_N > C_0$. One way to prevent this is to limit the equivalent capacity, C_N , in the entire VCT to a value less than or equal to C_0 . However, this is wasteful of link capacity. Another way is to exploit statistical multiplexing gain and admit a larger equivalent capacity such that overload is possible but very unlikely (i.e., $C_0 < C_N < BC_0$, where B is the number of base stations in the VCT). When an overload occurs, the quality of service in the overloaded base station is temporarily degraded. One of the performance metrics that we are considering is the overload probability, P_o , with respect to the maximum equivalent capacity in the VCT, C_N . Let C_t be the equivalent capacity used in a test base station. Then, the underload probability is given by

$$P_u = \Pr[C_t \leq C_0], \quad (6.1)$$

and the overload probability is given by

$$P_o = \Pr[C_0 < C_t \leq C_N] = 1 - P_u. \quad (6.2)$$

The pertinent parameters that govern the behaviour of a VCT in terms of connection admission and probability of handoff, i.e., mobile user migrating outside of its home region, are B , C_N and P_o . A large value of B means a small probability of handoff, but requires a larger amount of standby capacity. B can be considered as a “reuse” factor which needs to be chosen to give the best tradeoff in terms of probability of handoff and standby capacity requirement. A performance metric for CAC is the maximum useable

equivalent capacity, C_N , for a tolerable overload probability and a given number of base stations.

Considering K -classes of traffic, we have

$$C_t = \sum_{k=1}^K \sum_{i=1}^{n_{jk}} C_{ik}, \quad (6.3)$$

where n_{jk} is the number of class k connections in the j th base station and C_{ik} is the equivalent capacity of the i th connection of the class k connections. The maximum equivalent capacity for the VCT is given by

$$C_N = \sum_{j=1}^B \sum_{k=1}^K \sum_{i=1}^{n_{jk}} C_{ik}. \quad (6.4)$$

Let M_i be the number of class i traffic users that can be supported on one base station for a wireless ATM access network. The maximum equivalent capacity in a VCT, C_N , is varied such that the ratio among the K -classes of traffic is kept at a constant ratio of $R_1:R_2:\dots:R_K$. This equivalent capacity is then given by

$$C_N = n \left(\sum_{k=1}^K M_k C_{ik} \right), \quad (6.5)$$

where $n = 2, 3, 4, \dots$ and $C_0 < C_N < BC_0$. The connections in the VCT are assumed to be equally and independently distributed among the base stations in the VCT. The underload probability is then given by

$$P_u = \sum_{k_1=0}^{K_1} P_{k_1} \sum_{k_2=0}^{K_2} P_{k_2} \dots \sum_{k_K=0}^{K_K} P_{k_K}, \quad (6.6)$$

where

$$P_{k_i} = \binom{nM_i}{k_i} \left(\frac{1}{B} \right)^{k_i} \left(1 - \frac{1}{B} \right)^{nM_i - k_i},$$

and

$$K_j = \min \left[\left\lfloor \frac{C_0 - \sum_{m=1}^{j-1} k_m C_{im}}{C_{ij}} \right\rfloor, nM_j \right], i, j = 1, 2, \dots, K.$$

The symbol $\lfloor x \rfloor$ denotes the greatest integer smaller than or equal to x . The overload probability is then given by equation (6.2). Let C_R be the equivalent capacity that must be reserved at the root of the virtual connection tree for all connections in the VCT. It is given by

$$C_R = B \times \frac{53}{58} C_N. \quad (6.7)$$

The constant fraction in equation (6.7) is due to the data block (cell) size in the wired ATM network and the packet size in the wireless ATM network (see Section 2.3.1.8). The variable B in equation (6.7) is due to the sum of the resources that need to be reserved for all the base stations in the VCT which enable a mobile to move from one base station to another within the VCT without handoff. This is done using the VCNs assigned during the connection setup phase and the paths of these connections traverses through the root of the VCT. Let C be the link capacity of the root ATM switch. If $C_R \leq C$, then the corresponding value of the number of base stations is the number of base stations that can be supported in the VCT. The largest value of B that can satisfy this condition is the upper limit that can achieve a certain overload probability. The standby capacity, C_S , is related to C_R by

$$C_S = \frac{B-1}{B} C_R = (B-1) \left(\frac{53}{58} C_N \right). \quad (6.8)$$

The term $(B-1)$ in equation (6.8) is due to the other base stations in the VCT that each of the connections of the mobiles in the VCT can switch to by reserving standby capacity in the VCT. From equation (6.8), the larger the number of base stations in a VCT, B (diameter of the VCT), the larger the standby capacity, C_s , required.

Next, let us consider the VCTs to have base stations overlaying each other in a linear manner (highways and streets) for a one-dimensional mobility model with 2 directions of movement. Let p be the probability that a mobile user hands off to adjacent VCTs. Assuming that the mobile user is equally distributed among the base stations in the VCT and the probability of migrating to the adjacent base stations to be equally distributed, the probability, p , is given by

$$p = 2\left(\frac{1}{B} \cdot \frac{1}{2}\right) + (B-2)\left(\frac{1}{B} \cdot 0\right) = \frac{1}{B}, \quad (6.9)$$

where the first term in (6.9) is due to the mobile user's handoffs to adjacent VCTs on both ends of the VCT where the mobile user is in, and the second term is due to the mobile user moving to adjacent base stations in the VCT.

Next, let us consider a two-dimensional mobility model with 6 directions of movement; that is, we are considering hexagonal cells. Let p be the probability that a mobile user hands off to surrounding VCTs. Assuming that the mobile user is equally distributed among the base stations in the VCT and the probability of migrating to the surrounding base stations to be equally distributed, the probability, p , is given by

$$p = \left(\frac{1}{B}\right)\left(\frac{1}{6}\right)\sum_{i=1}^6 N_i \cdot i, \quad (6.10)$$

where i is the number of ways that a mobile user can move out of the VCT and N_i is the number of cells in the VCT that allows the mobile user to do so with i ways.

Let the number of mobile users in a VCT be M ; it is given by

$$M = n \sum_{k=1}^K M_k . \quad (6.11)$$

Let X be the number of mobile users at the ends of a VCT which handoff to the adjacent VCTs for the one-dimensional mobility model and it is the number of mobile users in the VCT which handoff to the surrounding VCTs for the two-dimensional mobility model. Then it is binomially distributed with pdf given by

$$p_X(x) = \binom{M}{x} p^x (1-p)^{M-x} , \quad (6.12)$$

and mean value given by

$$\bar{X} = Mp . \quad (6.13)$$

Assuming that the time spent by a mobile user in a cell, T_{in} , is exponentially distributed with a mean rate of $1/\bar{T}_{in}$, the mean frequency of handoffs to adjacent/surrounding VCTs, \bar{F} , for the one-dimensional mobility model or the two-dimensional mobility model is given by

$$\bar{F} = \frac{\bar{X}}{\bar{T}_{in}} . \quad (6.14)$$

6.3 Numerical and Simulation Results

The numerical results presented in this section are obtained using the analysis of Section 6.2 and by simulation. We consider 3 classes of traffic for both the overload probability analyzed in Section 6.2 and the % overload period in this simulation study.

The % overload period is defined as the sum of overload periods in a base station over the warm-up time to the end of the simulation time. The results are obtained from a simulation model of the VCT based on the SMPL simulation kernel described in [79]. Each simulation point has been obtained by running the simulation for a duration of 10^6 s with five simulation runs. We assume that, upon newly entering a given cell site, the time spent by a portable user in the cell is exponentially distributed with a mean value of 10 s.

Let M_{video} , M_{voice} and M_{data} be the number of video, voice and data users that can be supported in one base station for a wireless ATM access network. We use the scenario from [12], where $M_{video} = 2$, $M_{voice} = 100$ and $M_{data} = 100$. We consider a VCT with the following parameters: the number of base stations in the VCT is $B = 3$ to 10; the maximum capacity in a base station is $C_0 = 20$ Mbps; the equivalent capacity of a class 1 (video) connection in a base station is $C_{i1} = 6$ Mbps; the equivalent capacity of a class 2 (voice) connection in a base station is $C_{i2} = 20$ kbps; the equivalent capacity of a class 3 (data) connection in a base station is $C_{i3} = 10$ kbps. The maximum equivalent capacity in a VCT, C_N , is varied such that the ratio among the video, voice and data traffic is kept at a constant ratio of 12:2:1 ($M_{video} C_{i1} : M_{voice} C_{i2} : M_{data} C_{i3}$). This equivalent capacity is then given by

$$C_N = n(M_{video} C_{i1} + M_{voice} C_{i2} + M_{data} C_{i3}), \quad (6.15)$$

where $n = 2, 3, 4, \dots$ and $C_0 < C_N < BC_0$.

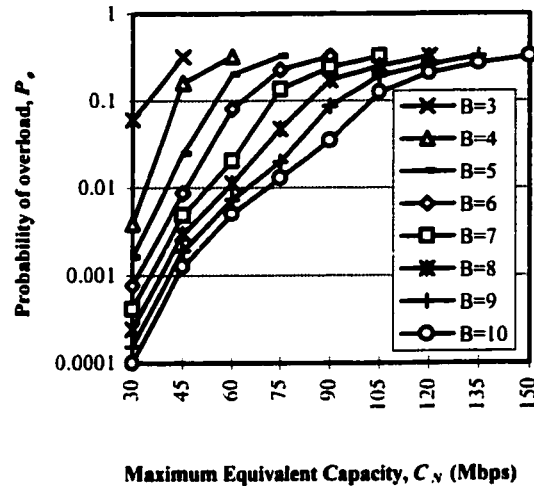


Fig. 6.1. Maximum equivalent capacity connection admissibility based upon guaranteed overload probability

Fig. 6.1 shows the overload probability as a function of the maximum equivalent capacity admitted to a VCT, C_v , with the number of base station, B , varying from 3 to 10. For an overload probability of 1 %, the maximum equivalent capacities that can be admitted to the VCT for $B = 4$ to 10 are shown in Table 6.1. Note that with $B = 3$, an overload probability of 1 % cannot be achieved. $B = 4$ is the lower limit that can achieve an overload probability of 1 %. From Table 6.1, for $C = 155$ Mbps, $B = 4$ ($C_R < C$), while for $C = 622$ Mbps, $B = 4$ to 9. Therefore, to implement the VCT concept to avoid the need to involve the network call processor for every cell handoff in a cellular ATM network, we have to allocate a large amount of standby capacity, C_s . Let us first consider the one-dimensional mobility model. From Table 6.1, as B increases, the frequency of handoffs between VCTs decreases. However, this gain will require a larger standby capacity as B increases. So, the selection of the value of B is a tradeoff between the frequency of handoffs between VCTs and the corresponding standby capacity. Inspection

of Table 6.1 shows that the standby capacity is a more sensitive parameter than the mean frequency of handoff to adjacent regions.

Table 6.1. Number of base stations in a VCT that can be supported by a root ATM switch for an overload probability of 1 %

B	C_N (Mbps)	C_R (Mbps)	C_S (Mbps)	\bar{F} (s^{-1})	$C=155$ Mbps	$C=622$ Mbps
4	34	124.3	93.2	11.4	×	×
5	39	178.2	142.6	10.5		×
6	46	252.2	210.2	10.3		×
7	53	339.0	290.6	10.2		×
8	59	413.3	377.4	9.9		×
9	64	526.3	467.9	9.8		×
10	71	648.8	583.9	9.6		

Fig. 6.2 shows the % overload period as a function of the maximum equivalent capacity admitted to a VCT, C_N , with the number of base station, B , varying from 3 to 10. For example, if the desired value of C_N is 60 Mbps at 1 % overload period, the number of base stations has to be at least 8. As shown in Table 6.2, a proportionally large amount of standby capacity is required.

Table 6.2 shows the number of base stations in a VCT that can be supported by a root ATM switch for 1 % of overload period. From Table 6.2, for $C = 155$ Mbps, $B = 4$, while for $C = 622$ Mbps, $B = 4$ to 9. The results obtained here is similar to that obtained by the overload probability approach.

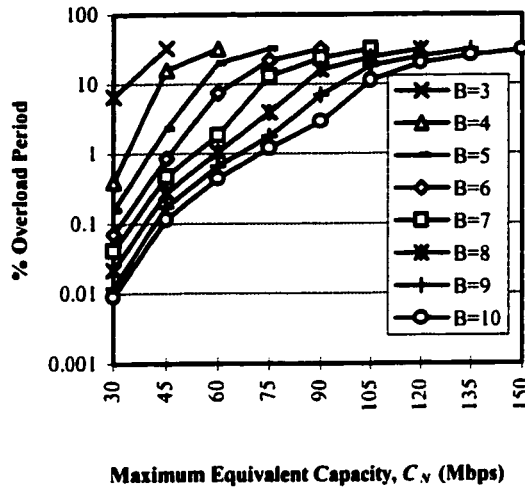


Fig. 6.2. Maximum equivalent capacity connection admissibility based upon % overload period

Table 6.2. Number of base stations in a VCT that can be supported by a root ATM switch for 1 % of overload period

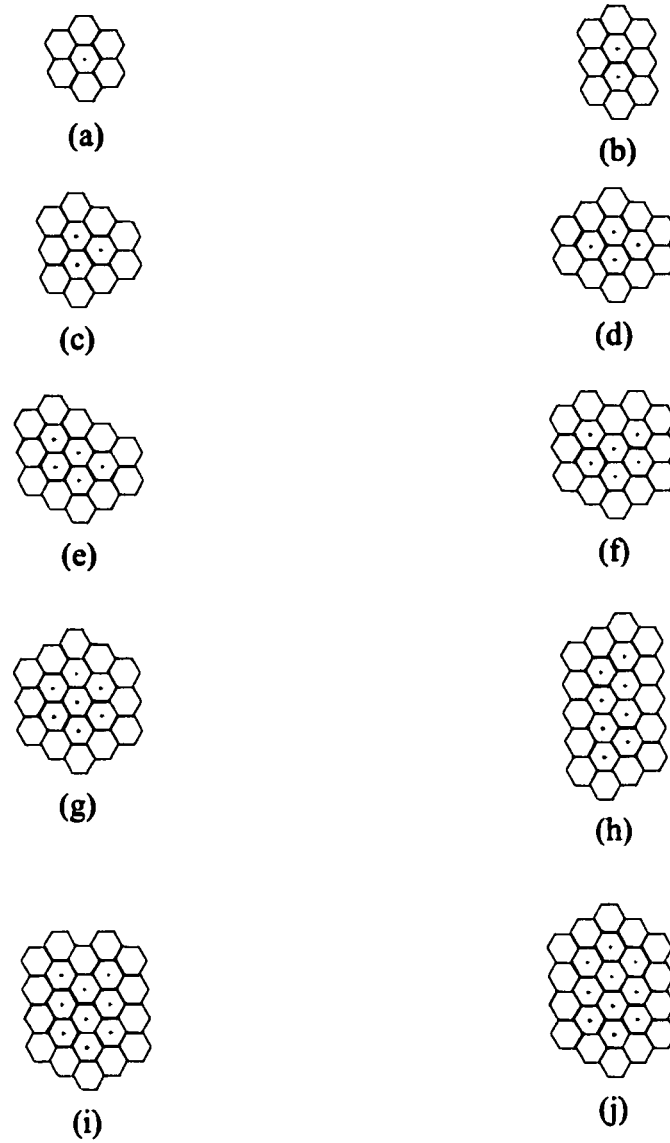
B	C_V (Mbps)	C_R (Mbps)	C_S (Mbps)	\bar{F} (s^{-1})	$C=155$ Mbps	$C=622$ Mbps
4	33	120.6	90.5	11.1	×	×
5	38	173.6	138.9	10.2		×
6	45	246.7	205.6	10.1		×
7	52	332.6	285.1	10.0		×
8	59	431.3	377.4	9.9		×
9	64	526.3	467.9	9.8		×
10	71	648.8	583.9	9.6		

Next, let us consider the two-dimensional mobility model. For each value of B , there are many possible configurations for grouping the hexagonal cells in a VCT. In general, it has been observed that the value of p is minimum when the cells are “tightly clustered”, while the value of p is maximum when the cells are connected in a linear manner. In this thesis, only configurations that allow the same configurations to be connected together efficiently (without cells being excluded) are considered.

Fig. 6.3 shows the configurations for the hexagonal cells in a VCT with the minimum values of p for each value of B from 1 to 10. Fig. 6.4 shows the configuration for the hexagonal cells arranged in a linear manner in a VCT resulting in the maximum value of p . Let p_{min} be the minimum value of p and p_{max} be the maximum value of p . From equation (4.10) and Fig. 6.4, it can be shown that p_{max} is given by

$$p_{max} = \frac{2B+1}{3B}, \quad B \geq 2. \quad (4.15)$$

Using the overload probability approach, the maximum equivalent capacities that can be admitted to the VCT for $B = 4$ to 10 are shown in Table 6.3. From Table 6.3, as B increases, the minimum and maximum mean frequency of handoffs to surrounding increases (in general) except for some points. The reason for one of these exceptions at $B=8$ is that the configuration for grouping the cells in the VCT does not allow the same VCT configurations to be connected together efficiently. For example, with the configuration shown in Fig. 6.5, the minimum value of p is 0.4167 and the minimum value of the mean frequency of handoff to surrounding VCTs is only 33.1. Table 6.4 shows similar results based on the % overload period approach as compared with the overload probability approach.



⬡ - A hexagonal cell in a VCT

⬡ - A hexagonal cell in surrounding VCTs

Fig. 6.3. Configurations for hexagonal cell(s) in a VCT with the minimum values of p : (a) $B=1$, (b) $B=2$, (c) $B=3$, (d) $B=4$, (e) $B=5$, (f) $B=6$, (g) $B=7$, (h) $B=8$, (i) $B=9$ and (j) $B=10$



Fig. 6.4. Configuration for hexagonal cells in a VCT with the maximum value of p

Table 6.3. Minimum and maximum mean frequency of handoffs to surrounding VCTs based on the overload probability

B	$C_N(\text{Mbps})$	p_{min}	p_{max}	$\bar{F}_{min} (\text{s}^{-1})$	$\bar{F}_{max} (\text{s}^{-1})$
4	34	0.5833	0.7500	26.7	34.3
5	39	0.5333	0.7333	28.0	38.5
6	46	0.5000	0.7222	31.0	44.7
7	53	0.4286	0.7143	30.6	51.0
8	59	0.4583	0.7083	36.4	56.3
9	64	0.4074	0.7037	35.1	60.6
10	71	0.3667	0.7000	35.1	66.9

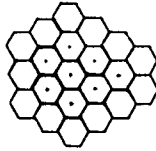


Fig. 6.5. Configuration for hexagonal cells in a VCT which does not allow the same VCT configurations to be connected together efficiently for $B=8$ but gives the minimum value of p

Table 6.4. Minimum and maximum mean frequency of handoffs to surrounding VCTs based on the % overload period

B	$C_N(\text{Mbps})$	p_{min}	p_{max}	$\bar{F}_{min} (\text{s}^{-1})$	$\bar{F}_{max} (\text{s}^{-1})$
4	33	0.5833	0.7500	25.9	33.3
5	38	0.5333	0.7333	27.3	37.5
6	45	0.5000	0.7222	30.3	43.8
7	52	0.4286	0.7143	30.0	50.0
8	59	0.4583	0.7083	36.4	56.3
9	64	0.4074	0.7037	35.1	60.6
10	71	0.3667	0.7000	35.1	66.9

From Table 6.3 or 6.4, the probability of handoff to surrounding VCTs is relatively large. Therefore, it is necessary to consider mechanisms to handle inter-VCT handoffs.

In a cellular network, let us consider multiple VCTs (clusters). The clusters can be arranged in a pattern as in Fig. 6.3. With hexagonal cells, it is easier to use symmetrical clusters, e.g., 7-cell cluster. This would be similar to frequency reuse patterns. Each cluster or a group of clusters can be managed by a single Mobile Switching Centre (MSC). A MSC is involved in connection setup, connection teardown and connection handoff. In this way, inter-cluster handoffs within the same MSC are intra-switch handoffs while inter-cluster handoffs from different MSC are inter-switch handoffs. Investigation of handoff strategies is outside the scope of this thesis. There are techniques for intra-switch handoffs [81-83] and inter-switch handoffs [84-85] reported in the literature. In other words, there is a hierarchical handoff management. The first level is a single cluster where the handoff is managed as in the VCT using standby resources. The second level is inter-cluster handoffs, or intra-switch or inter-switch handoffs.

6.4 Summary

The VCT concept has been proposed to avoid the need to involve the network call processor for every cell handoff attempt in micro-cellular ATM network [47]. A homogeneous model is considered [2]. Our model extends the model in [47] to account for heterogeneous traffic using the concept of equivalent capacity. Our CAC model to a VCT is described in Section 2.6.

The VCT concept utilizes a lot of standby resources to overcome the problem of frequent invocation of the network call processor. If there is another way of overcoming this problem using less standby resources, this direction should be pursued.

Numerical and simulation results indicate that, by using overload probability at a base station or the % overload period in a base station as a performance measure, the maximum equivalent capacity to a virtual connection tree can readily be determined. The tradeoff of using the proposed approaches is that the larger the value of the number of base stations in the virtual connection tree, B (the smaller the probability of handoffs to adjacent/surrounding virtual connection trees, in general), the larger the amount of standby capacity is required. Both one-dimensional and two-dimensional mobility models are considered in this chapter.

The equivalent capacities of the traffic sources considered in this chapter are used to set the token generation rates of the leaky buckets in Chapter 4.

Chapter 7

Conclusions

7.1 Overview

As stated in Chapter 2, the major objectives are to investigate MAC, UPC and CAC to the VCT in a cellular wireless ATM access network. A wireless ATM MAC protocol which allows seamless integration from the wireless domain to the wireline ATM network taking into consideration the various QoS and traffic characteristics of different service classes has been designed in Chapter 2.

Some MAC performance results obtained by simulation and an approximate analysis for delay-sensitive traffic like voice and MMPP video have been presented in Chapter 3. These results show that acceptable QoS for voice, MMPP video and data can be achieved in a wireless segment that supports 100 voice, 100 data and 2 MMPP video users of average rates.

In Chapter 4, the UPC based on a leaky bucket is studied by simulation for heterogeneous traffic and by analysis for voice and MMPP video traffic. For real-time voice traffic with the total packet/cell loss of 0.5 percent, the total buffer size of the leaky bucket is about 130. For real-time MMPP video traffic with a cell loss of 10^{-4} , the total buffer size of the leaky bucket is about 14000. For non-time critical data traffic, the BER is about 10^{-10} . This cannot be met by a physical transmission layer with BER of 10^{-4} . FEC or ARQ must be used for retransmission if there is an error for data traffic.

In Chapter 5, the uplink MAC and UPC based on a leaky bucket are studied by simulation for data, voice and MPEG video traffic. The simulation results show that

acceptable QoS for voice, MPEG video and data can be achieved in a wireless segment that supports 100 voice, 100 data and 5 MPEG video users of average rates with Protocol 1 and supports 100 voice, 100 data and 19 MPEG video users of average rates with Protocol 2. For real-time MPEG video traffic with a cell loss of 10^{-4} , the total buffer size of the leaky bucket is about 190 for Protocol 1 with 5 MPEG video users and about 8000 for Protocol 2 with 19 MPEG video users.

In Chapter 6, the problem of CAC of heterogeneous traffic within a VCT and two proposed CAC approaches based on equivalent capacity have been studied. The performance of these approaches is studied by simulation and analysis. Results indicate that, by using overload probability at a base station or % overload period as a performance measure, the maximum equivalent capacity to a VCT can readily be determined. The tradeoff of using these approaches is that the larger the value of the number of base stations in the VCT (the smaller the probability of migrating to adjacent/surrounding VCTs, in general), the larger the amount of standby capacity is required.

7.2 Contributions

The contributions of this research work are summarized below:

- We proposed an enhanced TDMA/DR MAC protocol over the TDMA/DR protocol [1-4]. Our protocol allows statistical multiplexing for voice users by using burst switching in which packets are transmitted only during the “on” period. Packets are not transmitted during the “off” period. Thus, more voice users can be accommodated. There is a packing algorithm in the base station that packs up the gaps in the information slots for voice users. Furthermore, bandwidth is more efficiently allocated. In our protocol, the request slots are divided into *used* and *available* request slots.

The *used* request slots relieve real-time VBR traffic (e.g., MMPP video or MPEG video) of the need to contend for request slot in every frame. Therefore, the queueing delay for transmitting the packets from this type of real-time traffic is reduced. In the *available* request slots, real-time traffic (e.g., voice) is given priority over non-real-time traffic (e.g. data). Thus, real-time traffic will not be delayed by non-real-time traffic.

- We have presented approximate analyses for the mean queueing delays and queueing delay distributions for real-time traffic like voice and MMPP video. These analyses give insights to the components that constitute the mean queueing delays and queueing delay distributions. The simulation results do not give these insights. Furthermore, only simulation results are given in [1-4, 10].
- We have also presented an analysis for calculating the probability of outstanding voice requests for a finite population instead of a infinite population in [80]. In actual computation for the state distribution of this probability, the number of voice users must be dimensioned to a large but finite number for the infinite population analysis. However, for the finite population analysis, the number of states is just the number of voice users plus one.
- We have found the distribution of the number of video packets arriving in a time interval for a MMPP video user (equation (3.43)) and the distribution of the number of video packets arriving in a time interval for the superposition of a number of MMPP video users (equation (3.45)). Without these distributions, the approximate queueing delay analysis for the MMPP video traffic and the approximate analysis for output process from the MAC protocol for a MMPP video user would not be possible.

- We have presented an approximate analysis for the output process from the MAC protocol for a MMPP video traffic. This analysis gives insights to the components that constitute the output process. The simulation results do not give these insights.
- We proposed and extended the VCT approach to CAC for homogeneous traffic in [47] to accommodate heterogeneous traffic based on equivalent capacity. A theoretical analysis is formulated to calculate new performance metrics like the reserved capacity, standby capacity, probability of migrating to adjacent or surrounding VCTs and the mean frequency of handoff to these base stations. Both one-dimensional and two-dimensional mobility models are considered in the analysis.

Appendices

Appendix A. Flow diagrams for uplink MAC protocol

Fig. A.1, Fig. A.2 and Fig. A.3 show the flow diagrams for the algorithm followed by each portable terminal for data, voice and video traffic, respectively. Fig. A.4 shows the flow diagram for the algorithm followed by the base station for information slot allocation.

Let N_{voice} , N_{video} and N_{data} be respectively the number of voice, video and data information slots requested in a TDMA frame. We can identify the following four cases in which the allocation of information slots to voice, video and data traffic can be classified:

Case (1): $(N_{voice} + N_{video} + N_{data}) \leq N_I$ - sufficient information slots for all users,

Case (2): $(N_{voice} + N_{video} + N_{data}) > N_I$ and $(N_{voice} + N_{video}) \leq N_I$ - sufficient information slots for voice and video users, insufficient information slots for data users,

Case (3): $(N_{voice} + N_{video}) > N_I$ and $N_{video} \leq N_I$ - sufficient information slots for video users, insufficient information slots for voice users, no information slots for data users, and

Case (4): $N_{video} > N_I$ - insufficient information slots for video users, no information slots for voice and data users,

Once information slots have been assigned to the users by informing them through the downlink, users will transmit in their assigned information slot(s).

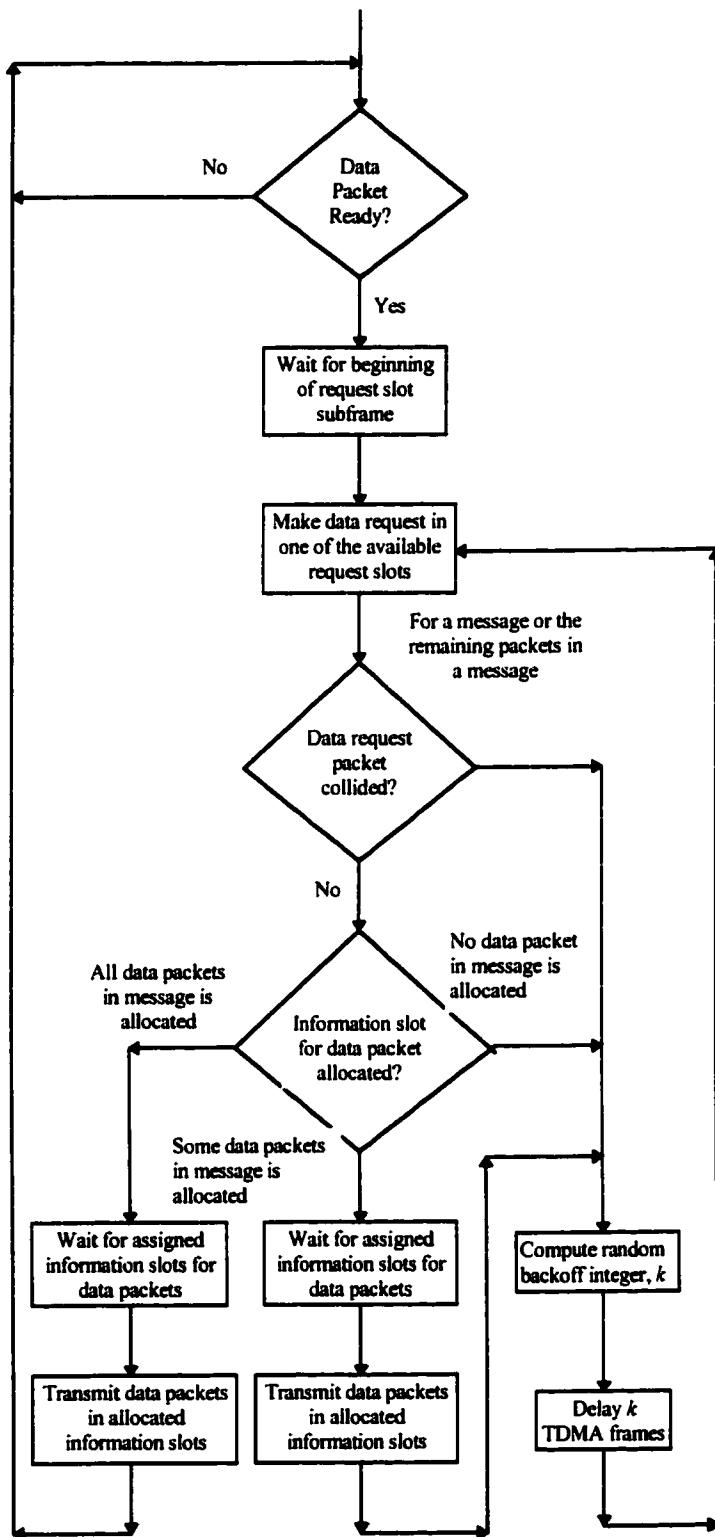


Fig. A.1. Flow diagram for the algorithm followed by each portable terminal for data traffic

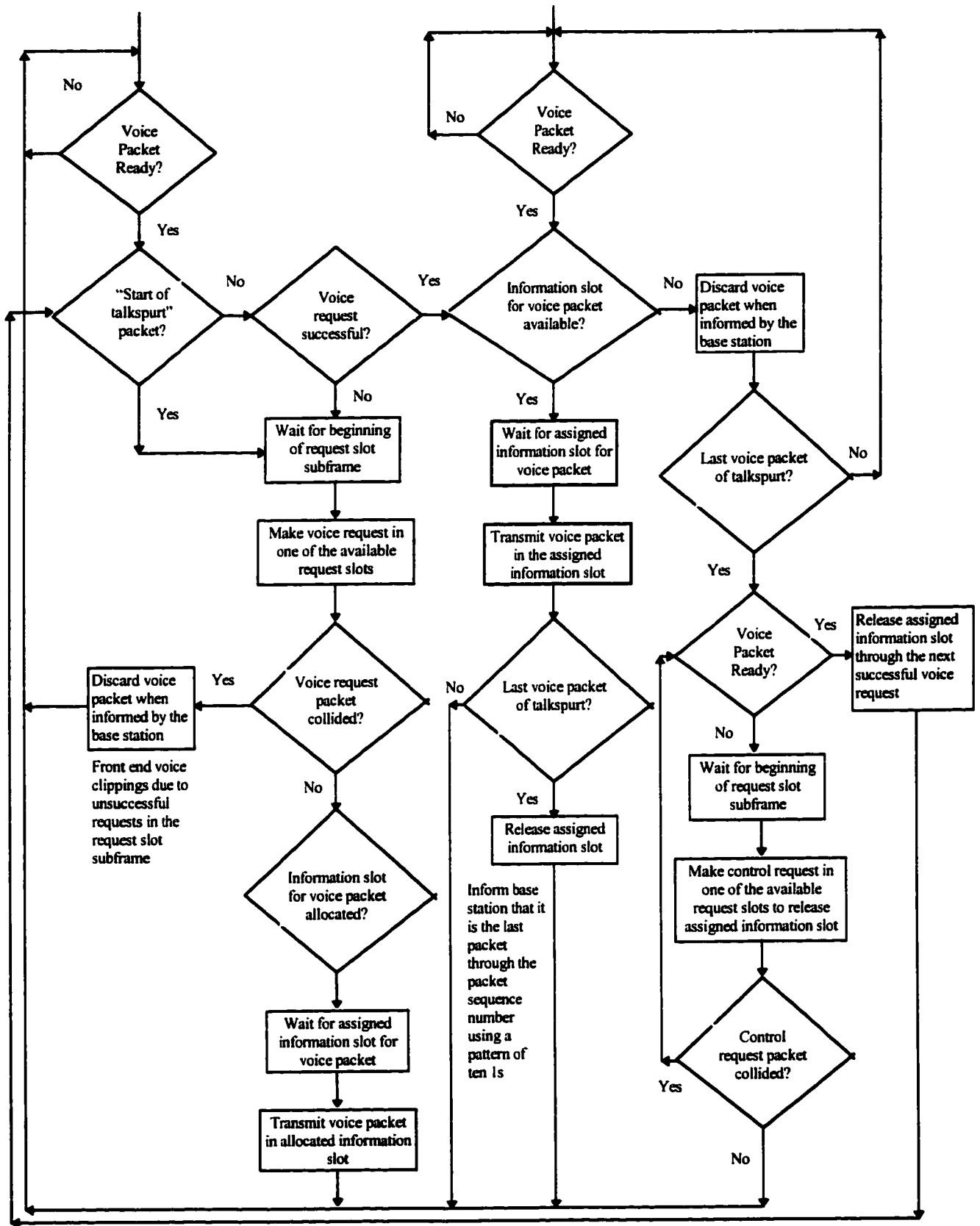


Fig. A.2. Flow diagram for the algorithm followed by each portable terminal for voice traffic

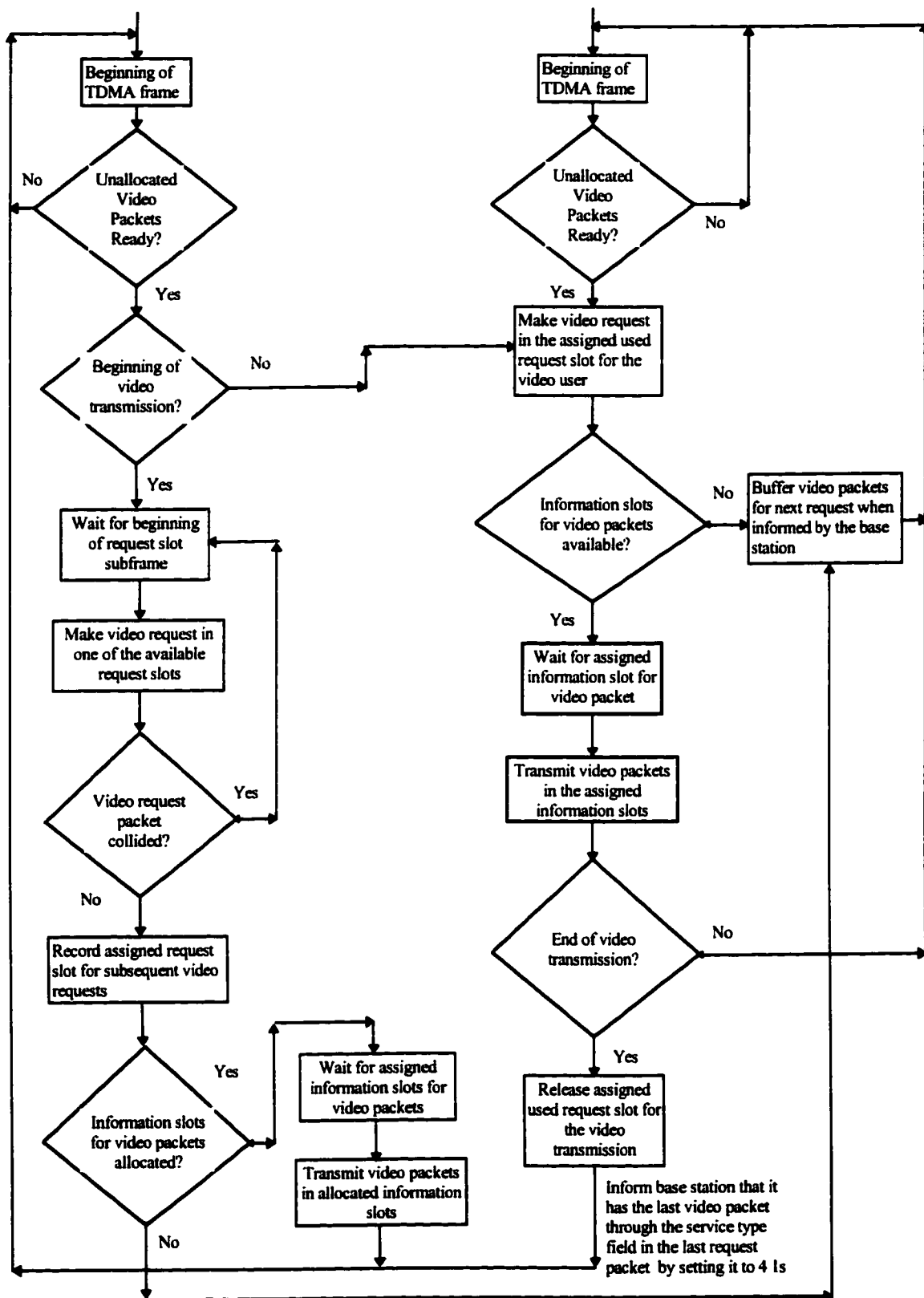


Fig. A.3. Flow diagram for the algorithm followed by each portable terminal for video traffic

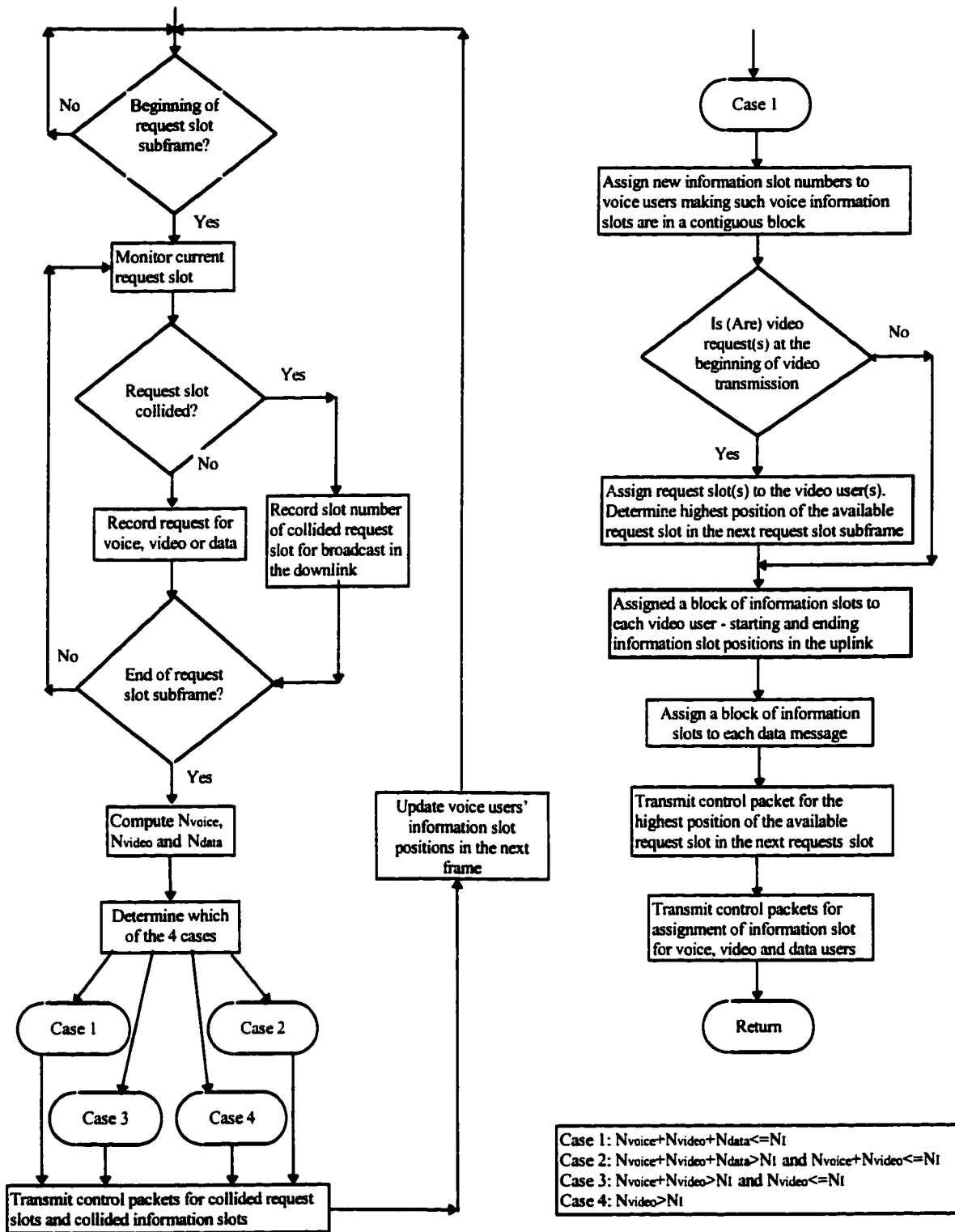


Fig. A.4a. Flow Diagram for the algorithm followed by the base station for information slot allocation (part 1)

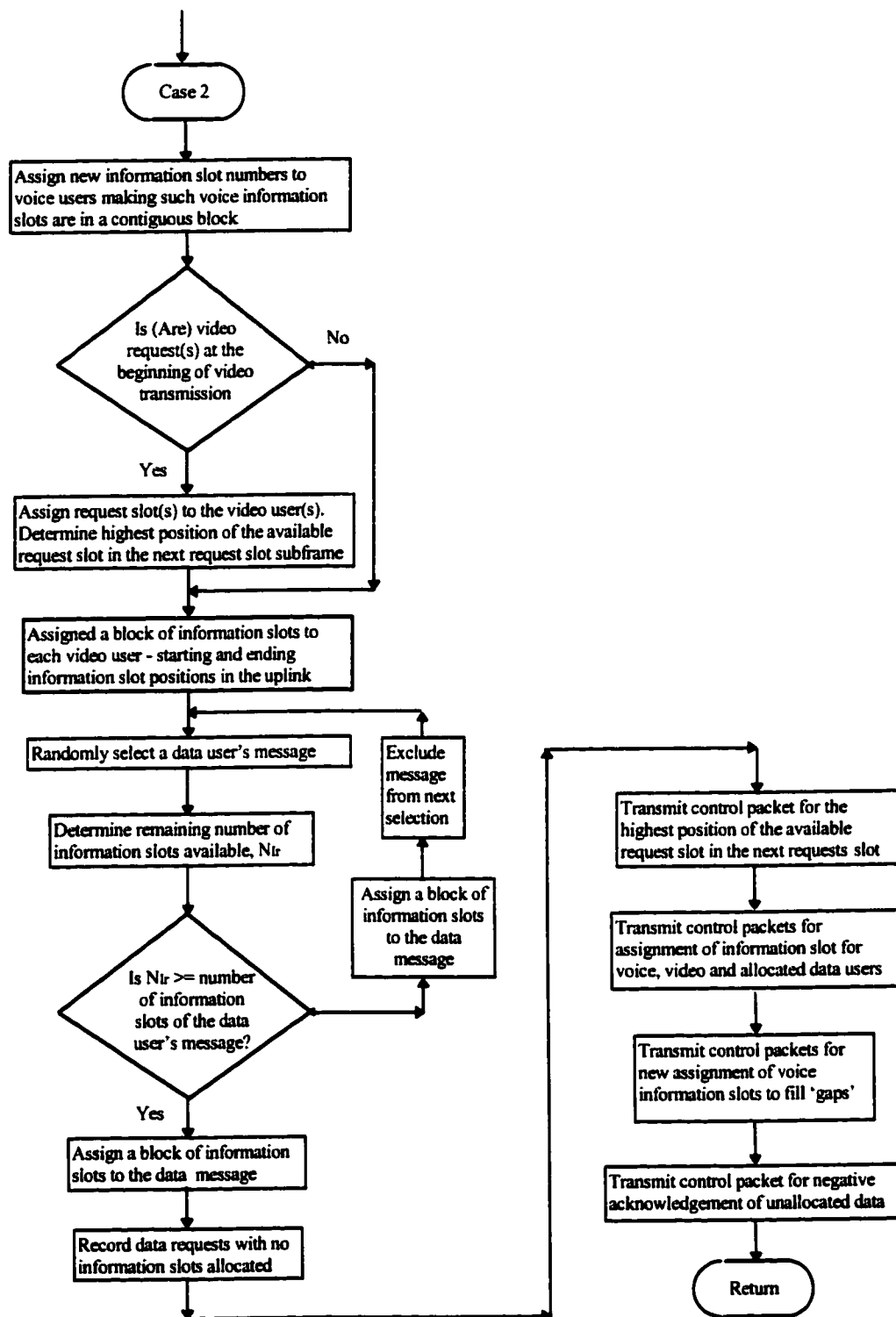


Fig. A.4b. Flow Diagram for the algorithm followed by the base station for information slot allocation (part 2)

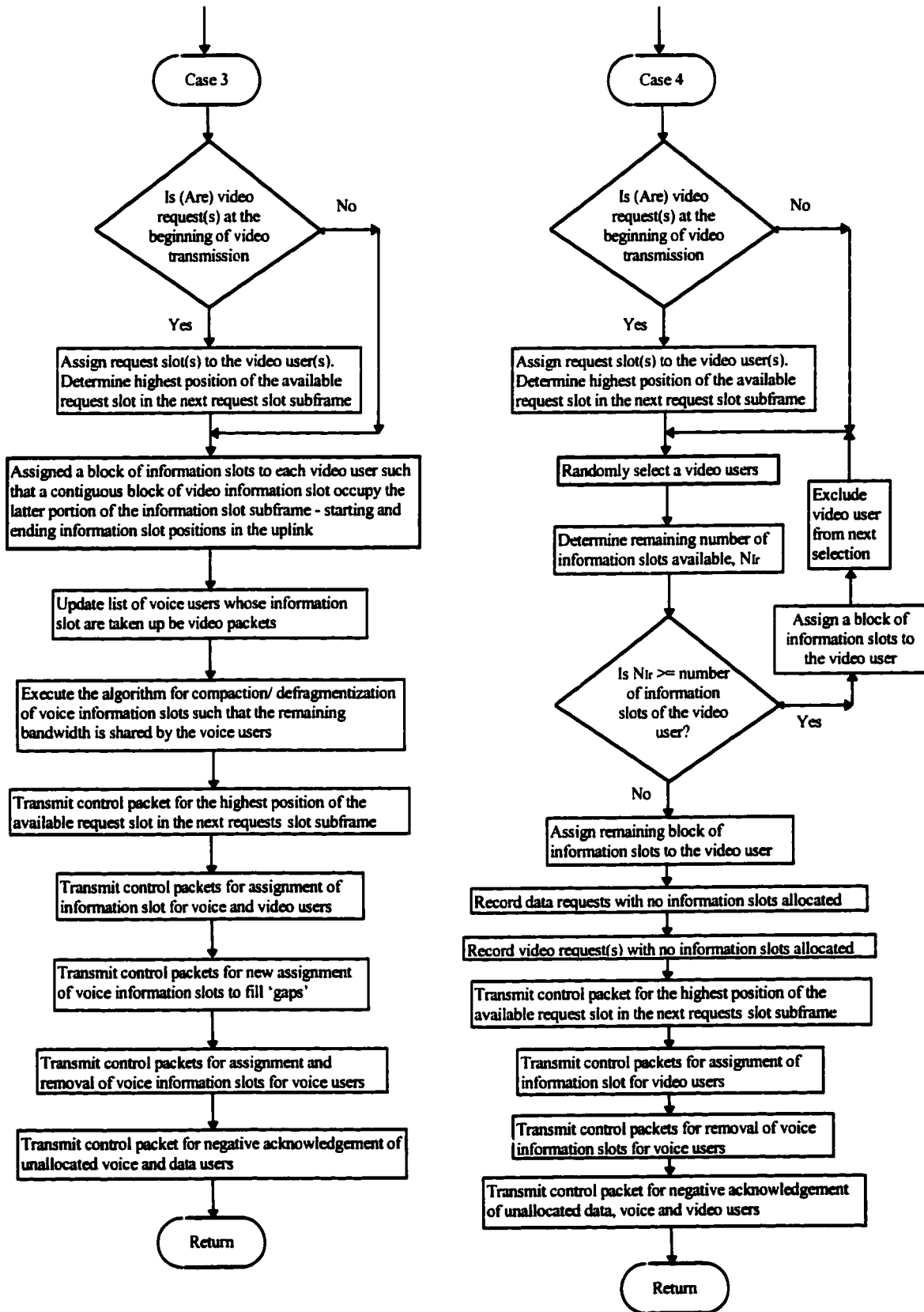


Fig. A.4c. Flow Diagram for the algorithm followed by the base station for information slot allocation (part 3)

Appendix B. Derivation of the probability of the number of frame delay, F , for voice packets

$$\begin{aligned}
\Pr[F=0] &= \sum_{\substack{c_{i-1}=0 \\ c_{i-1} \neq 1}}^{M_v} \Pr[C_{i-1} = c_{i-1}] \sum_{a_i=1}^{\infty} P[A_i = a_i] / (1 - \Pr[A_i = 0]) \Pr[K_{D,i} = a_i + c_{i-1} - 1] \\
&= \sum_{\substack{c_{i-1}=0 \\ c_{i-1} \neq 1}}^{M_v} \Pr[C_{i-1} = c_{i-1}] \sum_{a_i=1}^{\infty} \left[\frac{(\lambda T_{TDMA})^{a_i} e^{-\lambda T_{TDMA}}}{a_i! (1 - e^{-\lambda T_{TDMA}})} \right] \binom{N_A}{1} \left(\frac{1}{N_A} \right) \left(\frac{N_A - 1}{N_A} \right)^{a_i + c_{i-1} - 1} \\
&= \frac{e^{-\lambda T_{TDMA}}}{1 - e^{-\lambda T_{TDMA}}} \left(\frac{N_A}{N_A - 1} \right) \left[e^{\lambda T_{TDMA} \left(\frac{N_A - 1}{N_A} \right)} - 1 \right] \sum_{\substack{c_{i-1}=0 \\ c_{i-1} \neq 1}}^{M_v} \Pr[C_{i-1} = c_{i-1}] \left(\frac{N_A - 1}{N_A} \right)^{c_{i-1}}
\end{aligned} \tag{B.1}$$

Next, let us consider the case where $c_{i-1} = 0$ for $\Pr[F = 1]$, we have

$$\begin{aligned}
\Pr[F=1]_{c_{i-1}=0} &= \Pr[C_{i-1} = 0] \sum_{a_i=2}^{\infty} P[A_i = a_i] / (1 - \Pr[A_i = 0] - \Pr[A_i = 1]) \\
&\times \sum_{s_i=1}^{a_i-1} \Pr[K_{s,i} = s_i] \sum_{c_i=s_i+1}^{a_i} \Pr[C_i = c_i | C_{i-1} = 0] \sum_{a_{i+1}=0}^{\infty} \Pr[A_{i+1} = a_{i+1}] \Pr[K_{D,i+1} = a_{i+1} + c_i - 1] \\
&= \Pr[C_{i-1} = 0] \sum_{a_i=2}^{\infty} \frac{(\lambda T_{TDMA})^{a_i} e^{-\lambda T_{TDMA}}}{a_i! (1 - e^{-\lambda T_{TDMA}} - \lambda T_{TDMA} e^{-\lambda T_{TDMA}})} \sum_{s_i=1}^{a_i-1} \binom{N_A}{1} \left(\frac{1}{N_A} \right) \binom{a_i - 1}{s_i} \left(\frac{1}{N_A} \right)^{s_i} \\
&\times \sum_{c_i=s_i+1}^{a_i} \Pr[C_i = c_i | C_{i-1} = 0] \sum_{a_{i+1}=0}^{\infty} \frac{(\lambda T_{TDMA})^{a_{i+1}} e^{-\lambda T_{TDMA}}}{a_{i+1}!} \left(\frac{N_A - 1}{N_A} \right)^{a_{i+1} + c_i - 1} \\
&= \Pr[C_i = 0] \left(\frac{e^{-2\lambda T_{TDMA}} e^{\lambda T_{TDMA} \left(\frac{N_A - 1}{N_A} \right)}}{1 - e^{-\lambda T_{TDMA}} - \lambda T_{TDMA} e^{-\lambda T_{TDMA}}} \right) \left(\frac{N_A}{N_A - 1} \right) \\
&\times \sum_{a_i=2}^{\infty} \frac{(\lambda T_{TDMA})^{a_i}}{a_i!} \sum_{s_i=1}^{a_i-1} \binom{a_i - 1}{s_i} \left(\frac{1}{N_A} \right)^{s_i} \sum_{c_i=s_i+1}^{a_i} \Pr[C_i = c_i | C_{i-1} = 0] \left(\frac{N_A - 1}{N_A} \right)^{c_i} \\
&= \Pr[C_i = 0] \left(\frac{e^{-\lambda T_{TDMA} \left(\frac{N_A + 1}{N_A} \right)}}{1 - e^{-\lambda T_{TDMA}} - \lambda T_{TDMA} e^{-\lambda T_{TDMA}}} \right) \left(\frac{N_A}{N_A - 1} \right) \\
&\times \sum_{a_i=2}^{\infty} \frac{(\lambda T_{TDMA})^{a_i}}{a_i!} \sum_{s_i=1}^{a_i-1} \binom{a_i - 1}{s_i} \left(\frac{1}{N_A} \right)^{s_i} \sum_{c_i=s_i+1}^{a_i} \Pr[C_i = c_i | C_{i-1} = 0] \left(\frac{N_A - 1}{N_A} \right)^{c_i} \\
&= \frac{e^{-\lambda T_{TDMA} \left(\frac{N_A + 1}{N_A} \right)}}{1 - e^{-\lambda T_{TDMA}} - \lambda T_{TDMA} e^{-\lambda T_{TDMA}}} \left(\frac{N_A}{N_A - 1} \right) \Pr[C_i = 0] \\
&\times \sum_{a_i=2}^{M_v} \frac{(\lambda T_{TDMA})^{a_i}}{a_i!} \sum_{s_i=1}^{a_i-1} \binom{a_i - 1}{s_i} \left(\frac{1}{N_A} \right)^{s_i} \sum_{c_i=s_i+1}^{a_i} \Pr[C_i = c_i | C_{i-1} = 0] \left(\frac{N_A - 1}{N_A} \right)^{c_i}
\end{aligned} \tag{B.2}$$

assuming the tail distribution of A_i has a small probability. Similarly, considering the case

where $c_{i-1} \geq 2$ for $F = 1$, we have

$$\begin{aligned}
\Pr[F = 1]_{c_{i-1} \geq 2} &= \Pr[C_{i-1} = c_{i-1}] \sum_{a_i=1}^{\infty} \Pr[A_i = a_i] / (1 - \Pr[A_i = 0]) \\
&\times \sum_{s_i=1}^{a_i + c_{i-1} - 1} \Pr[K_{s_i} = s_i] \sum_{c_i=s_i+1}^{a_i + c_{i-1}} \Pr[C_i = c_i | C_{i-1} = c_{i-1}] \sum_{a_{i+1}=0}^{\infty} \Pr[A_{i+1} = a_{i+1}] \Pr[K_{D_{i+1}} = a_{i+1} + c_i - 1] \\
&\approx \frac{e^{-\lambda T_{DMM}} \left(\frac{N_A - 1}{N_A}\right)}{1 - e^{-\lambda T_{DMM}}} \left(\frac{N_A}{N_A - 1}\right) \Pr[C_i = c_i] \sum_{a_i=1}^{M_v} \frac{(\lambda T_{DMM})^{a_i}}{a_i!} \\
&\times \sum_{s_i=1}^{\min(a_i + c_{i-1} - 1, M_v - 1)} \binom{\min(a_i + c_{i-1} - 1, M_v - 1)}{s_i} \left(\frac{1}{N_A}\right)^{s_i} \sum_{c_i=s_i+1}^{\min(a_i + c_{i-1}, M_v)} \Pr[C_i = c_i | C_{i-1} = c_{i-1}] \left(\frac{N_A - 1}{N_A}\right)^{c_i}
\end{aligned} \tag{B.3}$$

Therefore, from equations (B.2) and (B.3), we have equation (3.20).

Bibliography

- [1] N. D. Wilson, R. Ganesh, K. Joseph and D. Raychaudhuri, "Packet CDMA Versus Dynamic TDMA for Multiple Access in an Integrated Voice/Data PCN", *IEEE Journal on Selected Areas in Communications*, Vol. 11, No. 6, pp. 870-884, August 1993.
- [2] D. Raychaudhuri and N. Wilson, "Multimedia Transport in Next-Generation Personal Communication Networks", *IEEE International Conference on Communications '93*, pp. 858-862, 1993.
- [3] D. Raychaudhuri and N. Wilson, "Multimedia Personal Communication Networks (PCN): System Design Issues", *Wireless Communications: Future Directions*, edited by J. M. Holtzman and D. J. Goodman, Kluwer Academic Publishers, pp. 289-304, 1993.
- [4] D. Raychaudhuri, "ATM Based Transport Architecture for Multiservices Wireless Personal Communication Networks", *IEEE International Conference on Communications '94*, pp. 559-565, 1994.
- [5] M. J. McTiffin, A. P. Hulbert, T. J. Ketseoglou, W. Heimsch and G. Crisp, "Mobile Access to an ATM Network using a CDMA Air Interface", *IEEE Journal on Selected Areas in Communications*, Vol. 12, No 5, pp. 900-908, June 1994.
- [6] R. R. Gejji, "Mobile Multimedia Scenario Using ATM and Microcellular Technologies", *IEEE Transactions on Vehicular Technology*, Vol. 43, No. 3, pp. 669-703, August 1994.
- [7] R. Wyrwas, W. Zhang, M. J. Miller and R. Anjaria, "Multiple Access Options for Multi-Media Wireless Systems", *Wireless Communications: Future Directions*, edited by J. M. Holtzman and D. J. Goodman, Kluwer Academic Publishers, pp. 289-304, 1993.
- [8] I. M. Leslie, D. R. Mcauley and D. L. Tennenhouse, "ATM everywhere?", *IEEE Network Magazine*, pp. 40-46, March 1993.
- [9] K. Y. Eng, M. J. Karol, M. Veeraraghavan, E. Ayanoglu, C. B. Woodworth and P. Pancha, R. A. Valenzuela, "BAHAMA: A Broadband Ad-Hoc Wireless ATM Local-Area Network", *IEEE International Conference on Communications '95*, pp. 1216-1223, 1995.
- [10] M. J. Karol, Z. Liu and K. Y. Eng, "Distributed-Queueing Update Multiple Access (DQRUMA) for Wireless Packet (ATM) Networks", *IEEE International Conference on Communications '95*, pp. 1224-1231, 1995.
- [11] T. C. Wong, K. C. Chua and J. W. Mark, "QoS Issues in Interconnected Wireless and Wireline ATM Networks - A Cellular Wireless ATM Network", Technical Report WL_ATM-001-06-95, Centre for Wireless Communications, National University of Singapore, 1995.

- [12] K. C. Chua, T. C. Wong and J. W. Mark, "Design of a Cellular Wireless ATM Access Network", IEEE Personal, Indoor and Mobile Radio Communications Record '96, Vol. 2, pp. 618-622, Taipei, Taiwan, 15-18 Oct 1996.
- [13] D. J. Goodman, R. A. Valenzuela, K. T. Gayliard and B. Ramamurthi, "Packet Reservation Multiple Access for Local Wireless Communications," IEEE Transactions on Communications, Vol. 37, No. 8, pp. 885-890, 1989.
- [14] D. J. Goodman, "Cellular Packet Communications," IEEE Transactions on Communications, Vol. 38, No. 8, pp. 1272-1280, August 1990.
- [15] S. Nanda, D. J. Goodman and U. Timor, "Performance of PRMA: A Packet Voice Protocol for Cellular Systems," IEEE Transactions on Vehicular Technology, Vol. 40, No. 3, pp. 584-598, August 1991.
- [16] D. J. Goodman and S. X. Wei, "Efficiency of Packet Reservation Multiple Access," IEEE Transactions on Vehicular Technology, Vol. 40, No. 1, pp. 170-176, February 1991.
- [17] M. Frullone, G. Falcia, P. Grazioso, G. Riva and A. M. Serra, "On the Performance of Packet Reservation Multiple Access with Fixed and Dynamic Channel Allocation," IEEE Transactions on Vehicular Technology, Vol. 42, No. 1, pp. 78-86, February 1993.
- [18] W. C. Wong, "Dynamic Allocation of Packet Reservation Multiple Access Carriers," IEEE Transactions on Vehicular Technology, Vol. 42, No. 4, pp. 385-392, November 1993.
- [19] R. A. Ziegler and G. P. Pollini, "An Experimental Implementation of the PRMA Protocol for Wireless Communication," IEEE INFOCOM, pp. 909-912, 1993.
- [20] G. Wu, K. Mukumoto and A. Fuda, "Analysis of an Integrated Voice and Data Transmission System using Packet Reservation Multiple Access," IEEE Transactions on Vehicular Technology, Vol. 43, No. 2, pp. 289-297, May 1994.
- [21] R. H. M. Hafez, D. D. Falconer, G. Stamatelos and S.A. Mahmoud, "Fundamental issues in Millimeter Wave Indoor Wireless Networks," Wireless '93 conference Record, Calgary, July 1993.
- [22] K.-C. Chen, "Medium Access Control of Wireless LANs for Mobile Computing," IEEE Network Magazine, pp. 50-64, September/October, 1994
- [23] N. Abramson, "Multiple Access in Wireless Digital Networks," Proceedings of the IEEE, Vol. 82, No. 9, pp. 1360-1370, September 1994.
- [24] W. C. Y. Lee, "Mobile Communications Design Fundamentals," Second Edition, Chapter 9, Cellular CDMA, pp. 313-318, John Wiley and Sons, 1993.

- [25] G. D. Stamoulis, M. E. Anagnostou and A. D. Georgantas, "Traffic Source Models for ATM networks: a survey," *Computer Communications*, Vol. 17, No. 6, pp. 428-438, June 1994.
- [26] V. S. Frost and B. Melamed, "Traffic Modeling for Telecommunications Networks", *IEEE Communications Magazine*, pp. 70-81, March 1994.
- [27] R. O. Onvural, "Asynchronous Transfer Mode Networks: Performance Issues," Artech House, 1994.
- [28] H. Akimaru and K. Kawashima, "Teletraffic: Theory and Applications," Springer-Verlag, 1993.
- [29] K. Sriram and W. Whitt, "Characterizing superposition arrival processes in packet multiplexers for voice and data," *IEEE Journal on Selected Areas in Communications*, Vol. sac-4, No. 4, pp. 833-846, September 1986.
- [30] S. Nanda, D. J. Goodman and U. Timor, "Performance of PRMA: A Packet Voice Protocol for Cellular Systems," *IEEE Transactions on Vehicular Technology*, Vol. 40, No. 3, pp. 584-598, August 1991.
- [31] G.-L. Wu and J. W. Mark, "Computational Methods for Performance Evaluation of a Statistical Multiplexer Supporting Bursty Traffic," *IEEE/ACM Transactions on Networking*, Vol. 4, No. 3, pp. 386-397, June 1996.
- [32] G.-L. Wu and J. W. Mark, "Computational Methods for Performance Evaluation of an ATM Multiplexer Supporting Bursty Traffic," *IEEE International Conference on Communications Record '93*, pp. 1020-1026, 1993.
- [33] D. Dubois, N. D. Geoganas and E. Horlait, "A QoS Selector for Multimedia Applications on ATM Networks," *IEEE International Conference on Communications '94*, pp. 160-164, 1994.
- [34] P. Mermelstein, A. Jalali and H. Leib, "Integrated Services on Wireless Multiple Access Network," *IEEE International Conference on Communications '93*, pp. 863-867, 1993.
- [35] O. T. W. Yu and V. C. M. Leung, "B-ISDN Architectures and Protocols to Support Wireless Personal Communications Internetworking," , *IEEE Personal, Indoor and Mobile Radio Communication Record '95*, pp. 768-772, 1995.
- [36] M. Barton and T. R. Hsing, "Architecture for Wireless ATM Networks," , *IEEE Personal, Indoor and Mobile Radio Communication Record '95*, pp. 778-782, 1995.

- [37] S. Dastango, "A Multimedia Access Control Protocol for ATM Based Mobile Networks," *IEEE Personal, Indoor and Mobile Radio Communication Record '95*, pp. 794-798, 1995.
- [38] N. Movahhedinia, G. Stamatelos and H. M. Hafez, "A slot Assignment Protocol for Indoor Wireless ATM Networks using the Channel Characteristics and the Traffic Parameters," *IEEE GLOBECOM Record '95*, pp. 327-331, 1995.
- [39] P. Agrawal, E. Hyden, P. Krzyzanowski, P. Mishra, M. B. Srivastava and J. A. Trotter, "SWAN: A Mobile Multimedia Wireless Network," *IEEE Personal Communications*, pp. 18-33, April 1996.
- [40] Z. Lui, M. J. Karol, M. E. Zarki and K. Y. Eng, "Time-Frequency Slicing with Distributed-Queueing Request Update Multiple Access (DQRUMA) for Multi-Rate Wireless Packet (ATM) Networks," in "Multiaccess, Mobility and Teletraffic for Personal Communications," B. Jabbari, P. Godlewski and X. Lagrange (Editors), Kluwer Academic Publishers, pp. 293-306, 1996.
- [41] D. Makrakis, R. S. Mander and P. Panantoni-Kazakos, "A New Medium Access Control Protocol for Integrated Traffic Personal Communication Networks," in "Multiaccess, Mobility and Teletraffic for Personal Communications," B. Jabbari, P. Godlewski and X. Lagrange (Editors), Kluwer Academic Publishers, pp. 337-350, 1996.
- [42] A. Acampora, "Wireless ATM: A Perspective on Issues and Prospects," *IEEE Personal Communications*, pp. 8-17, August 1996.
- [43] E. Ayanoglu, K. Y. Eng and M. J. Karol, "Wireless ATM: Limits, Challenges, and Proposals," *IEEE Personal Communications*, pp. 18-34, August 1996.
- [44] D. Falconer, "A System Architecture for Broadband Millimeter-Wave Access to an ATM LAN," *IEEE Personal Communications*, pp. 36-41, August 1996.
- [45] D. Raychaudhuri, "Wireless ATM Networks: Architecture, System Design and Prototyping," *IEEE Personal Communications*, pp. 42-49, August 1996.
- [46] B. Walke, D. Petras and D. Plassmann, "Wireless ATM: Air Interface and Network Protocols of the Mobile Broadband System," pp. 50-56, August 1996
- [47] A. S. Acampora and M. Naghshineh, "An Architecture and Methodology for Mobile-Executed Handoff in Cellular ATM Network," *IEEE Journal on Selected Areas in Communications*, vol. 12, no. 8, pp. 1365-1375, October 1994.
- [48] R. Guerin, H. Ahmadi and M. Naghshineh, "Equivalent Capacity and its Applications to Bandwidth Allocation in High-Speed Networks," *IEEE Journal on Selected Areas in Communications*, vol. 9, no. 7, pp. 968-981, September, 1991.

- [49] H. Saito and K. Shiimoto, "Dynamic Call Admission Control in ATM Network," *IEEE Journal on Selected Areas in Communications*, vol. 9, No. 7, pp. 982-989, September, 1991.
- [50] M. Naghshineh and A. S. Acampora, "QOS Provisioning in Micro-cellular Networks Supporting Multimedia Traffic," *IEEE INFOCOM, Conference Record '95*, pp. 1075-1084, 1995.
- [51] M. Naghshineh and M. Schwartz, "Distributed Call Admission Control in Mobile/Wireless Networks," *IEEE Personal, Indoor and Mobile Radio Communications, Conference Record '95*, pp. 289-293, 1995.
- [52] G. M. Stamatelos and J. F. Hayes, "Admission-Control Techniques with application to broad networks," *Computer Communications*, vol. 17, no. 9, pp. 663-673, September, 1994.
- [53] D. Hong and T. Suda, "Congestion Control and Prevention in ATM Networks," *IEEE Network Magazine*, pp. 10-16, July, 1991.
- [54] G. Gallassi, G. Rigolio and L. Verri, "Resource Management and Dimensioning in ATM Networks," *IEEE Network Magazine*, pp. 8-17, May, 1990.
- [55] M. Sidi, W.-Z. Liu, I. Cidon and I. Gopal, "Congestion Control Through Input Rate Regulation," *IEEE GLOBECOM Record '89*, pp. 1764-1768, 1989.
- [56] A. W., Berger, "Performance Analysis of a Rate Control Throttle Where Tokens and Jobs Queue," *IEEE INFOCOM Record '90*, pp. 30-38, 1990.
- [57] A. I. Elwalid and D. Mitra, "Stochastic Fluid Models in the Analysis of Access Regulation in High Speed Networks," *IEEE INFOCOM Record '91*, pp. 1626-1632, 1991.
- [58] M. Butto, E. Cavallero and A. Tonietti, "Effectiveness of the 'leaky Bucket' Policing Mechanism in ATM Networks," *IEEE Journal on Selected Areas in Communications*, Vol. 9, No. 3, pp. 335-342, April, 1991.
- [59] K. Bala, I. Cidon and K. Sohraby, "Congestion Control for High Speed Packet Switched Networks," *IEEE INFOCOM Record '90*, pp. 520-526, 1990.
- [60] G.-L. Wu and J. W. Mark, "Discrete Time Analysis of Leaky-Bucket Congestion Control," *Computer Networks and ISDN Systems*, Vol. 26, pp. 79-94, 1993.
- [61] K. Sohraby and M. Sidi, "On the Performance of Bursty and Correlated Sources Subject to Leaky Bucket Rate-Based Access Control Schemes," *IEEE INFOCOM Record '91*, pp. 426-434, 1991.

- [62] D. P. Heyman, "A Performance Model of the Credit Manager Algorithm," *Computer Networks and ISDN Systems*, Vol. 24, pp. 81-91, 1992.
- [63] A. W. Berger, A. E. Eckberg, T.-C. Hou and D. M. Lucantoni, "Performance Characterizations of Traffic Monitoring, and Associated Control, Mechanisms for Broadband 'Packet' Networks," *IEEE GLOBECOM Record '90*, pp. 350-354, 1990.
- [64] M. C. Chuah, R. L. Cruz, "Approximate Analysis of Average Performance of (σ, ρ) Regulators," *IEEE INFOCOM Record '90*, pp. 874-880, 1990.
- [65] L.-N. Wong and M. Schwartz, "Access Control in Metropolitan Area Networks," *IEEE International Conference on Communications Record '90*, pp. 1591-1595, 1990.
- [66] J. S. Turner, "New Directions in Communications (Or Which Way to the Information Age?)," *IEEE Communications Magazine*, pp. 8-15, October, 86.
- [67] J. S. Turner, "The Challenge of Multipoint Communication," *Traffic Engineering for ISDN Design and Planning*, M. Bonatti and M. Decina (Editors), Elsevier Science Publishers B. V. (North-Holland), pp. 263-279, 1988.
- [68] P. Tran-Gia, "Discrete-Time Analysis of Usage Parameter Control Functions in ATM Systems," *Architecture and Protocols for High-Speed Networks*, O. Spaniol, A. Danthine, W. Effelsberg (Editors), Kluwer Academic Publishers, pp. 111-131, 1994.
- [69] G. Gallassi, G. Rigolio and L. Fratta, "ATM: Bandwidth Assignment and Bandwidth Enforcement Policies," *IEEE GLOBECOM Record '89*, pp. 1788-1793, 1989.
- [70] R. Krishnan and J. A. Silvester, "The Effect of Variance Reduction on Performance of the Leaky Bucket," *IEEE International Conference on Communications Record '95*, pp. 1974-1980, 1995.
- [71] H. Heiss and E. Wallmeier, "Performance Comparison of Three Policy Mechanisms Based on their Maximum Throughput Functions," *Teletraffic Science and Engineering: The Fundamental Role of Teletraffic in the Evolution of Telecommunications Networks*, J. Labetoulle and J. W. Roberts (Editors), pp. 1405-1414, 1994.
- [72] E. P. Rathgeb, "Modeling and Performance Comparison of Policing Mechanisms for ATM Networks," *IEEE Journal on Selected Areas in Communications*, Vol. 9, No. 3, pp. 325-334, April, 1991.
- [73] F. P. Kelly, "Effective Bandwidths at Multi-Class Queues," *Queueing Systems*, Vol. 9, pp. 5-16, 1991.
- [74] R. J. Gibbens and P. J. Hunt, "Effective Bandwidths for Multi-Type UAS Channel," *Queueing Systems*, Vol. 9, pp. 17-28, 1991.

- [75] Z. Zhang and A. S. Acampora, "Equivalent Bandwidth for Heterogeneous Sources in ATM Networks, IEEE International Conference on Communications '94, pp. 1025-1031, 1994.
- [76] G. Kesidis, J. Walrand and C. -S. Chang, "Effective Bandwidths for Multiclass Markov Fluids and other ATM Sources,' IEEE/ACM Transactions on Networking, Vol. 1, No. 4, pp. 424-428, August, 1993.
- [77] A. I. Elwalid and D. Mitra, "Effective Bandwidth of General Markovian Traffic Sources and Admission Control of High Speed Networks," IEEE/ACM Transactions on Networking, Vol. 1, No. 3, pp. 329-343, June 1993.
- [78] K. M. Rege, "Equivalent Bandwidth and Related Admission Criteria for ATM Systems - A Performance Study," International Journal of Communication Systems, Vol. 7, pp. 181-197, 1994.
- [79] M. H. Macdougall, "Simulating Computer Systems: Techniques and Tools," The MIT Press, 1987.
- [80] H. W. Lee and J. W. Mark, "Combined Random/Reservation Access for Packet Switched Transmission Over a Satellite with On-Board Processing: Part I - Global Beam Satellite", IEEE Transactions on Communications, Vol. COM-31, No. 10, pp. 1161-1171, October 1983.
- [81] H. Mitts, H. Hansen, J. Immonen and S. Veikkolainen, "Lossless handover for wireless ATM," Annual International Conference on Mobile Computing and Networking Record '96, pp. 85-96, 1996.
- [82] H. Mitts, H. Hansen, J. Immonen and S. Veikkolainen, "Lossless handover for wireless ATM," Mobile Networks and Applications, Vol. 1, No. 3, pp. 299-312, 1996.
- [83] S. N. Mukhi and J. W. Mark, "A Feedback-Based Handoff Algorithm for Wireless ATM Networks," To appear in Proc. of WCNC '99, September 22-24, 1999, New Orleans, Louisiana, USA.
- [84] W. Chen "Impact of anchor re-routing based inter-switch handoffs in wireless ATM access networks," IEEE International Conference on Communications Record '96, Vol. 1, pp.235-239, 1996.
- [85] K. Jang, K. Kang, J. Shim and D. Kim, "Dynamic wired-resource reservation scheme with a connection rerouting method on ATM-based PCN," Annual International Conference on Universal Personal Communications Record '97, Vol. 2, pp. 738-745, 1997.
- [86] P. Sholander, L. Martinez, L. Tolendino and B. A. Mah, "The Effects of User Mobility on Usage Parameter Control (UPC) in Wireless ATM Systems," IEEE International Performance, Computing and Communications Conference Record '98, pp. 216-221, 1998.

- [87] M. Ritter and P. Tran-Gia, "Performance Analysis of Cell Rate Monitoring Mechanisms in ATM Systems," Third International Conference on Local and Metropolitan Communication Systems, Edited by T. Hasegawa, G. Pujolle, H. Takagi and Y. Takahashi, Vol. 3, pp. 129-150, Chapman and Hall, 1995.
- [88] "Broadband Network Traffic - Performance Evaluation and Design of Broadband Multiservice Networks, Final Report of Action COST 242," Edited by J. Roberts, U. Mocci and J. Virtamo, pp. 504-505, Springer, 1996.
- [89] H. Nguyen, "Video Coding and Modeling with Applications to ATM Multiplexing," Ph.D. Thesis, University of Waterloo, 1993.
- [90] T. C. Wong, J. W. Mark and K. C. Chua, "Delay Performance Analysis of MMPP Video Traffic in Wireless ATM Network," 32nd Annual Conference on Information Sciences and Systems Record '98, Vol. 1, pp. 353-358, Princeton, New Jersey, U.S.A., 18-20 Mar 1998.
- [91] T. C. Wong, J. W. Mark and K. C. Chua, "Connection Admission Control in a Cellular Wireless ATM Access Network," IEEE International Conference on Communications Record '98, Vol. 2, pp. 1094-1098, Atlanta, Georgia, U.S.A., 7-11 Jun 1998.
- [92] T. C. Wong, J. W. Mark and K. C. Chua, "Access and Control in a Cellular Wireless ATM Networks," in preparation.